Greenhouse gasses emissions and their trends over the last three decades across Africa

Mounia Mostefaoui[1], Philippe Ciais[2], Matthew J. McGrath[2], Philippe Peylin[2], Prabir K. Patra[3], Yolandi Ernst[4]

[1]Laboratoire de Météorologie Dynamique/IPSL, École Normale Supérieure, PSL Research University, Sorbonne University, École Polytechnique, IP Paris, CNRS, Paris, France.
[2]Laboratoire des Sciences du Climat et de l'Environnement, 91190 Gif-sur-Yvette, France.
[3]Research Institute for Global Change, JAMSTEC, Yokohama 2360001, Japan.
[4]Global Change Institute, University of the Witwatersrand, Johannesburg, South Africa.

Correspondence to: mounia.mostefaoui@polytechnique.edu

Key words: greenhouse gasses, anthropogenic emissions and removals, fossil fuels, land-use, land-use change and forestry, Africa, bottom-up, top-down atmospheric inversions, UNFCCC inventories, Global Carbon Project, PRIMAP-hist, IPCC sectors, climate change, Paris Agreement, Global Stocktake, Monitoring, Reporting and Verification.

Abstract. A key goal of the Paris Agreement (PA) is to reach net-zero Greenhouse Gasses (GHG) emissions by 2050 globally, which requires mitigation efforts from all countries. Africa's rapidly growing population and GDP makes this continent important for GHG emission trends. In this paper, we study the emissions of carbon dioxide (CO_2), methane (CH_4) and nitrous oxide (N_2O) in Africa over three decades (1990-2018). We compare bottom-up (BU) approaches including UNFCCC national inventories, FAO, PRIMAP-hist, process-based ecosystem models for CO_2 fluxes in the Land Use, Land Use Change and Forestry (LULUCF) sector, and global atmospheric inversions. For inversions, we applied different methods to separate anthropogenic CH_4 emissions. The ~~bottom-up~~ BU inventories show that over the decade 2010-2018, less than ten countries represented more than 75% of African fossil CO_2 emissions. With a mean of 1373 $MtCO_2$ yr^{-1}, total African fossil CO_2 emissions over 2010-2018 represent only 4% of global fossil emissions. Yet, these emissions grew by +34% from 1990-1999 to 2000-2009 and by +31% over 2000-2009 to 2010-2018, which represent more than a doubling in 30 years. This growth rate is more than twice faster than the global growth rate of fossil CO_2 emissions. The anthropogenic emissions of CH_4 grew by 5% from 1990-1999 to 2000-2009 and by 14.8% from 2000-2009 to 2010-2018. The N_2O emissions grew by 19.5% from 1990-1999 to 2000-2009; and by 20.8% from 2000-2009 to 2010-2018. When using the mean of estimates from UNFCCC reports (including the land use sector), with corrections from outliers, Africa was a mean source of greenhouse gasses of 2622^{3239}_{2186} $MtCO_2e$ yr^{-1} from all ~~bottom-up~~ BU estimates (sub- and superscript indicating min-max range uncertainties), and of $+2637^{5873}_{1761}$ $MtCO_2e$ yr^{-1} from top-down (TD) methods, during their overlap period from 2001 to 2017. Although the mean values are consistent, the range of ~~(top-down)~~ TD estimates is larger than the one of ~~bottom-up~~ BU estimates, indicating that sparse atmospheric observations and transport model errors do not allow us to use inversions to reduce the uncertainty of ~~bottom-up~~ BU estimates. A main source of uncertainty comes from CO_2 fluxes in the land-use sector (LULUCF) for which the spread across inversions is larger than 50%, especially in Central Africa. Moreover, estimates from national UNFCCC communications differ widely depending on whether the large

sinks in a few countries are corrected to more plausible values using more recent national sources following the methodology of Grassi et al. (2022). The median of CH_4 emissions from inversions based on satellite retrievals and ~~in situ~~ surface station networks are consistent with each other within 2% at continental scale. The inversion ensemble also provides consistent estimates of anthropogenic CH_4 emissions with ~~bottom up~~ BU inventories such as PRIMAP-hist. For N_2O, inversions systematically show higher emissions than inventories, on average about 4.5 times more than PRIMAP-hist, either because natural N_2O sources cannot be separated accurately from anthropogenic ones in inversions, or because ~~bottom up~~ BU estimates ignore indirect emissions and under-estimate emission factors. Future improvements can be expected thanks to a denser network for monitoring atmospheric concentrations. This study helps to introduce methods to enhance the scope of use of various published datasets and allows to compute budgets thanks to recombinations of those data products. Our results allow to understand uncertainty and trends of emissions and removals in a region of the world where few observations exist and most inventories are based on default IPCC guidelines values. The results can therefore serve as a support tool for the Global Stocktake (GST) of the Paris Agreement. The referenced datasets related to figures are available at: https://doi.org/10.5281/zenodo.7347077 (Mostefaoui et al., 2022).

Introduction

Large global reductions of greenhouse gasses (GHG) emissions are needed to avoid "dangerous anthropogenic interference with the climate system" (IPCC, 2021). The Paris Agreement (PA) aims at limiting global warming below 2°C and reaching "net-zero GHG emissions by 2050" (UNFCCC, 2015). To improve the monitoring of emissions trends, the PA has an Enhanced Transparency Framework (ETF) by which countries will have to report their GHG emissions and removals under a standardized format starting in 2024 (Perugini et al., 2021; UNFCCC, 2021) through Biennial Transparency Reports (BTR), with the ambition to use up-to-date data and best available science to improve national inventories. This represents a challenge for many developing countries, where emissions inventories have been irregular.

Recent analyses predict a fast increase of African emissions correlated with demographic growth. The African population is expected to double from 1.2 billion in 2019 to 2.5 billion at the 2050 horizon (UN, 2019). Using the TIAM-ECN Integrated Assessment Model (IAM) developed with data from the International Energy Agency (IEA), van der Zwaan et al., (2018) concluded that greenhouse gasses (GHG) emissions from Africa will become substantial at the global scale by 2050. In Shared Socio-economic Pathways (SSP) projection scenarios, Africa and the Middle East are grouped together despite having very different geographies, per capita emissions and Gross Domestic Product (GDP) (IIASA, 2017). According to IAM projections, the minimum projected share of Africa in global emissions would be close to 10% by 2050 for a business-as-usual pathway. An "explosive growth in African combustion emissions"' (Liousse et al., 2014) could not be excluded from 2030 to 2050, if no drastic mitigation policies are implemented (IPCC, 2021). If a stringent emissions reduction pathway limiting global warming to +2 °C is adopted, Africa could contribute to around 20% of global emissions by 2050, becoming the second largest worldwide emitting region. Further, under stringent climate policy scenarios, CH_4 and N_2O emissions in Africa were projected to contribute 80% of the total emissions of these two gasses in 2050 (van der Zwaan et al., 2018). Therefore, Africa will become an important global emission contributor under any mitigation pathway with a demographical and industrial development increase.

There are 56 African countries represented in the United Nations. National emissions reports to the United Nations Convention Framework on Climate Change (UNFCCC) are available for 53 countries, including all major African emitters. Africa as a whole ranks fifth worldwide in terms of territorial fossil fuels use with a total of 1449 $MtCO_2e$, in-between the Russian Federation and Japan (Friedlingstein et al., 2020). The global share of Africa is ~ 4% of fossil CO_2 (FCO_2) emissions, ~ 16

% of CH_4 emissions (Saunois et al., 2020) and ~ 25% of N_2O emissions (Tian, 2020). South Africa is the biggest FCO_2 emitter in the continent, and ranked twelve on the global scale, just after Brazil.

Despite projections of strong growth of emissions and population in Africa, the continent is under-studied and lacks up-to-date comprehensive assessments of GHG emissions and removals, given sporadic and often outdated reports by individual countries. The literature tends to be scarce about African countries, and their emissions have rarely been analyzed comprehensively using the results from both statistical inventories that are also referred to as bottom-up (BU) methods, and from top-down (TD) atmospheric inversions. Country reports estimate GHG emissions through statistical inventories using estimates of national sectoral activity data multiplied by emissions factors, with three levels of refinements depending on countries, named Tier 1 for default emissions factors, Tier 2 for country-specific emissions factors / activity data and Tier 3 for more emissions factors / activity with tailored representation at the scale of process. Other BU inventories for assessing national emissions also exist: they are based on the same approach as country-reported inventories but use their own parameters for activity data and emissions factors coming from research groups, international statistical agencies, etc. Process-based ecosystem models developed by the research community are not used by countries. They are based on the representations of complex ecosystem processes and can also be viewed as a BU method. Besides, another approach is named "top-down" and refers to atmospheric inversions. Inversions consist in estimating causes (emissions and sinks) based on consequences (concentrations). The inverse modeling approach consists in adjusting a priori fluxes to the atmospheric transport in order to be as adjusted as possible with observation data by minimizing a cost function. This is a mathematically complex problem under constrained because every point of the globe is an unknown emission, and there is only a limited number of observations: "regularization" techniques are used to find a unique solution. The African ground-based atmospheric network used by inversions is very sparse. There are only three currently active surface flasks over this whole continent, located in Namibia (Gobabeb), in the Seychelles (Mahe Island), and in South Africa (Cape Point). The one in Algeria (Assekrem) was terminated on 26/08/2020, and the one in Kenya has been inactive since 21/06/2011. The characteristics of the surface flasks in Africa, available on the NOAA website are summarized in Table S1. Inversion results are therefore uncertain due to this small number of atmospheric stations over the continent (Nickless et al., 2020).

A previous analysis of African emissions was solely focused on FCO_2 emissions during the decade 2000-2009 (Canadell et al., 2009). A first budget for the period 1990-2009 was provided at the continental scale with the RECCAP1 project (Valentini et al., 2014). Ayompe et al. (2020) studied recent FCO_2 emissions trends, using International Energy Agency (IEA) data. Other studies are region-

specific or sector-specific, focusing exclusively on agriculture (Bombelli et al., 2009), on natural ecosystems in Sub-Saharan Africa (Kim et al., 2016) or in individual countries such as Kenya (Zhu et al., 2018).

Paying attention not only to commonly identified big emitters like South Africa, but also to medium emitters and to emerging emitters is important, not only in terms of scientific assessment, but also for financial and climate policy purposes under the PA. The Monitoring, Reporting and Verification (MRV) provisions of the PA indeed require scientific and policy tools to verify the pledges made by all the signatory countries. Instruments for financial transfers for mitigation and adaptation like the Green Fund on Climate Change (GCF) and the REDD+ initiatives cover the African scope and will require scientific assessment of trends for impact evaluation and credibility purposes, and as an incentive for continued investments. As part of the Global Stock Take (GST) under article 14 of the PA aiming at assessing "collective progress", all signatory parties will have to show their contributions to the global mitigation efforts. These efforts will be evaluated within a MRV system which includes the requirement for developing countries to submit their Biennial Update Reports (BUR) on a biennial basis starting in 2024. As no standard global reporting framework has been required to date, we anticipate that the data available for the first stocktake in 2023 will be very heterogeneous. As a continent gathering non-Annex I countries exclusively, the African case is featured by the scarcity of national official inventories which have been provided to date on a voluntary basis through National Communication (NC) and BUR. BU estimates of emissions established by independent scientific methods are also discussed in the present study. In this context, different and complementary observation-based methods assessing national GHG emissions and sinks are needed.

The aim of this paper is to evaluate relative merits of different existing types of datasets for the assessment of African emissions and removals and their trends for CO_2, CH_4 and N_2O during the last three decades. In this paper, we standardize the metrics and scope of application for different categories of GHG emissions to discuss budgets. We also validate and benchmark different independent datasets to evaluate the possibility to use them as a verifying tool for official country-reported data. In order to cover all GHG sectors, we also describe recombinations of different historical datasets for the last 30 years that are necessary to fill the gap for some missing past sectoral emissions. This study offers a comparison of data products originally combined to compute a budget and an evaluation of their relative merits. The different data products discussed here include different ~~bottom-up (~~BU~~)~~ approaches, including official countries communications to the UNFCCC and estimations from the Food and Agriculture Organization (FAO), Carbon Dioxide Information Analysis Center (CDIAC), global inventories for anthropogenic emissions (PRIMAP-hist which integrates combinations of

various datasets including FAO and Global Carbon Project (GCP)), and process-based models for land CO_2 fluxes with 14 Dynamic General Vegetation Models (DGVM) from the TRENDY version 9 ensemble (Table 1). We also analyze and combine TD products to discuss individual gas and to compute budgets: three atmospheric global inversions for CO_2 land fluxes; 22 inversions for CH_4 emissions (11 ~~in situ~~ inversion models using surface station data and 11 satellite inversion models) and CH_4 wildfire emissions from the Global Fires Emission Dataset (GFED) version 4. We used three inversion models for N_2O fluxes (PyVAR model, TOMCAT-INVICAT model, and MIROC4-ACTM model (see Table 1). Inversions only solve for total fluxes or at best for groups of sectors, whereas BU estimates have a larger number of sectors. In Table 2, we present the correspondence between 'sectors' defined by the TD and BU methods. For all datasets, we chose an atmospheric convention with negative values representing removals from the atmosphere (i.e. land sink). We deliver an original comparison of BU estimates from national inventories, global inventories, and process-based models, with TD estimates from atmospheric inversions over Africa. The work is carried out for large countries or groups of small countries, as inversions do not have the capability to constrain fluxes over small areas given their coarse grid and sparse atmospheric data. Based on the benchmarking and relative merits evaluation of the various data products presented above, the scientific questions addressed in this study are: 1) How consistent are the mean values and trends of GHG emissions across ~~bottom up~~ BU estimates in Africa? 2) How consistent are the different inversion model results? 3) How do inversions compare with BU estimates? 4) What is the net GHG balance of the African continent from different observation-based methods, including CO_2 sinks and sources in the land-use sector? 5) What are the main sources of uncertainties?

The manuscript is organized into two main sections. First, a material and methods section describes the regional breakdown and input data (section 1). We present our results for the whole Africa and for six groups of aggregated countries (section 2) with a specific analysis of CO_2 emissions and sinks, divided between FCO_2 (section 2.1), fluxes in the land use, land use change and forestry (LULUCF) sector (section 2.2), and emissions of non-CO_2 greenhouse gasses (sections 2.3 and 2.4). Conclusions are drawn about uncertainties of African GHG net emissions and removals assessment.

1 Methods, ~~and~~ datasets and datasets usage

This study covers the period from 1990 to 2018, and emissions and sinks of CO_2, CH_4 and N_2O. We used 1990 as a base year since reporting to the UNFCCC mostly started in that year and is often used as a reference comparison year in national pledges of the PA. The last year of analysis is 2018,

reflecting the availability of inversion data and avoiding further uncertainty due to poorly understood emissions changes before and after the COVID19 crisis. This period allows the analysis of decadal features. It also has the advantage of being covered by several datasets, listed in Table 1. We considered different ~~bottom up (~~BU~~)~~ approaches, including official countries communications to the UNFCCC and estimations from the Food and Agriculture Organization (FAO), global inventories for anthropogenic emissions (PRIMAP-hist which integrates combinations of various datasets including FAO, GCP, EDGAR v4.3.2, Andrew 2018 cement data, BUR, Common Reporting Format (CRF), UNFCCC data, and BP), and process-based models for land CO_2 fluxes with 14 Dynamic General Vegetation Models (DGVM) from the TRENDY version 9 ensemble (Table 1). We used three atmospheric global inversions for CO_2 land fluxes; 22 inversions for CH_4 emissions; and three inversions for N_2O fluxes (Table 1). For preliminary data quality control, we checked the consistency of prior fluxes by plotting them separately (Fig. S1). Inversions only solve for total fluxes or at best for groups of sectors, whereas BU estimates have a larger number of sectors. In Table 2, we present the correspondence between 'sectors' defined by the TD and BU methods. For all datasets, we chose an atmospheric convention with negative values representing removals from the atmosphere (i.e. land sink). No specific standard guidelines currently exist for defining uncertainties of BU and TD data products. Given that some of our estimates are based on a small number of models / estimates, we cannot calculate the full distribution e.g. with a 95% confidence interval, but we rather reported ranges with min / max. Assuming that the unknown distributions would be Gaussian, like in Schulze et al. (2018), we could infer a 2-sigma (≈ 95%) confidence interval if we assume that min-max are equivalent to 3-sigma, but in view of the small numbers of estimates e.g. for N_2O with only 3 inversions, we prefer to just give the min-max range. Moreover, for national inventories, as all African countries are non-Annex I, they do not deliver confidence intervals but Grassi et al. (2022) estimated for CO_2 LULUCF fluxes uncertainties of 50 % for the average of non-Annex-1 countries. Here uncertainty estimates are understood as the spread among minimum and maximum values from one methodology. A main source of uncertainty in the comparison of country-reported data with other data products is the inclusion or not of natural fluxes additionally to anthropogenic emissions sectors. For the comparability of the different data products presented in this study, we discuss only the mean value over the period of overlapping data availability. Referenced datasets are available at https://doi.org/10.5281/zenodo.7347077 (Mostefaoui et al., 2022).

Table 1. List of BU and TD methods used. (For more details, see also Saunois et al. (2020) for CH_4, Friedlingstein et al. (2020) for FCO_2; UNFCCC country-reported data; Gütschow et al. (2021) for PRIMAP-hist).

Dataset name	Method	CO_2	CH_4	N_2O	Spatial resolution	Time period covered
Inversions						
Global Carbon Budget ensemble (2020) [(1)]	TD	×			from 1° × 1° to 6° × 4°	2000-2019
Global Methane Budget ensemble [(2)] **(2020)**	TD		×		from 1° × 1° to 6° × 4°	2000-2017 [(3)]
Global N_2O Budget ensemble [(4)] **(2020)**	TD			×	from 2.8° × 2.8° to 5.6° × 5.6°	1998-2017
DGVMs						
TRENDYv9 [(5)]	BU				0.5° × 0.5° (land surface) or 1° × 1°	1990-2019
Other BU inventories						
PRIMAP-hist (excluding LULUCF)	BU	×	×	×	country	1990-2019
GCB (CDIAC) (excluding LULUCF)	BU	×			0.1° × 0.1°	1990-2019
UNFCCC	BU	×			country	1990-2015
FAO ($LULUCF\ CO_2$)	BU	×			country	1990-2019
GFEDv4 (wildfires only)	BU		×		0.25° × 0.25°	1997–2016

(1) See 3 inversions details in the supplementary Table S6~~5~~.
(2) See 22 inversions details in the supplementary Table S7~~6~~.
(3) Variations from 2003-2015, 2000-2015, 2010-2017: see detailed period coverage for each dataset in the supplementary Table S7~~6~~.
(4) See 3 inversion details in the supplementary Table S8~~7~~.
(5) See supplementary Table S5 for the14 products.

Table 2. Sectoral reconciliation between categories defined in TD and BU methods.

Gas	Sector label choice for BU and TD	TD inversions	BU inventories
CO_2	Net land flux	Total Net Biome Productivity (NBP) after subtraction of prior prescribed Fossil CO_2	Energy + Industrial Processes and Product Use + Agriculture + Waste + Biomass burning
CH_4	Total anthropogenic emissions	Fossil + Anthropogenic Biomass burning + Agriculture & Waste - Wildfires	Energy + Industrial Processes + Agriculture +Waste + Biomass burning
N_2O	Total	Total	All IPCC sectors

1.1 Regional breakdown

As some countries are small emitters and their area is too small to be resolved by inversions, and in some cases even by DGVMs, we grouped African countries into six regions shown in Fig. S2~~1~~ and listed in Table S2~~1~~. The grouping followed national borders and biomes similarity considering the Köppen-Geiger climate zones (Beck et al., 2018), magnitudes of fossil fuel emissions, and per capita emissions (Fig. S2~~1~~, Fig. S3~~2~~ and Fig. S8~~7~~). We also grouped a maximum of about ten countries per region.

1.2 Inventories datasets

PRIMAP-hist anthropogenic emissions assessment for CO_2, CH_4, and N_2O

The PRIMAP-hist version 2.2 BU dataset is derived from Gütschow et al., (2021) and combines UNFCCC reports with a gap-filling method to produce a time series of annual anthropogenic emissions for different IPCC sectors. PRIMAP-hist does not cover the LULUCF sector for CO_2 due to the high uncertainties. PRIMAP-hist does not include emissions from shipping and international aviation, but includes cement as part of FCO_2 emissions. We use data from the HISTCR scenario (data accessed from https://www.pik-potsdam.de/paris-reality-check/primap-hist/ in April 2022) from country-prioritized dataset, which mainly uses UNFCCC (BUR and NC) data, unless such data are missing, in that case PRIMAP-hist uses extrapolated data from EDGAR (2021), FAO (2021) and BP Statistical Review of World Energy (2021).

Global Carbon Project (GCP) fossil CO_2 emissions

We used country-level FCO_2 data published by the global CO_2 budget by the Global Carbon Project (GCP) (Friedlingstein et al., 2020) separated per fuel type (gas, oil and coal) and including fossil fuel use in the combined industry, ground transportation and power sectors, natural gas flaring, cement production, and process-related emissions (e.g. fertilizers and chemicals). Data for African countries coming among others from the Carbon Dioxide Information Analysis Center (CDIAC) compiled until 2018 (Gilfillan & Marland, 2021), BP Statistical Review of World Energy (BP, 2020), and recent estimates of cement production and clinker-to-cement ratios (Andrew, 2020).

UNFCCC inventories for CO_2 in the LULUCF sector

We used UNFCCC submissions for LULUCF CO_2 fluxes from NC and BUR reports downloaded from the UNFCCC website (https://unfccc.int/) in March 2021, and further processed into .csv tables by Deng et al., (2021). Those estimates are based on different accounting methods following the IPCC Guidelines (IPCC, 2006; IPCC, 2019). Country-reported data quality control, quality assurance and verification process follow 2006 IPCC guidelines detailed in Chapter 6 QA/QC procedures of this document. African countries, being Non-Annex I countries, do not report emissions every year. Figure 1 shows the number of BUR and NC provided each year per African region. The years 1990, 1994, 1995, 2000 and 2005 are featured with several updates, while most of the other years have few updates. About every two years, all regions have at least one update. Note that flexibility for BUR is given to Least Developed Countries (LDCs), that include 33 out of 56 African countries, and to Small Islands Developing States (SIDS), that include six African countries (Table S4~~3~~).

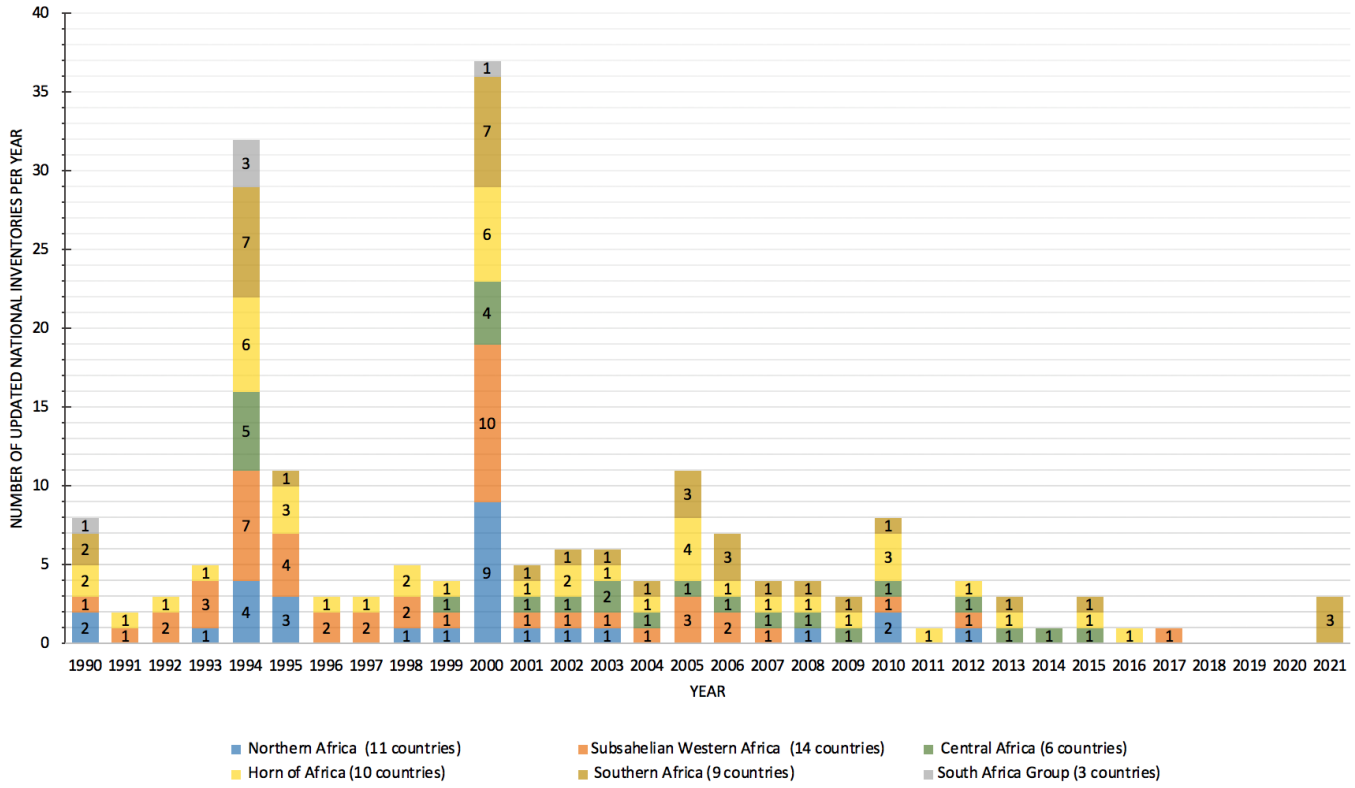

Figure 1. Number of UNFCCC reports for LULUCF CO_2 fluxes in National Communications and Biennial Update Reports, per group of countries defined in Table S2~~1~~.

Non-Annex I African countries can use older versions of the IPCC guidelines (IPCC, 2006; IPCC, 2019a). This induces uncertainties from changes in accounting methods between versions, with recent guidelines having more detailed sectors and sources. There is no data for Libya, Equatorial Guinea, Malawi and Sierra Leone during the whole period. UNFCCC data are missing in some years for Rwanda, Sao Tome & Principe, Senegal, South Sudan, Angola. There is no data during 1990-1998 for Liberia.

We noticed that NC and BUR lack details regarding the methods used, the sources for activity data and emissions factors, and most of them are in French language. BUR in .pdf format include a non-standardized table for emissions. The reader is sometimes referred to the "national coordinator for climate change service" with no link to any database or contact person.

Because the PA targets human-induced emissions, countries use the proxy of "Managed lands" for the LULUCF sector, as defined by the IPCC guidelines (https://www.ipcc-nggip.iges.or.jp/public/2006gl/vol4.html; last accessed in August 2022). Managed lands are areas where LULUCF CO_2 fluxes are assigned to some anthropogenic activities. Several African NC and BUR do not contain information on their managed lands areas. We thus looked at REDD+ national reports (https://redd.unfccc.int/submissions.html?topic=6; last accessed in August 2022) to get this information

(Fig. S32 and Table S98). LULUCF CO_2 fluxes on managed lands result from either direct anthropogenic effect such as land use change and forestry, or indirect effects (such as change in CO_2 and climate) on land remaining in the same land use, e.g. forest remaining forest (Grassi et al., 2022). The vast majority of African countries use a Tier 1 IPCC accounting method which does not distinguish between these different effects. Tier 1 methods use a classification with only three out of six possible types of land: "forest land", "cropland" and "grassland", and do not give spatially explicit land use data. Tier 2 methods include fluxes from six land use types: forest, cropland and grassland, wetlands, urban and other land-use, for the case of land remaining under the same land use type, and for the case of conversions between land use types. In Africa, only South Africa and Zambia used Tier 2 methods for some LULUCF CO_2 subsectors.

Processing of the UNFCCC LULUCF CO_2 data and outliers correction

We processed the UNFCCC LULUCF CO_2 data for outlier corrections (Table S54). For Guinea-Bissau, and Tanzania, we identified inconsistent values from successive communications with substantially differing numbers. For Guinea, Madagascar, Zimbabwe, Congo, Mali, the Central African Republic (CAF), Angola and Mauritius we identified changes of more than one order of magnitude between two consecutive reports and likely implausibly large carbon sinks considering their national forest area. The computations of per area emissions and removals showed discrepancies, which points out the need for further examination and inspection of more recent reports in NDC and REDD+ reports (Table S54). Our corrections explained in the supplementary section are consistent with those proposed by Grassi et al. (2022) who diagnosed 'biophysically impossible' sequestration rates with a threshold value larger than 10 $tCO_2/ha\ yr^{-1}$ over an area greater than 1 Mha. For Namibia, Nigeria and the Democratic Republic of the Congo (DRC), it was challenging to select a best estimate between recent and past reports. For those countries, corrections using more recent data than BUR/NC have high uncertainties, as noted by Grassi et al. (2022). This includes the absence of any sink for DRC for instance, contrary to sinks consistently reported over time and large forested area in this country's previous reports to the UNFCCC. We therefore systematically looked at corrected values for both case scenarios (with and without Namibia, Nigeria and DRC data corrections). In total, we corrected 13 outliers as shown in Table S54, consistently with Grassi et al. (2022).

Food and Agriculture Organization of the United Nations (FAO) LULUCF CO_2 fluxes

We used data from LULUCF CO_2 fluxes over 1990-2019 from the FAO Global Forests Resource Assessments (FAO FRA; data License: CC BY-NC-SA 3.0 IGO, extracted from: https://fra-data.fao.org; date of Access: May 2022). According to the 2005 FAO categories and definitions, forest is land covering at least 0.5 hectares and having vegetation taller than 5 meters with a canopy cover higher than 10%. Other

wooded lands refer to land that are not classified as "forest" but that are wider than 0.5 ha, have a canopy cover of 5%-10% or combine trees, shrubs and bushes with cover higher than 10%. The FAO data for forests comprise carbon stock changes from both aboveground and belowground living biomass pools. They are independent from country-reported UNFCCC emissions and removals. The FAO estimates are based on activity data, areas of forest land and CO_2 emissions and removals factors. The FAO data reports: 1) net emissions and removals from "forest land remaining forest land" and from "land converted to forest" grouped together, and 2) emissions from "net forest conversion", i.e. deforestation. In contrast, the UNFCCC accounting uses a 20-years window for CO_2 fluxes from land use change, while land-use change fluxes from land-converted-to-forest are reported separately from those of 'forest remaining forest'.

1.3 Dynamic Global Vegetation Models (DGVM) datasets

We used Net Biome Productivity (NBP) from 14 Dynamic Global Vegetation Models (DGVM) from the TRENDY v9 ensemble covering the period 1990-2019. The different models described in Friedlingstein et al. (2019) are: CABLE, CLASS, CLM5, DLEM, ISAM, JSBACH, JULES, LPJ, LPX, OCN, ORCHIDEE-CNP, ORCHIDEE-SDGVM, and SURFEX (Table S6~~5~~). DGVM are forced by historical reconstructions of land cover change, atmospheric CO_2 concentration and climate since 1901. Detailed cropland management practices are generally ignored, except for the harvest of crop biomass. Forest harvest is prescribed from historical statistics in 11 models (Table A1, of Friedlingstein et al., (2020)). The models simulate carbon stock changes in biomass, litter and soil pools. From the difference between simulations with and without historical land cover change, a flux called 'land use emissions' can be obtained from DGVM. This flux includes the indirect effects of climate and CO_2 on lands affected by land use change, and a foregone sink called "loss or gain of atmospheric sink capacity", which is absent from the methods used by UNFCCC and FAO. Pongratz et al. (2014) delivered the following definition of loss of sink capacity as "the CO_2 fluxes in response to environmental changes on managed land as compared to potential natural vegetation. Historically, the potential natural vegetation would have provided a foregone sink as compared to human land use." Thus, land use change fluxes from DGVM were not compared with other estimates. Note that DGVM do not explicitly separate managed and unmanaged land. Thus, we used all forest lands to calculate their mean CO_2 fluxes.

1.4 Atmospheric inversions datasets

CO_2 inversions

We used the net land CO_2 fluxes excluding fossil fuel emissions (hereafter, net ecosystem exchange) from three global inversions of the Global Carbon Project that cover a long period (see Table A4 of Friedlingstein et al., 2020), including : CarbonTrackerEurope (CTRACKER-EU-v2019; van der Laan-Luijkx et al., 2017), the Copernicus Atmosphere Monitoring Service (CAMSV18-2-2019; Chevallier et al., 2005), and one variant of Jena CarboScope (JENA, sEXTocNEET_v2020; Rödenbeck et al., 2005). The GCP inversion protocol recommends to use as a fixed prior the same gridded dataset of FCO_2 emissions (GCP-GridFED). However, some modelers used different interpolations of this dataset, and one group used a different gridded dataset (Ciais et al., 2021). We applied a correction to the estimated total CO_2 flux by subtracting a common FCO_2 flux from each inversion (Figure S1~~8~~ and Methodological Supplementary 1 ~~2~~). The resulting land atmosphere CO_2 fluxes, or net ecosystem exchange, cannot be directly compared with inventories aiming to assess C stock changes, given the existence of land-atmosphere CO_2 fluxes caused by lateral processes. This issue was discussed by Ciais et al. (2021) and a practical correction of inversions was proposed by Deng et al. (2022) based on new datasets for CO_2 fluxes induced by lateral processes involving river transport, crop and wood product trade. We applied here the same correction to all CO_2 inversions.

CH_4 inversions

We used the CH_4 emissions from global inversions over 2000-2017 from the Global Methane Budget (Saunois et al., 2020) (Table 1). This ensemble includes 11 models using GOSAT satellite CH_4 total-column observations covering 2010-2017, and 11 models assimilating surface stations data (SURF) since 2000 (Table S5~~4~~). Surface inversions are constrained by very few stations for Africa, while the GOSAT satellite data has a better coverage. One could thus expect GOSAT inversions to give more robust results. Inversions deliver an estimate of surface net CH_4 emissions, although some of them solve for fluxes in groups of sectors, called 'super-sectors'. We have not used in situ for dataset validation per se, only the GOSAT data were evaluated against Total Carbon Column Observing Network (TCCON) independent ground based total column-averaged abundance of CH_4 (XCH_4). In the inversion dataset, net CH_4 surface emissions were interpolated into a $0.8° \times 0.8°$ resolution, regridded from coarser resolution fluxes and separated into 'super-sectors' either using prior emission maps or posterior estimates for those inversions solving fluxes per supersector, following Saunois et al. (2020). More specifically, these five super-sectors are: 1) Fossil Fuel, 2) Agriculture and Waste, 3) Wetlands, 4) Biomass and Biofuel Burning (BBUR), and 5) Other natural emissions. We separated CH_4 anthropogenic emissions from inversions using Method 1 and Method 2 proposed by Deng et al. (2021). Method 1 relies on the separation calculated by each inversion except for the BBUR supersector from which wildfire emissions were subtracted based on the Global Fires Emission Dataset (GFED) version 4 (van der Werf et al., 2017). Method 2 removes from total emissions the median

of natural emissions from inversions (Deng et al. 2022). The two methods gave similar results and only Method 1 was used in the results section.

N_2O inversions

We used three N_2O atmospheric inversions from the global N_2O budget synthesis (Tian, 2020) and from Deng et al. (2022) (~~-~~Tables S1~~,~~ and S7) : PyVAR CAMS (Thomson et al., 2014), MATCM_JMASTEC (Rodgers, 2000), (Patra et al., 2018), and TOMCAT (Wilson et al., 2014; Monks et al., 2017). We used the total N_2O flux from inversions including natural emissions, given that natural emissions estimates are highly uncertain for Africa. Inversion results are therefore not directly comparable with the PRIMAP-hist inventory which only contains anthropogenic emissions.

1.5 Metrics to compare gasses and ancillary data and data usage

We express emissions of non-CO_2 gasses in megatons of carbon dioxide equivalent ($MtCO_2e$) using the Global Warming Potential over a 100-year time horizon (GWP100) values from the fourth IPCC Assessment Reports (IPCC AR4, WGI Chapter 2, 2007), consistent with PRIMAP-hist and historical country-reported data. We used AR4 GWP100 because many African countries have been following the 2006 IPCC guidelines referring to AR4 GWP100 2019 refinement to IPCC guidelines, which do not recommend any specific metrics, therefore we are following IPCC guidelines used by countries. The multiplicative coefficients to use to change AR4 to AR6 GWP100 values are: 1.19 for fossil CH_4, 1.09 for non-fossil CH_4, and 0.92 for N_2O. We used population data from the United Nations population (World Population Prospects 2019, 2022), for computing per capita FCO_2 emissions and their disparities, based on Gini indices (Dortman et al., 1979) for measuring statistical dispersions among a given population (methodological supplementary M2~~1~~). We also used African GDP data (World Bank, 2017).

2 Results and discussion

2.1 Fossil CO_2 emissions

2.1.1 Continental, regional and country changes

411 **(a)**

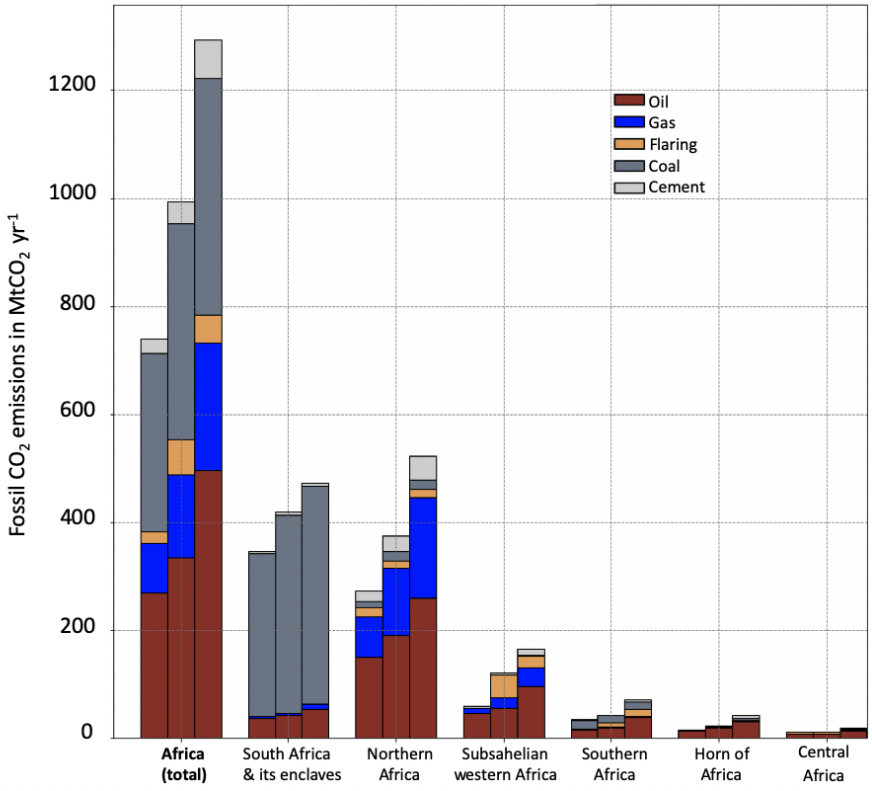

412

413 **(b)**

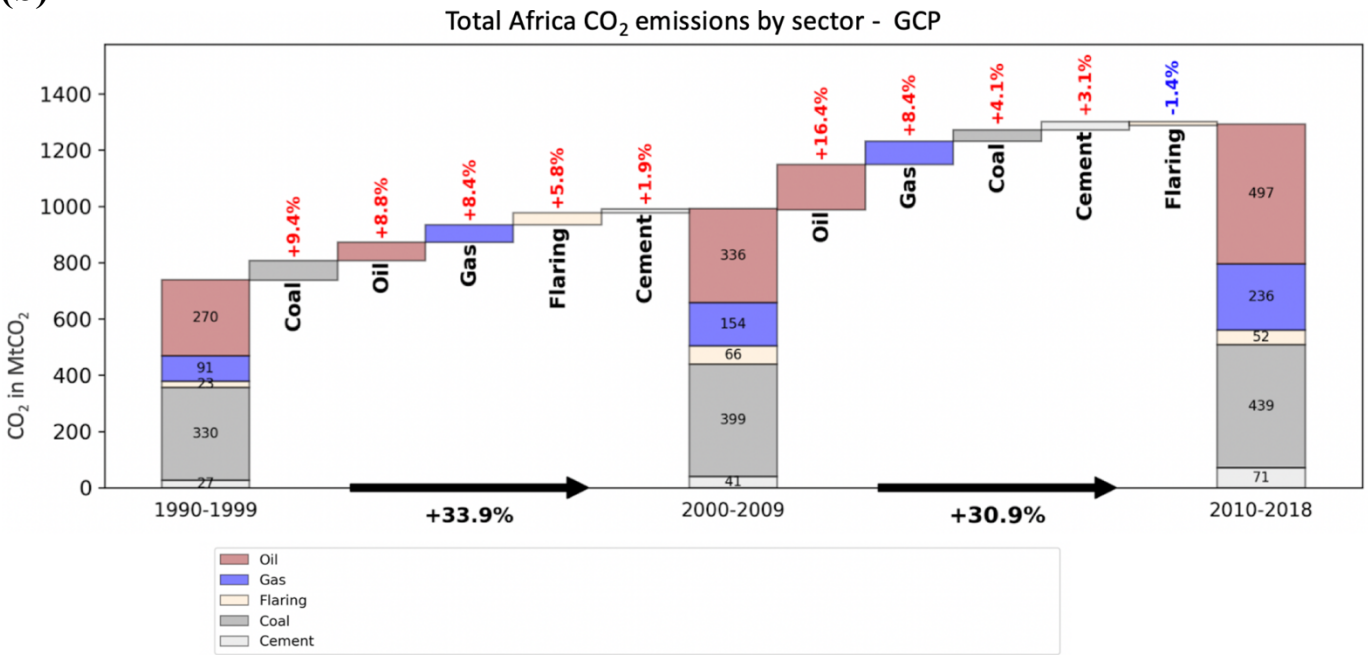

414

415

416

417

(c)

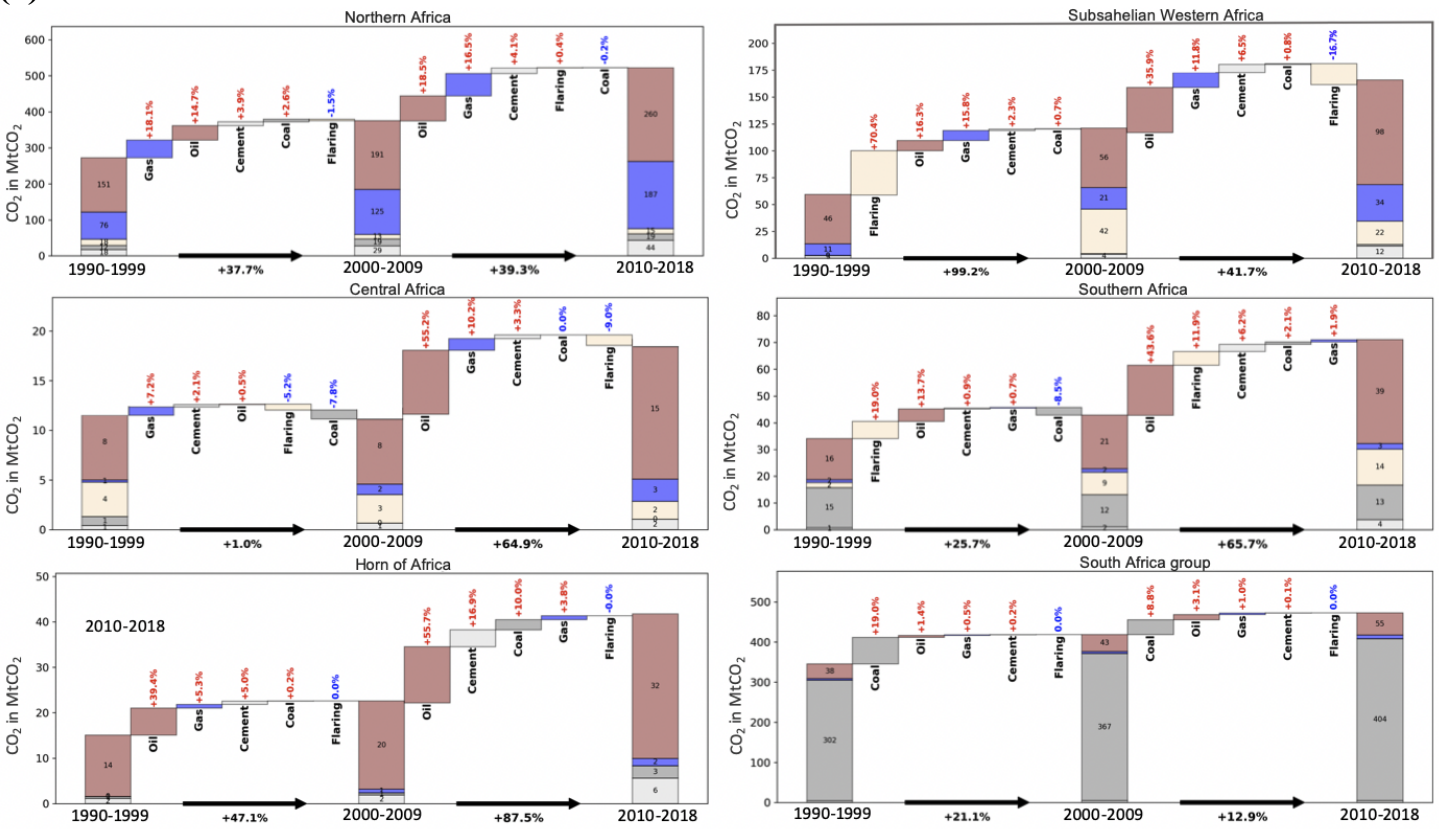
Northern Africa
Subsahelian Western Africa
Central Africa
Southern Africa
Horn of Africa
South Africa group
CO2 in MtCO2
1990-1999
2000-2009
2010-2018
+37.7%
+39.3%
+99.2%
+41.7%
+1.0%
+64.9%
+25.7%
+65.7%
+47.1%
+87.5%
+21.1%
+12.9%

Figure 2. (a) African fossil fuel CO_2 emissions per fuel type and for cement per region over 1990-1999, 2000-2009 and 2010-2018. (b) Contribution of each fuel type to the change of African emissions. (c) Same for different regions regrouping several countries. Data from GCP (2019).

a) FCO_2 total anthropogenic emissions mean 1999-2008 in Mt yr^{-1} (GCP).

b) Differences expressions in percentage between FCO_2 total anthropogenic mean emissions 2009-2018 and mean 1999-2008 divided by average value for both decades (GCP).

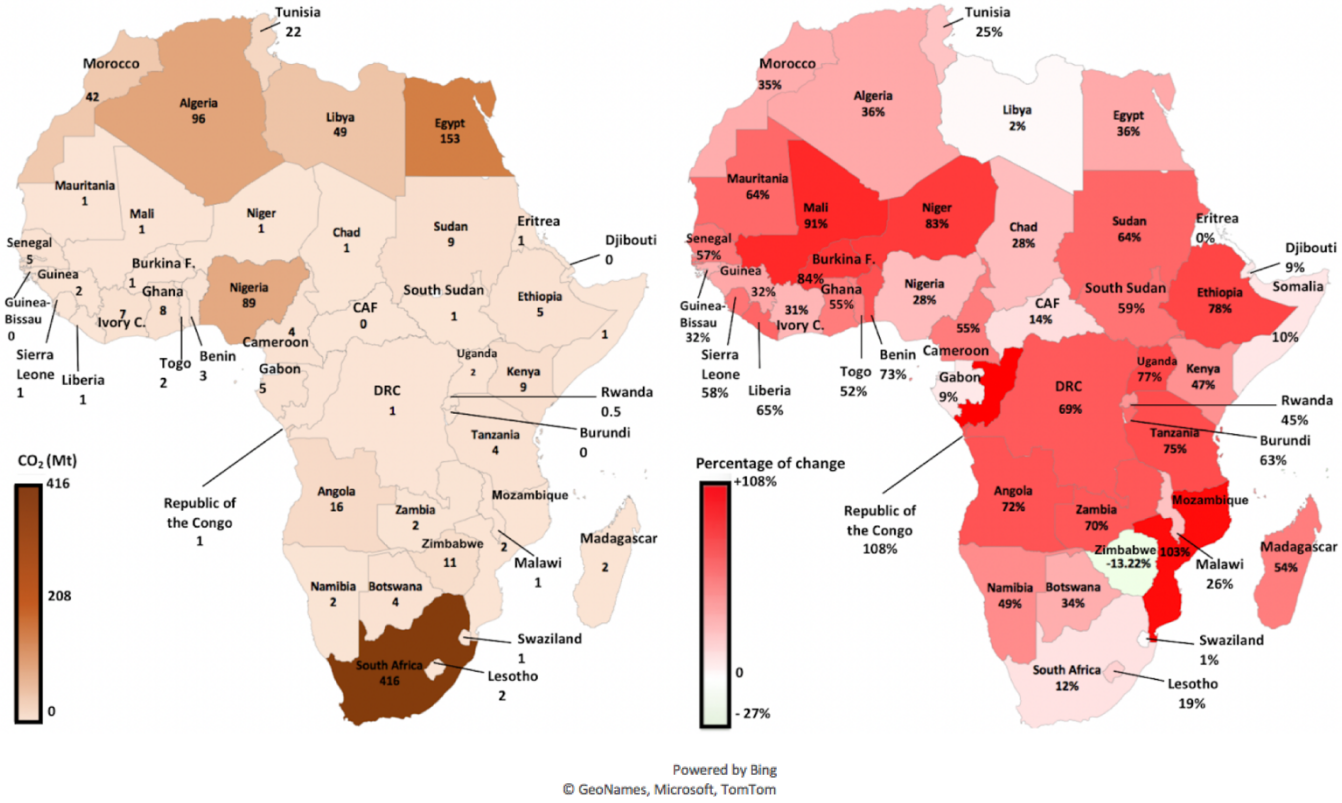

c) CH_4 total anthropogenic emissions mean 1999-2008 in $MtCO_2e\ yr^{-1}$ (PRIMAP-hist).

d) Differences between CH_4 total anthropogenic mean emissions 2009-2018 and mean 1999-2008 in $MtCO_2e\ yr^{-1}$ (PRIMAP-hist).

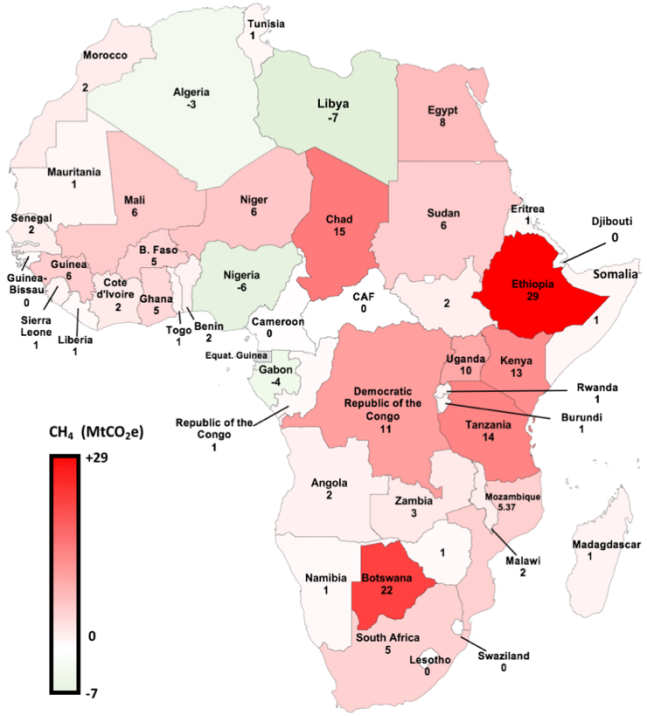

Powered by Bing
© GeoNames, Microsoft, TomTom

e) N_2O total anthropogenic emissions mean 1999-2008 in $MtCO_2e\ yr^{-1}$ (PRIMAP-hist).

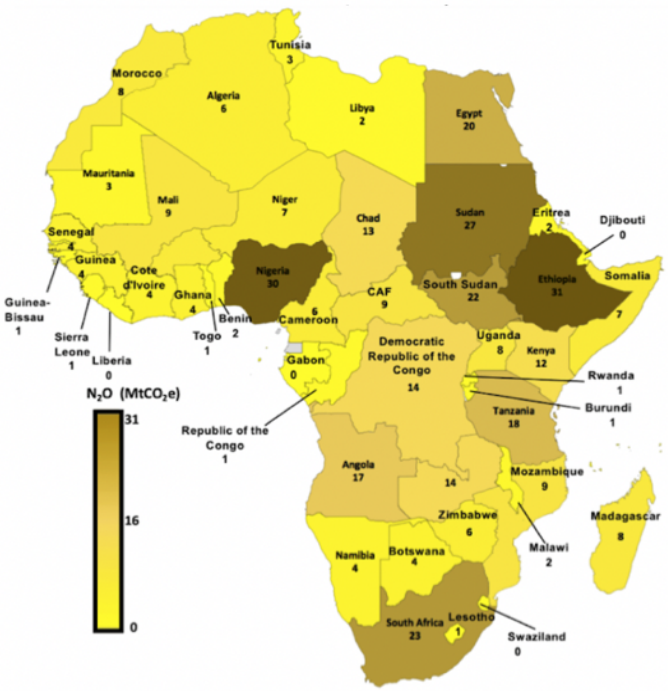

f) Differences between N_2O total anthropogenic mean emissions 2009-2018 and mean 1999-2008 in $MtCO_2e\ yr^{-1}$ (PRIMAP-hist).

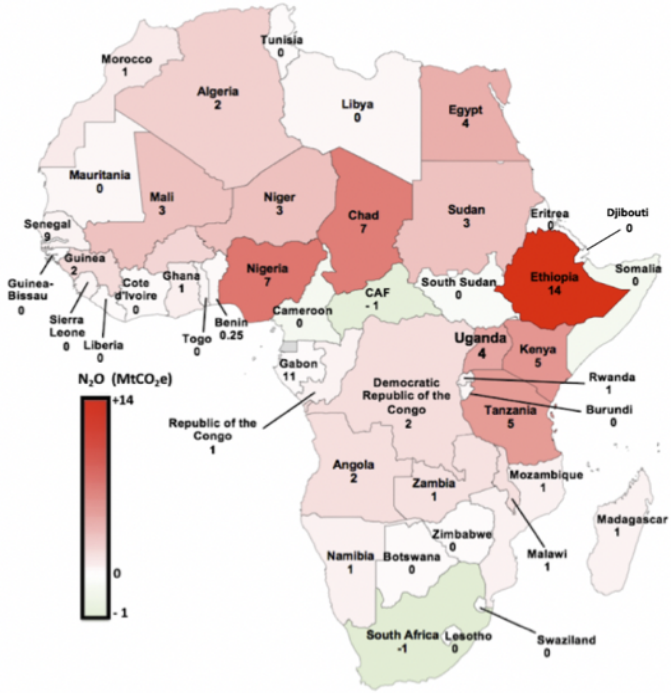

Powered by Bing
© GeoNames, Microsoft, TomTom

Figure 3 (a). Maps of average fossil fuel CO_2 emissions for African countries during 1999-2008 in $MtCO_2e\ yr^{-1}$ and (b) change from 1999-2008 to 2009-2018 using data from GCP in $MtCO_2e\ yr^{-1}$ (Friedlingstein et al., 2019); (c-d) same but with anthropogenic CH_4 emissions from PRIMAP-hist in $MtCO_2e\ yr^{-1}$; (e-f) same for anthropogenic N_2O emissions from PRIMAP-hist in $MtCO_2e\ yr^{-1}$.

PRIMAP-hist and GCP

First, we compared GCP and PRIMAP-hist fossil CO_2 emissions. We found that most of the relative differences between these two datasets at country level considerably decreased with time, except for Mali. Those differences are less than 5% for most of the main African emitters during the last decade, except for South Africa where the difference is a bit larger than 10% (see maps in Fig. S8~~7~~). The largest relative difference between the two datasets comes from Mali in the decade 2009-2018, with FCO_2 emissions of 3 $MtCO_2\ yr^{-1}$ in GCP, compared to 1 $MtCO_2\ yr^{-1}$ in PRIMAP-hist. Given the relatively small differences, we chose to use only GCP for trends between decades, but when computing net budgets for the three main GHG, we show differences between the use of those two estimates.

The changes of African FCO_2 emissions per fuel type and for cement using the GCP data are shown in Fig. 2 (a). In Fig.2 (b), we show absolute values and relative contributions to the total change in each decade. During 2010-2018, total African FCO_2 emissions from oil (497 $MtCO_2\ yr^{-1}$) and coal (439 $MtCO_2\ yr^{-1}$) were roughly similar. While global FCO_2 emissions increased by +13 % over this period (Friedlingstein et al., 2019), African FCO_2 almost doubled in 2018 compared to 1990 levels, a relative increase comparable with that of China over the same period. From 1990-1999 to 2000-2009, the mean emissions increased by 33.9% from 741 $MtCO_2\ yr^{-1}$ to 996 $MtCO_2\ yr^{-1}$. All FCO_2 sectors contributed to this decadal increase. The contribution from coal (+9.4 %) was slightly larger but comparable to that from oil (+9 %) and gas (+8 %). From 2000-2009 to 2010-2018, emissions further increased by 31% from 996 $MtCO_2\ yr^{-1}$ to 1295 $MtCO_2\ yr^{-1}$. The oil and the gas fuels contributed the most to this increase with +16 % for oil, and +8 % for gas. Coal emissions increased by only +4.1 % and coal went from being the first source of African FCO_2 emissions over 2000-2009 to the second one over 2010-2018.

As for regional contributions to emissions changes between 1990-1999 and 2000-2009 shown in Fig. 2 (b) the main contribution to the total increase came from the region of South Africa where emissions increased from 302 $MtCO_2\ yr^{-1}$ to 367 $MtCO_2\ yr^{-1}$ (+21.1 %, coal being the largest contributor). The second largest contribution to the increase is from North Africa where oil was the largest contributor (emissions increased from 151 $MtCO_2\ yr^{-1}$ to 191 $MtCO_2\ yr^{-1}$; +15 %), and gas (+18%). The least increasing region was Central Africa. North Africa

experienced the largest increase from 1990-1999 to 2000-2009, and from 2000-2009 to 2010-2018 with successive increases of +38 % and +39 %, largely dominated by oil and gas (Fig. 4 (b)). As a result, during the period 2010-2018, Northern African countries were the dominant emitters with 545 $MtCO_2$ yr^{-1}. The group of South Africa (including Lesotho and Botswana) was the second biggest emitter region over 2010-2018, mainly due to coal emissions from the Republic of South Africa. The two least contributing African regions were the Horn of Africa and Central Africa.

At the country level, Figure 3a-b shows mean FCO_2 emissions and relative changes over the last two decades. The main emitters do not have the biggest relative changes. The four main emitters over 2000-2009 were South Africa (416 $MtCO_2$ yr^{-1}), Egypt (153 $MtCO_2$ yr^{-1}), Algeria (96 $MtCO_2$ yr^{-1}) and Nigeria (89 $MtCO_2$ yr^{-1}). Those four countries altogether represented 67% of the continental total emissions over 2000-2009 (987 $MtCO_2$ yr^{-1}). The largest relative increases from 2000-2009 to 2010-2018 are from Congo (+108 %), Mozambique (+103 %) and Mali (91%), compared to relative increases in the main emitters, the Republic of South Africa (+21 %), Egypt (+36%) and Algeria (+36%).

2.1.2 Variations of per capita and per GDP fossil fuel CO_2 emissions

Per capita emissions

Using ancillary data on population (Fig. S3~~2~~ and Fig. S3~~4~~) we computed the mean African per capita emissions of 1 tCO_2/cap yr^{-1} for 2009-2018 ~~(Fig. S2 and S3)~~, which is 5 times larger than during 1990-1998 (0.2 tC/cap yr^{-1}), and yet 5 times smaller than the global average (5 tCO_2/cap yr^{-1}). From 1999-2008 to 2009-2018, African per capita emissions increased by 30 %. African per capita FCO_2 emissions during 2009-2018 were 17 times less than in the USA (17 tCO_2/cap yr^{-1}), 7 times less than in China (7 tCO_2/cap yr^{-1}), 7 times less than in EU27+UK (7 tCO_2/cap yr^{-1}), and 2 time less than India (2 tCO_2/cap yr^{-1}). At the country level, the biggest per capita emissions over 2009-2018 were from the Republic of South Africa with 9 tCO_2/cap yr^{-1}, which ranks 14th worldwide, above China and just below Poland. The second biggest per capita emissions were from Libya (8 tCO_2/cap yr^{-1}). The smallest ones were from the DRC (0.1 tCO_2/cap yr^{-1}). For the first period 1990-1998, per capita emissions of African region ranked in this order: South Africa group (4 tCO_2/cap yr^{-1}) > Northern Africa (2 tCO_2/cap yr^{-1}) > Central African countries (1 tCO_2/cap yr^{-1}) > Southern countries (0.8 tCO_2/cap yr^{-1}) > Horn of Africa (0.5 tCO_2/cap yr^{-1}) > Sub-Sahelian Western Africa (0.3 tCO_2/cap yr^{-1}). For the second period 2009-2018, they ranked in this order: South Africa group (4 tCO_2/cap yr^{-1}) > Northern Africa (2 tCO_2/cap yr^{-1}) > Southern countries (1 tCO_2/cap yr^{-1}) and Horn of Africa (1 tCO_2/cap yr^{-1}) > Central Africa countries (1 tCO_2/cap yr^{-1}) > Sub-Sahelian Western Africa (0.4 tCO_2/cap yr^{-1}). At country scale during the first period of

1990-1998, the four African largest per capita emissions ranked in this order: Libya (9 tCO_2/cap yr^{-1} > the Republic of South Africa (9 tCO_2/cap yr^{-1}) > Gabon (5 tCO_2/cap yr^{-1}) > Algeria (3 tCO_2/cap yr^{-1}). The four African countries with the smallest per capita emissions ranked as following: Burundi (0.04 tCO_2/cap yr^{-1}) < Uganda, Ethiopia and Mali (0.1 tCO_2/cap yr^{-1}).

We also computed the GINI index for African per capita FCO_2 emissions for each of the last three decades, using data from (Friedlingstein et al., 2020) (see Methodological Supplementary M2). These GINI values were 0.7 for 1990-1998, 0.7 for 1999-2008, and 0.7 for 2009-2018, thus very stable over the last 30 years and close to 1, indicating high inequities among countries.

Emissions per GDP

Per exchange rate vs. per Purchasing Power Parities (PPP) GDP

According to the International Monetary Fund (IMF), the Gross Domestic Product (GDP) delivers an estimate "of the monetary value of goods and services produced in a country over a chosen period." GDP data from the World Bank (2015) is available for 30 African countries only (Fig. S54). The four countries with the biggest per $US exchange rate GDP (Fig. S65) are: Nigeria ($490 B) > South Africa ($350B) > Egypt ($330B) and Algeria ($330B) > Angola ($120B). The four countries with the smallest GDP in 2015 are: Gambia ($1.4B) and Seychelles ($1.4B) > Guinea-Bissau ($1B) > Comoros ($970 M). Emissions per $US GDP are shown in Fig. S65 The Purchasing Power Parities (PPP) calculated by the International Comparison Program (ICP) of the World Bank is a refined measure of what a given national currency can acquire in terms of goods or services in another country, removing the impact of currency exchange rates. Emissions per PPP$ GDP are shown in Fig. S76.

The mean of African emissions per unit PPP$ GDP in 2016 was 0.6 $kgCO_2$/PPP$ yr^{-1}, which is more than twice the global value, 3 times the mean value of the USA (0.2 $kgCO_2$/PPP$ yr^{-1}), and Europe (0.2 $kgCO_2$/PPP$ yr^{-1}). This points to a more carbon intensive economic growth in Africa than in developed countries, which may be an important barrier for future mitigation strategies as the GDP of Africa has grown by 112% in the last 30 years, and is projected to increase in the future by 3% per year (World Bank, 2022). At regional level, the largest values were: South Africa (0.4 $kgCO_2$/PPP$ yr^{-1}) > North Africa, Southern Countries and Sahelian Western Africa (0.2 $kgCO_2$/PPP$ yr^{-1}) > Central Africa and the Horn of Africa (0.1 $kgCO_2$/PPP$ of GDP). At country scale, the largest emitters per unit of GDP were Libya (0.7 $kgCO_2$/PPP$ yr^{-1}) and South Africa (0.7 $kgCO_2$/PPP$ yr^{-1}) > Lesotho (0.4 $kgCO_2$/PPP$ yr^{-1}) > Algeria (0.3 $kgCO_2$/PPP$ yr^{-1}) (Fig. S76.) The smallest emitters were: DRC (0.03 $kgCO_2$/PPP$ yr^{-1}) < Chad (0.04 $kgCO_2$/PPP$ yr^{-1}) < Burundi (0.06 $kgCO_2$/PPP$ yr^{-1}) < Uganda (0.07 $kgCO_2$/PPP$ yr^{-1}).

We also used GDP per unit exchange rate from the International Energy Agency (IEA, 2019). The mean African emissions per unit of $GDP_{exch.rate}$ was 0.5 $kgCO_2$ $/$ yr^{-1}, larger than elsewhere, except in Asia (0.6 $kgCO_2$/ $GDP_{exch.rate}$ yr^{-1}. As shown in Fig. S~~6~~5, over 2013-2017 the six biggest emitters were South Africa (0.7 $kgCO_2$/ $GDP_{exch.rate}$ yr^{-1}) > Libya (0.5 $kgCO_2$/ $GDP_{exch.rate}$ yr^{-1}) > South Sudan (0.4 $kgCO_2$/ $GDP_{exch.rate}$ yr^{-1}) > Zimbabwe, Benin and Algeria (0.3 $kgCO_2$/ $GDP_{exch.rate}$ yr^{-1}). The correlation coefficient between $GDP_{exch.rate}$ and FCO_2 emissions per $GDP_{exch.rate}$ was 0.3, suggesting that the countries with a high GDP do not always emit more CO_2 per unit GDP. For instance, South Africa ranked first with 0.7 $kgCO_2$/ $GDP_{exch.rate}$ yr^{-1} and second for GDP (350 $Billion); Nigeria ranked first for GDP (490 $Billion), but 21st for emissions per GDP (0.1 $kgCO_2$/ $GDP_{exch.rate}$ yr^{-1}). This may be related to the fact that countries with a high GDP are also more likely to create growth through sustainable activities.

2.2 LULUCF CO_2 fluxes

Outlier corrections

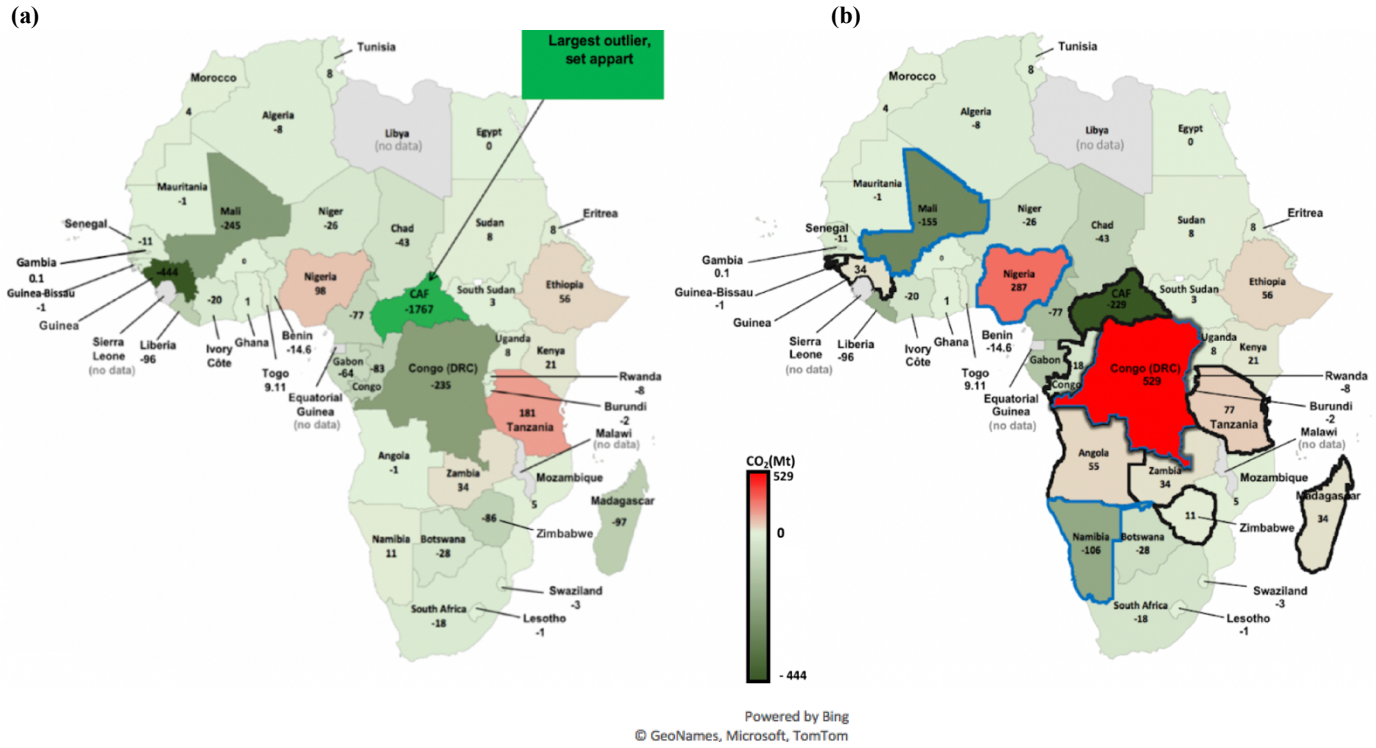

(c)

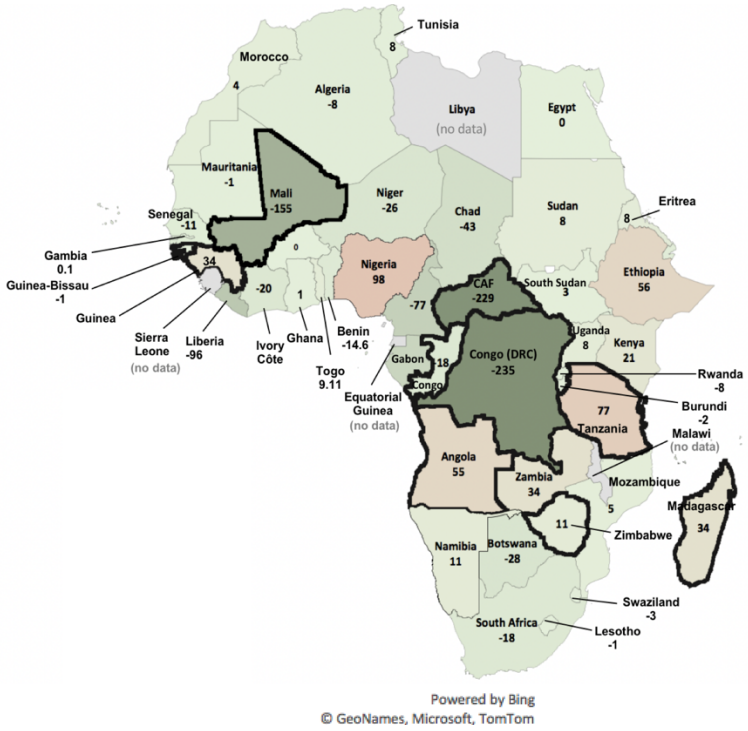

Figure 4. Map of national LULUCF CO_2 fluxes for 2001-2018 in $MtCO_2\ yr^{-1}$. (a) Before outliers' removals. (b) After outliers' removal according to Grassi et al. (2022). (c) After outlier removals (DRC, Namibia and Nigeria) from this study. Positive values represent a net C loss by ecosystems.

In this section, we analyze CO_2 fluxes from the LULUCF sector, based on UNFCCC data (section 1.1) which include forest lands, grasslands, croplands, and all possible conversions between them (IPCC, 2003; 2006). As shown in section 1.2 and Table S4, we found that some countries' reports are outliers with biophysically implausible CO_2 sinks and/or sudden unexplained very large changes between successive reports. Due to scarce data over 1990-1998 we focus on the period 2001-2018. In the following paragraph, we discuss four approaches to include UNFCCC data:

a) Uncorrected data, b) corrections following Grassi et al. (2022) for all countries, c) corrections following Grassi et al. (2022) except DRC, Namibia and Nigeria, d) Corrections following Grassi et al. (2022) except for DRC.

Figure 4 (a) shows UNFCCC data without correcting for outliers, based on BUR and NC data accessed in May 2022. The majority of countries are sinks, or small sources, except Tanzania and Nigeria being large sources. Very large (implausible) sinks are seen in Guinea and CAF. The continent is a CO_2 sink of -3309 $MtCO_2\ yr^{-1}$ during the period 2001-2018.

Figure 4 (b) shows the corrected fluxes according to Grassi et al. (2022) who excluded implausible large sink rates and used NDC and REDD+ reports instead of NC data for DRC, Congo, CAF, Guinea, Madagascar and the most recent BUR, NC and inventory data for Namibia, Angola, Zimbabwe and Nigeria (see their Table 7). Africa as a whole is a CO_2 source of 265 $MtCO_2\ yr^{-1}$. At regional scale, the mean CO_2 sources distributes as follows on four regions: Sub-Sahelian West Africa (235 $MtCO_2\ yr^{-1}$) > Horn of Africa (153 $MtCO_2\ yr^{-1}$) > Central Africa (144 $MtCO_2\ yr^{-1}$) > Southern Africa (14 $MtCO_2\ yr^{-1}$). The two sink regions are North Africa (-259 $MtCO_2\ yr^{-1}$) and South Africa (-23 $MtCO_2\ yr^{-1}$). At country scale, after the corrections of Grassi et al. (2022), the four countries with the larger sinks are: CAF (-229 $MtCO_2\ yr^{-1}$) > Mali (-155 $MtCO_2\ yr^{-1}$) > Namibia (-106 $MtCO_2\ yr^{-1}$) > Cameroon (-77 $MtCO_2\ yr^{-1}$). The four countries with largest sources are DRC (529 $MtCO_2\ yr^{-1}$) > Nigeria (287 $MtCO_2\ yr^{-1}$) > Tanzania (77 $MtCO_2\ yr^{-1}$) > Ethiopia (56 $MtCO_2\ yr^{-1}$). A main issue with the correction from Grassi is that it reports no sink in DRC which has an important forest coverage representing 68% of the country area (FAO, 2015) and for which a sink was consistently reported in previous NCs.

Figure 4 (c) shows LULUCF CO_2 in African countries that are consistent with Grassi et al. (2022) except for three countries: Namibia (we used 2000 NC3 instead of NIR2019), Nigeria (we used 2014 NC2 instead of 2017 BUR2) and DRC (we used 2015 NC3 instead of 2021 NDC). In that approach Africa becomes a net CO_2 sink of -589 Mt yr^{-1} over 2001-2018. At regional scale, the region of Central Africa (-620 $MtCO_2$) remains the main sink. But the values and ranking of the top sources rank as: Horn of Africa (153 $MtCO_2$) > Southern Africa (141 $MtCO_2$) > Sub-Sahelian West Africa (19$MtCO_2$). At country scale with this correction choice, the top sinks are: DRC (-235 $MtCO_2$) > CAF (-229 $MtCO_2$) > Mali (-155 $MtCO_2$); and the three top sources: Nigeria (98 $MtCO_2$) > Tanzania (77 $MtCO_2$) > Ethiopia (56 $MtCO_2$).

In the fourth approach where we use the corrections of Grassi et al. (2022) except for DRC where we kept the latest national communication instead of the most recent NDC, the continent is a net sink of -504 $MtCO_2\ yr^{-1}$ over 2001-2018. At regional scale, Central Africa is a large CO_2 sink, and the ranking of sink regions is: Central African group (-620 $MtCO_2\ yr^{-1}$) > North Africa (-259 $MtCO_2\ yr^{-1}$) > South Africa (-23 $MtCO_2\ yr^{-1}$). The ranking of the source regions stays unchanged. At the country scale, the main sink is DRC (-235 $MtCO_2\ yr^{-1}$). In the paper, we will mainly use data corrected following Grassi et al. (2022), but we want to raise a caution flag that adopting their correction for DRC had an enormous effect on the CO_2 budget of the continent, which becomes a source. Using the original latest national communication of DRC instead of the NDC used by Grassi et al., and our own corrections for Namibia and Nigeria instead of those of Grassi et al. increased the continental CO_2 uptake.

Comparison of UNFCCC managed land area and FAO forest and other wooded lands areas

Figure S10 shows a comparison of land areas reported in NC, BUR and REDD+ reports (https://redd.unfccc.int/submissions.html?mode=browse-bycountry) with FAO forest land areas (2015) and FAO forest land + other woodlands areas for the year 2015 (see Table S98). Consistent with Grassi et al. (2022), all forest lands in Africa are considered as managed. We found that FAO forest lands areas are closer to UNFCCC estimates than the sum of FAO forest and other woodlands area, except for DRC, Sudan, Senegal, Niger and Mauritania (Table S98). Forest areas in UNFCCC data using IPCC default method do not exactly match FAO data estimates of forest area.

LULUCF CO_2 fluxes from UNFCCC versus DGVM and inversions

A comparison between LULUCF CO_2 fluxes from UNFCCC, FAO, DGVMs and inversions is shown in Fig. 5 at the scale of the continent and for the six regions. The period of overlapping time series is 2001-2018. For the continent, DGVMs give a mean sink of -232 $MtCO_2$ yr^{-1} with a huge range from -1977 $MtCO_2$ yr^{-1} to 2095 $MtCO_2$ yr^{-1}. The years with the biggest sinks for DGVM (from the median of all models) are 2006 and 2018, and the years with the smallest sinks are 2005 and 2016 which seem related to widespread drought years across Africa. A key result shown by this figure is that the DGVMs and inversions show a huge spread, making them of little value to 'verify' inventories for LULUCF CO_2 fluxes in Africa. Yet, we observed that the median of all DGVM points to a sink for Africa, unlike the UNFCCC data with the correction from Grassi et al. (2022).

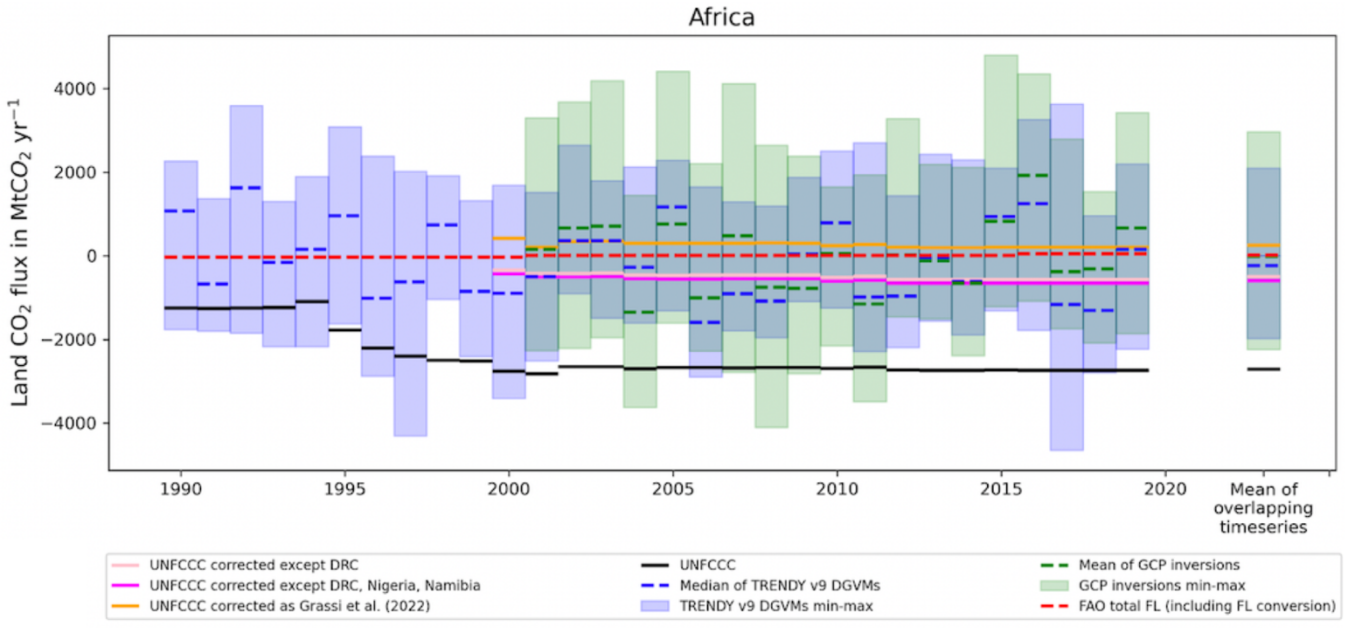

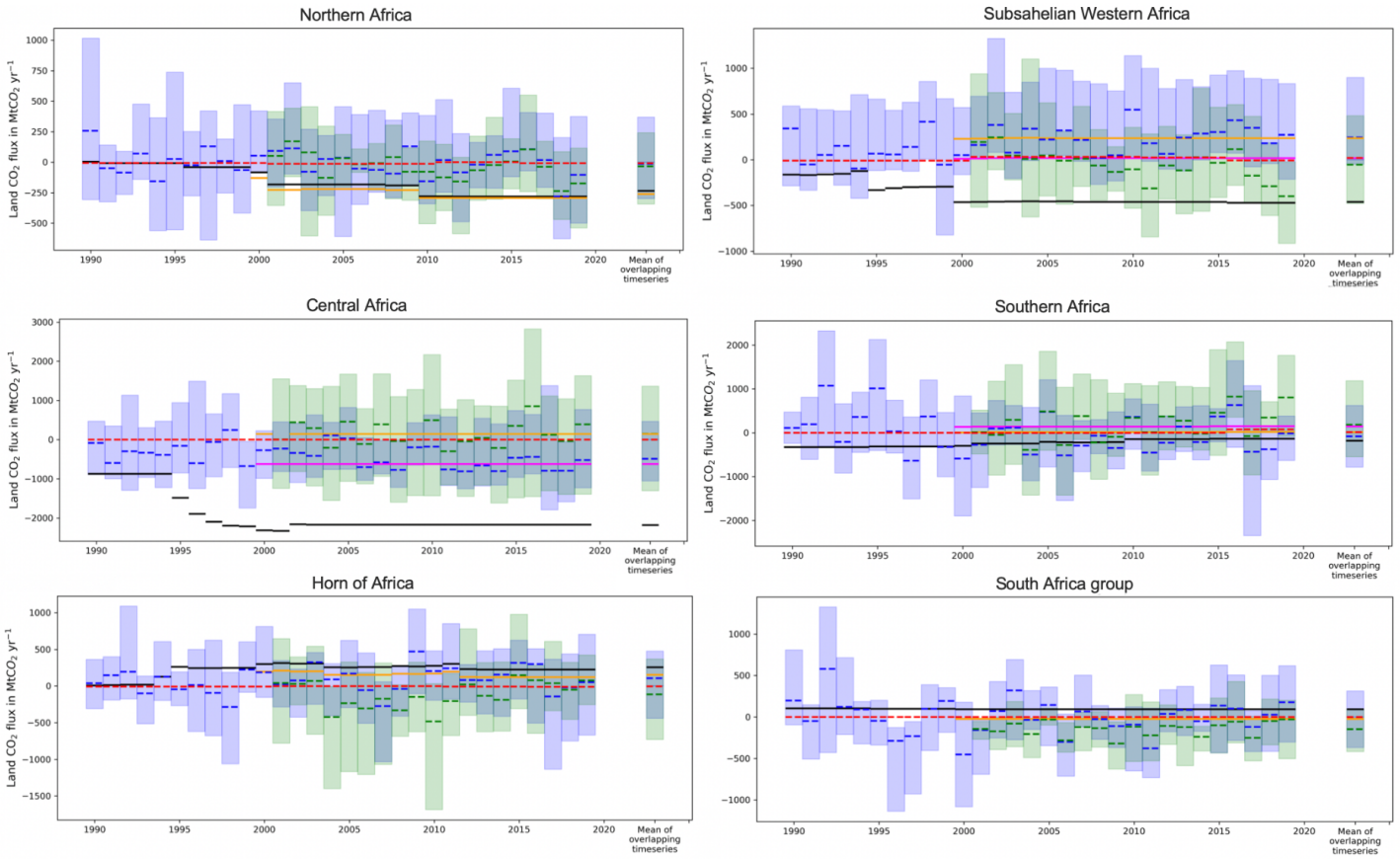

Figure 5. LULUCF CO_2 emissions and sinks: comparison between UNFCCC national greenhouse gas inventories, TRENDYv9 DGVMs and inversions, for total Africa and for each of the six African sub regions; as well as country details for the three lain outliers. The unit is in $MtCO_2\ yr^{-1}$ Shaded green areas represent the minimum and maximum ranges from inversions. Shaded blue represents the minimum and maximum ranges for TRENDYv9 DGVMs. Green dashes denote the mean of inversions, blue dashes denote the median of TRENDYv9 DGVMs, green dashes the median of inversions. Positive values represent a source while the negative values refer to a sink.

For three large countries, corrected UNFCCC values from Grassi et al. show a bigger discrepancy with other BU and TD methods than uncorrected ones (Fig. S9). In Namibia the corrected value gives a larger sink compared to other methods, while the uncorrected value is comparable. In DRC the corrected value which was a source seems a high overestimate compared to other methods, while the uncorrected UNFCCC value is close to median values from inversions, and to FAO. In Nigeria, the corrected value seems to be a high overestimation of a net source compared to other methods pointing to either a smaller source (FAO, inversions) or even a sink (DGVM).

682 The data in Figure 5 show that most methods agree on a small net sink for African LULUCF CO_2 fluxes,
683 except for corrections following Grassi et al (2022). But disagreements exist among different methods.
684 Inversions give a smaller net sink ($\text{mean}_{\text{min}}^{\text{max}}$) of -14 $^{2\,966}_{-2\,248}$ $MtCO_2$ yr^{-1} than DGVMs (-232 $^{2095}_{-1978}$ $MtCO_2$
685 yr^{-1}). The median value of inversions is nevertheless within the range of DGVMs. At the scale of Africa,
686 the inversions mean sink is ∼12 times smaller than the median from DGVMs. The min-max range of
687 inversions (5216 $MtCO_2$ yr^{-1}) is larger than the range of the DGVMs by 17%. DGVM and inversions show
688 a positive temporal correlation coefficient (r = 0.7) for annual trends (linear fit to time series).
689 UNFCCC values with the fourth approach point out to a net sink (-503 $MtCO_2$ yr^{-1}), similar to the third
690 one. Corrected values as in Grassi et al. (2022) give a net source estimate of 265 $MtCO_2$ yr^{-1}. FAO net
691 emissions and removals represent a small net source (18 $MtCO_2$ yr^{-1}). Differences between FAO and
692 UNFCCC, as explained in Grassi et al. (2022), could be due to the fact that FAO estimates of CO_2 fluxes
693 for forest remaining forest can be set to zero in absence of any national stock change inventory (Table 3).
694
695 **Table 3. Mean net LULUCF CO_2 (emissions and removals) over the overlapping period of the different**
696 **datasets (2001-2018), in $MtCO_2$ yr^{-1}.**

Region	Corrected UNFCCC (Grassi et al. 2022) with and without DRC correction.	Corrected UNFCCC but DRC/ Nigeria/ Namibia	Median TRENDY v9	Max TRENDY v9	Min TRENDY v9	Mean GCB inv.	Max GCB inv.	Min GCB inv.	FAO total FL with FL conversion
South Africa group	-23	-23	-5	312	-368	-147	96	-418	-1
Horn of Africa	153	153	108	475	-439	-115	367	-729	-5
Southern Africa	14	**141**	-81	622	-785	182	1186	-548	13
North Africa	-259	-259	-13	369	-299	-34	240	-343	-9
Subsahelian West Africa	236	**19**	245	900	-49	-53	481	-479	21
Central Africa	**144** (DRC with NDC2021) **-620** (DRC with NC3)	**-620**	-490	461	-1051	152	1362	-1303	-1
Africa total	**265** (DRC with NDC2021) **-503** (DRC with NC3)	**-589**	-232	2095	-1978	-14	2967	-2249	-1

697

At a regional scale, we note some agreement between different ~~bottom-up~~ BU approaches. First, for the South Africa region, the mean of DGVM medians during the overlapping period 2001-2018 (-5 $MtCO_2$ yr^{-1}) and the FAO estimate (-1 $MtCO_2$ yr^{-1}) are comparable and not too far from Grassi et al., 2022 (-23 $MtCO_2$ yr^{-1}). Second, for North Africa, the DGVM median (-13 $MtCO_2$ yr^{-1}) and the FAO mean estimate over the same period (-9 $MtCO_2$ yr^{-1}) are comparable. Finally, in Sub-Sahelian West Africa, the DGVM (236 $MtCO_2$ yr^{-1}) and UNFCCC corrected following Grassi et al., 2022 (245 $MtCO_2$ yr^{-1}) are also close to each other.

Northern Africa is the group where DGVM and inversions point to the closest values both in terms of sign (sink) and magnitudes with respectively small sinks of -13^{369}_{-299} $MtCO_2$ yr^{-1} and $-34^{240}_{-343}$$MtCO_2$ yr^{-1}. Looking at DGVM and inversions in the region of South Africa, we found that both DGVM and inversions point to a sink (respectively -5^{312}_{-368} $MtCO_2$ yr^{-1} and $-147\,^{96}_{-418}$ $MtCO_2$ yr^{-1}), however with a different magnitude. The region showing the highest discrepancies between inversions and DGVM values is Central Africa with a source in inversions ($152^{1362}_{-1303}$$MtCO_2$ yr^{-1}) and a sink for DGVM (-490^{461}_{-1051} $MtCO_2$ yr^{-1}). The Sub-Sahelian West Africa also shows discrepancies in both sign and magnitude with 245^{900}_{-49} $MtCO_2$ yr^{-1} for DGVM and $-53\,^{481}_{-479}$$MtCO_2$ yr^{-1} for inversions. The same is true for Southern Africa with $-81\,^{622}_{-785}$$MtCO_2$ yr^{-1} for DGMVs and $182^{1186}_{-548}$$MtCO_2$ yr^{-1} for inversions, and the Horn of Africa with $108^{475}_{-439}$$MtCO_2$ yr^{-1} for DGVM and $-115\,^{367}_{-729}$$MtCO_2$ yr^{-1} for inversions. At the regional scale, the inversions systematically give smaller sinks than DGVMs in the regions of Central Africa, Sub-Sahelian West Africa and North Africa after 2010 (Fig. 5).

We also computed the coefficient of correlation at the regional level between DGVM and inversions trends for each region. The highest correlation coefficients are in the South Africa region (r = 0.7), followed by Northern Africa (r = 0.6) and in Southern Africa (r = 0.5). The lowest correlation coefficients are for the group of Central African countries (r = 0.3), Sub-Sahelian Western countries (r = 0.2) and the Horn of Africa (r = 0.1).

2.3 CH_4 anthropogenic emissions

Total and sectoral bottom up CH_4 anthropogenic emissions and decadal changes

731 **(a)**

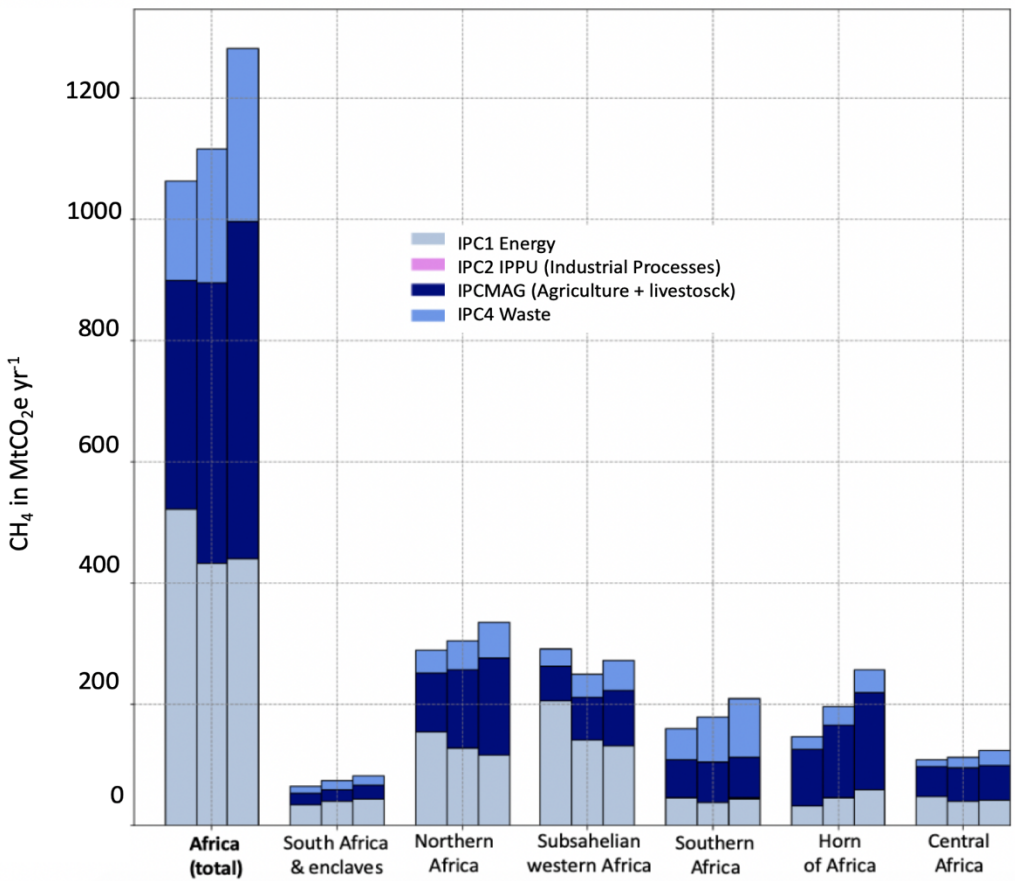

732

733 **(b)**

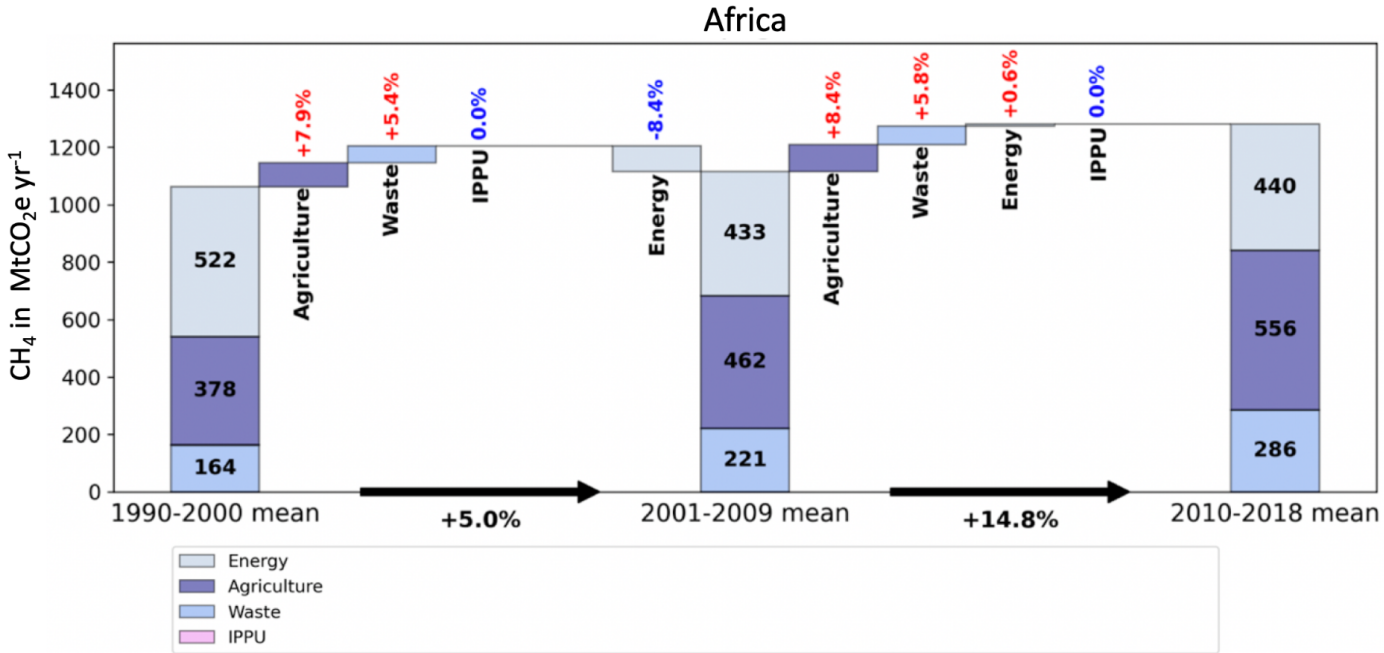

734

(c)

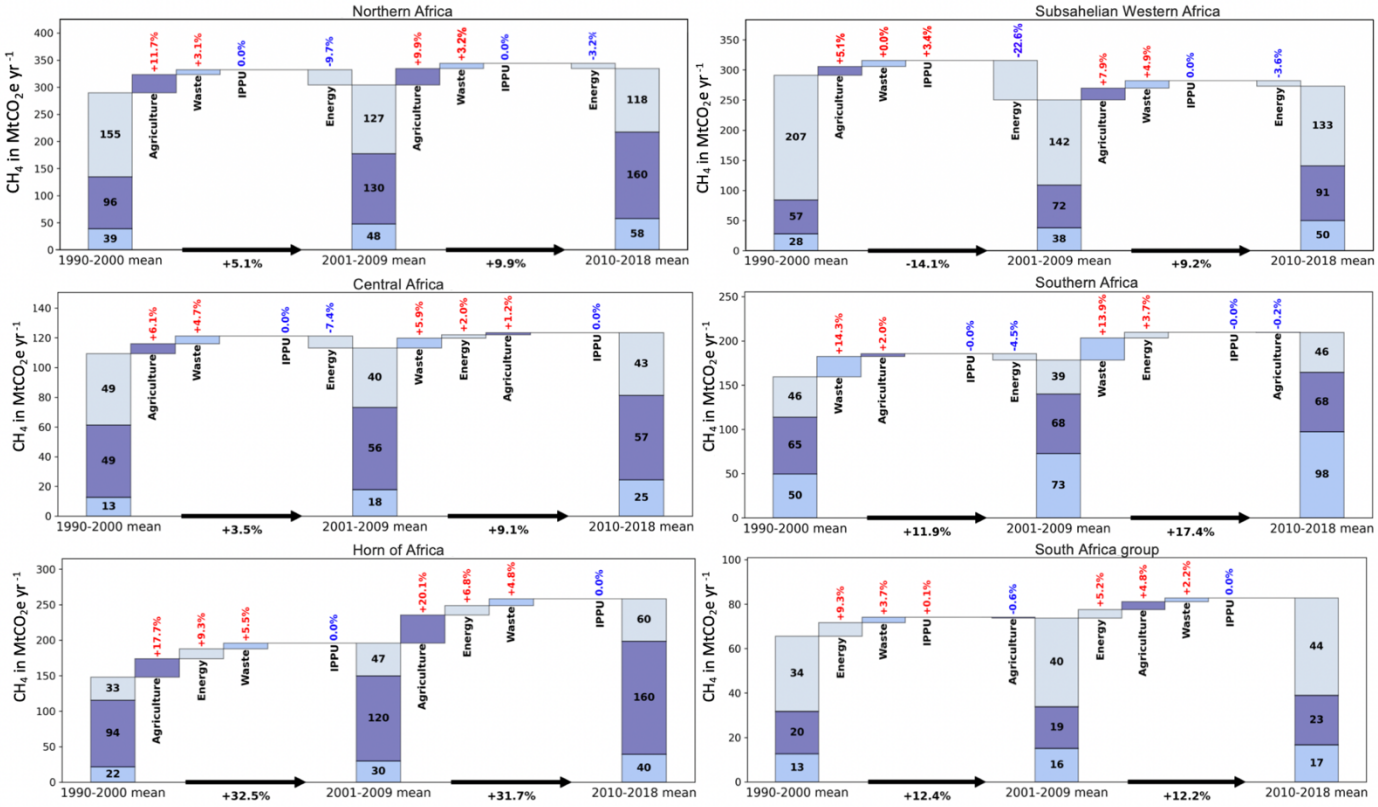

Figure 6. (a) African mean anthropogenic CH_4 emissions in $MtCO_2e\ yr^{-1}$ over three decades (1990-1998, 1999-2008, 2010-2018). (b) Contribution of each sector to the change of African emissions between the last three decades. (c) Same for different regions regrouping several countries. Data from PRIMAP-hist (2021).

Figure 6 shows anthropogenic CH_4 emissions from PRIMAP-hist grouped into four super-sectors (see section 1). A map of CH_4 emissions and their trends per country is given in Fig. 3c-d. LULUCF CH_4 emissions are not considered in PRIMAP-hist. African anthropogenic CH_4 emissions sum up to 1154 $MtCO_2e\ yr^{-1}$ over the last three decades. They increased from 1064 $MtCO_2e\ yr^{-1}$ in 1990-2000 to 1116 $MtCO_2e\ yr^{-1}$ in 2001-2009, and further to 1282 $MtCO_2e\ yr^{-1}$ over 2010-2018 (Fig. 6.a.) Over the last three decades, the main African CH_4 emitting super-sectors shifted from Energy (49% over 1990-2000) to Agriculture, mainly due to a North African contribution. At the regional level, the main contributing region to total emissions shifted over the last 30 years from Sub-Sahelian Western Africa (297 $MtCO_2e\ yr^{-1}$ for all sectors in 1990-2000) to North Africa (333 $MtCO_2e\ yr^{-1}$ for all sectors in 2010-2018).

North African emissions increased from 290 $MtCO_2e\ yr^{-1}$ in 1990-2000 to 305 $MtCO_2eq\ yr^{-1}$ in 2001-2009, and further to 333 $MtCO_2e\ yr^{-1}$ in 2010-2018. Sub-Sahelian emissions decreased from 297 $MtCO_2e\ yr^{-1}$ in 1990-2000 to 252 $MtCO_2e\ yr^{-1}$ in 2001-2009, and re-increased to 274 $MtCO_2e\ yr^{-1}$ in 2010-2018, a level smaller than in the first decade (Fig. 6b). The Horn of Africa emissions increased from 149 $MtCO_2e\ yr^{-1}$ over 1990-2000, to

197 $MtCO_2e\ yr^{-1}$ over 2001-2009, and further to 260 $MtCO_2e\ yr^{-1}$ over 2010-2018. The emissions from Southern Africa increased from 184 $MtCO_2e\ yr^{-1}$ in 1990-2000, to 180 $MtCO_2e\ yr^{-1}$ in 2001-2009, and further to 212 $MtCO_2e\ yr^{-1}$ in 2010-2018. Emissions from the Central African region increased from 111 $MtCO_2e\ yr^{-1}$ in 1990-2000, to 114 $MtCO_2e\ yr^{-1}$ in 2001-2009, and further to 125 $MtCO_2e\ yr^{-1}$ in 2010-2018. We also computed the GINI of African countries anthropogenic CH_4 per capita emissions and obtained the following values: 0.6 in 1990-1998, 0.5 in 1999-2008, 0.5 in 2009-2018, thus a trend of increasing 'inequality' between countries. As compared to per capita FCO_2 emissions, more homogeneity is observed for CH_4 per capita emissions. Similar to FCO_2 emissions, the GINI values remained stable over the three decades, showing a similar level of inequalities over time.

~~Bottom-up~~ BU versus inversions for total and anthropogenic CH_4 emissions

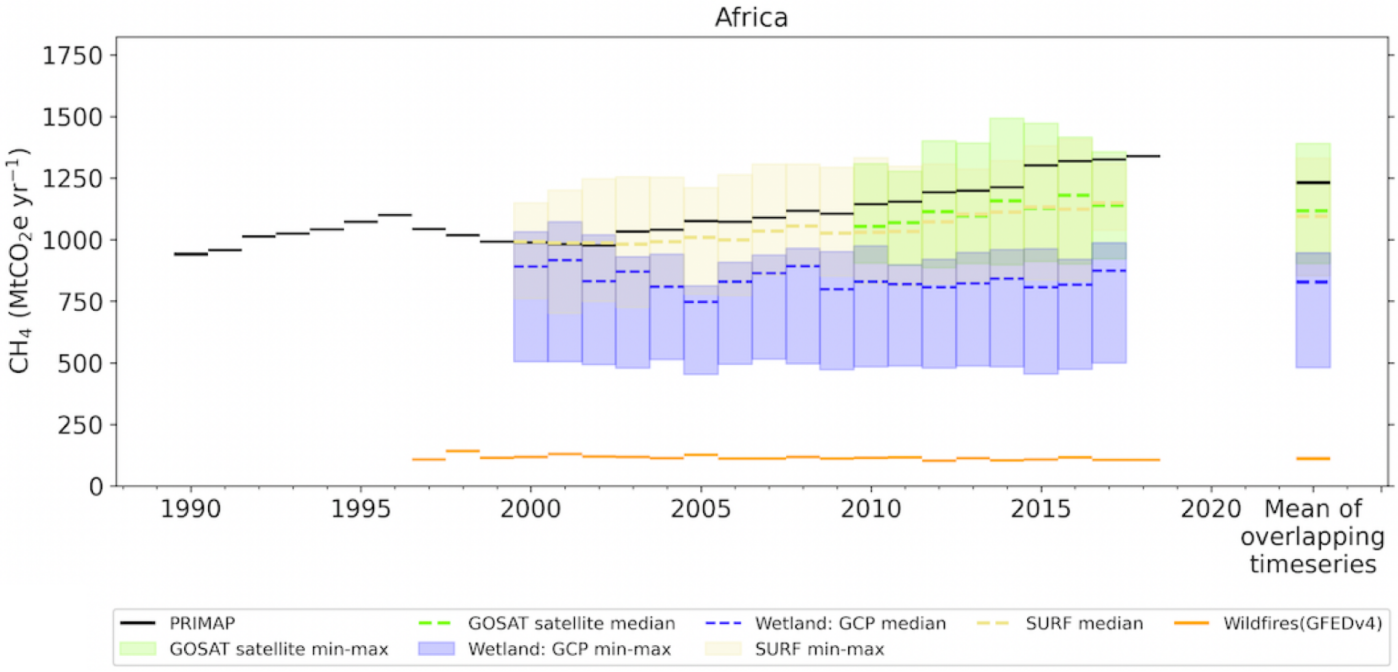

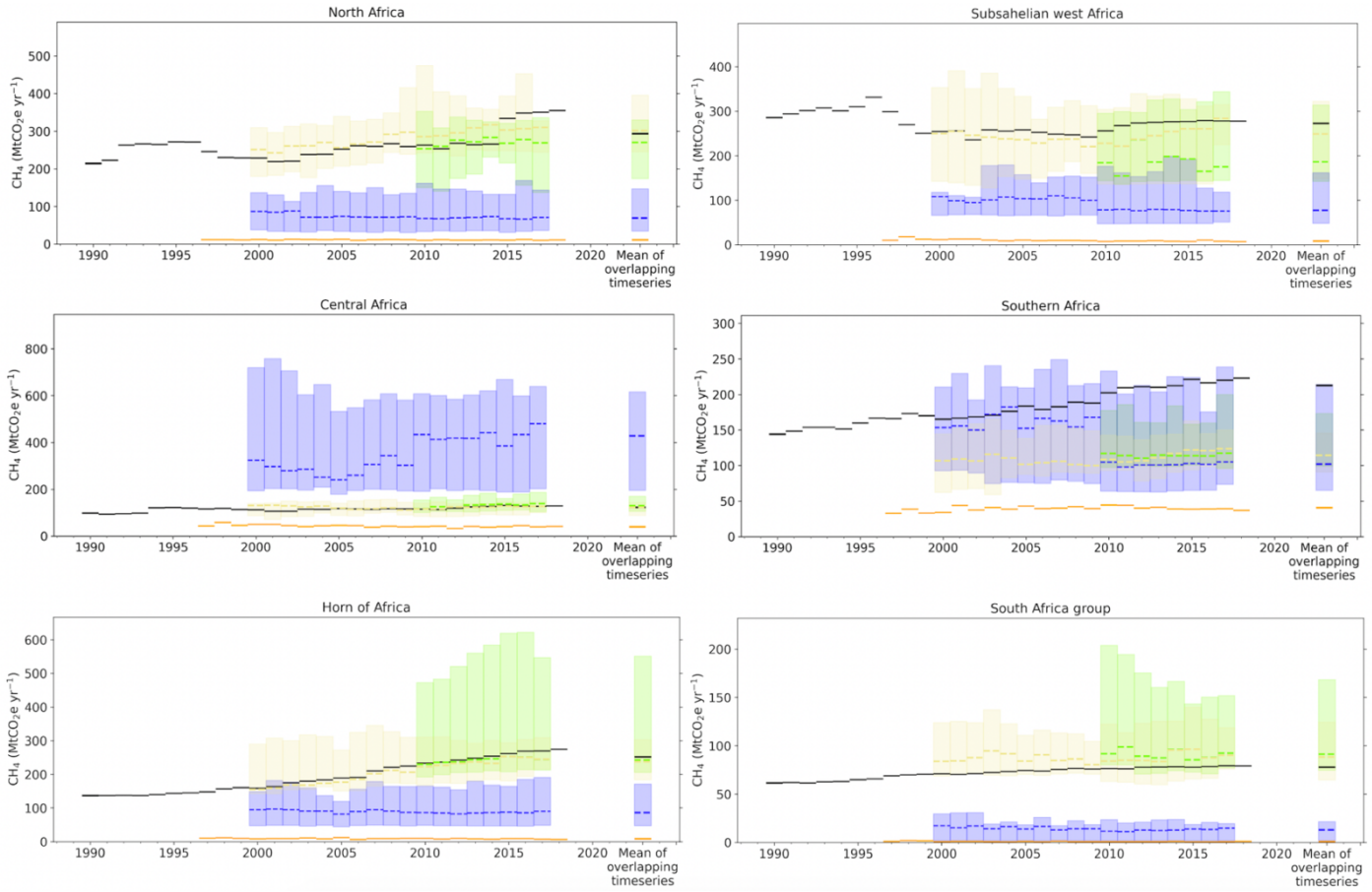

Figure 7. Comparison of total anthropogenic CH_4 emissions in $MtCO_2e\ yr^{-1}$ from the PRIMAP-hist inventory (black) and global inversions. Shaded green and yellow areas represent the minimum and maximum range from GOSAT satellite and surface inversions, respectively. Shaded blue areas represent the minimum and maximum ranges of wetlands natural emissions from inversions. The orange lines represent wildfire emissions from GFED4.

Figure 7 compares ~~bottom-up~~ BU anthropogenic emissions from PRIMAP-hist for the period 2000-2018 with inversions' anthropogenic emissions (see section 1). Wetlands natural emissions are shown in the figure only for information from the median and range of inversions. Over the overlapping time period, medians of both GOSAT and surface inversions are always smaller than PRIMAP-hist emissions, at continental and regional level, except for the Central African region. For the African continent, the mean and min-max of GOSAT inversions for anthropogenic CH_4 emissions over 2000-2018 is 1117^{1390}_{903} $MtCO_2e\ yr^{-1}$, very close to the mean of surface inversions of 1094^{1330}_{853} $MtCO_2e\ yr^{-1}$. A good agreement between GOSAT and surface inversions was also found in other high-emitting countries (Deng et al., 2021). In contrast, PRIMAP-hist gives a mean of CH_4 anthropogenic emissions of 1231 $MtCO_2e\ yr^{-1}$ over the period 2010-2017. The mean wetlands flux from inversions over 2010-2017 is of 827^{946}_{481} $MtCO_2e\ yr^{-1}$. Methane emissions from wildfires over Africa for the same period are less important, with a mean of 110 $MtCO_2e\ yr^{-1}$.

Regional emissions from PRIMAP-hist ranked in decreasing order are: North Africa (293 $MtCO_2e\ yr^{-1}$) > Sub-Sahelian west Africa (272 $MtCO_2e\ yr^{-1}$) > Horn of Africa (252 $MtCO_2e\ yr^{-1}$) > Southern Africa (212 $MtCO_2e\ yr^{-1}$) > Central Africa (123 $MtCO_2e\ yr^{-1}$) > South Africa (78 $MtCO_2e\ yr^{-1}$). For both GOSAT and surface inversions, the ranking of regions (Table S1~~0~~) is almost the same for surface inversions and PRIMAP-hist, with the exception of Central Africa and Southern Africa.

2.4 Results for N_2O emissions

N_2O PRIMAP-hist versus atmospheric inversions (total flux)

Total and sectoral N_2O anthropogenic emissions (PRIMAP-hist)

(a)

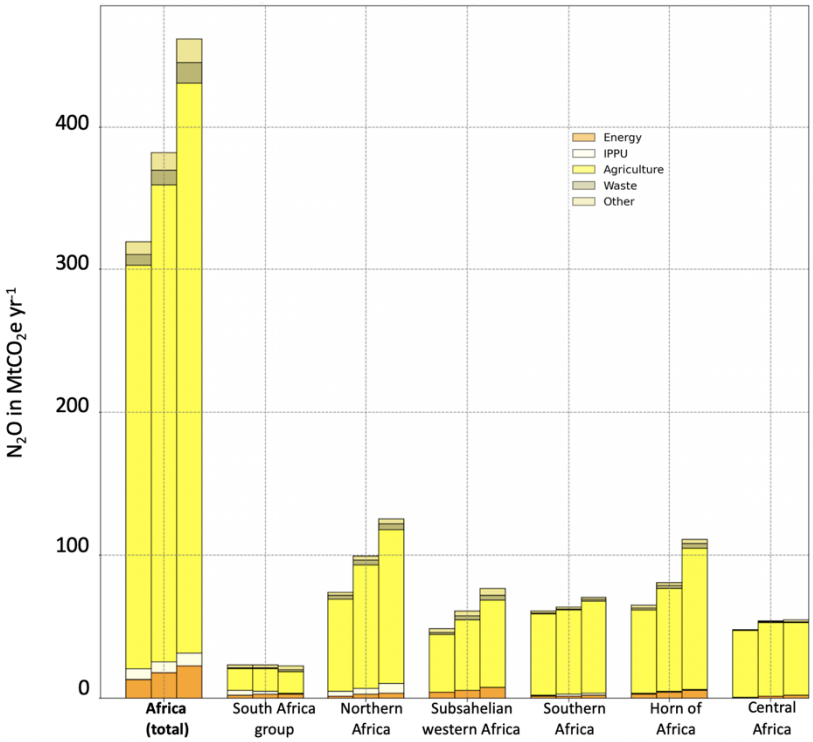

801 **(b)**

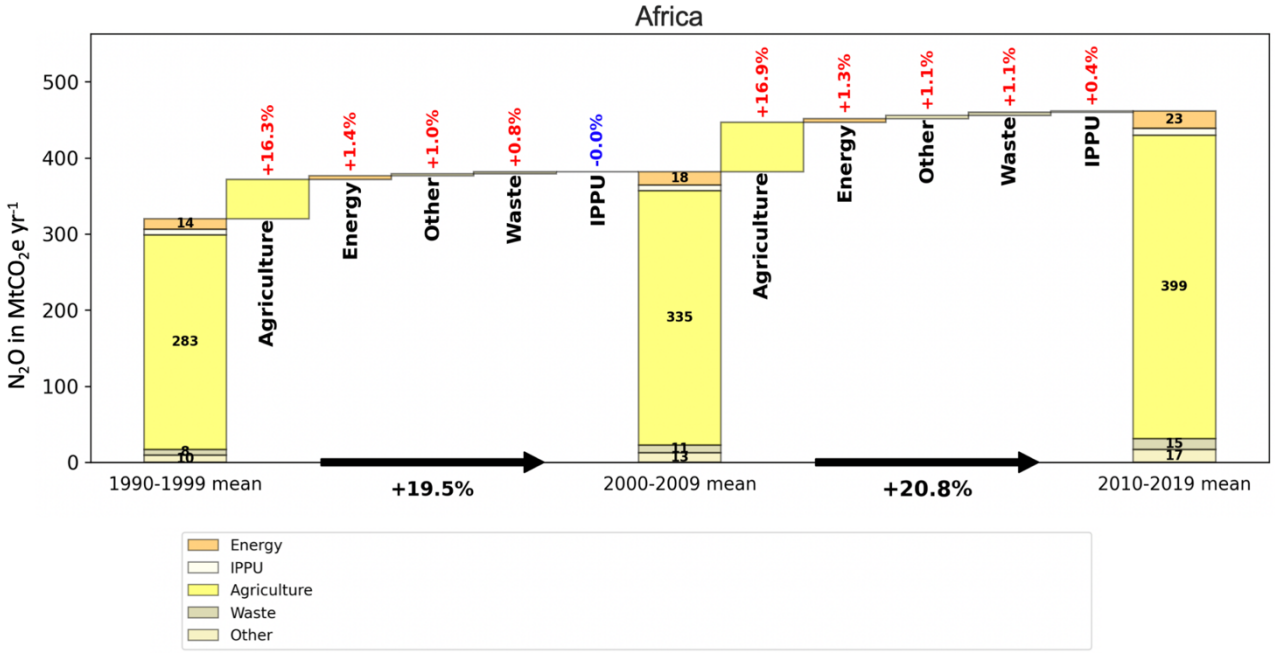

802

803 **(c)**

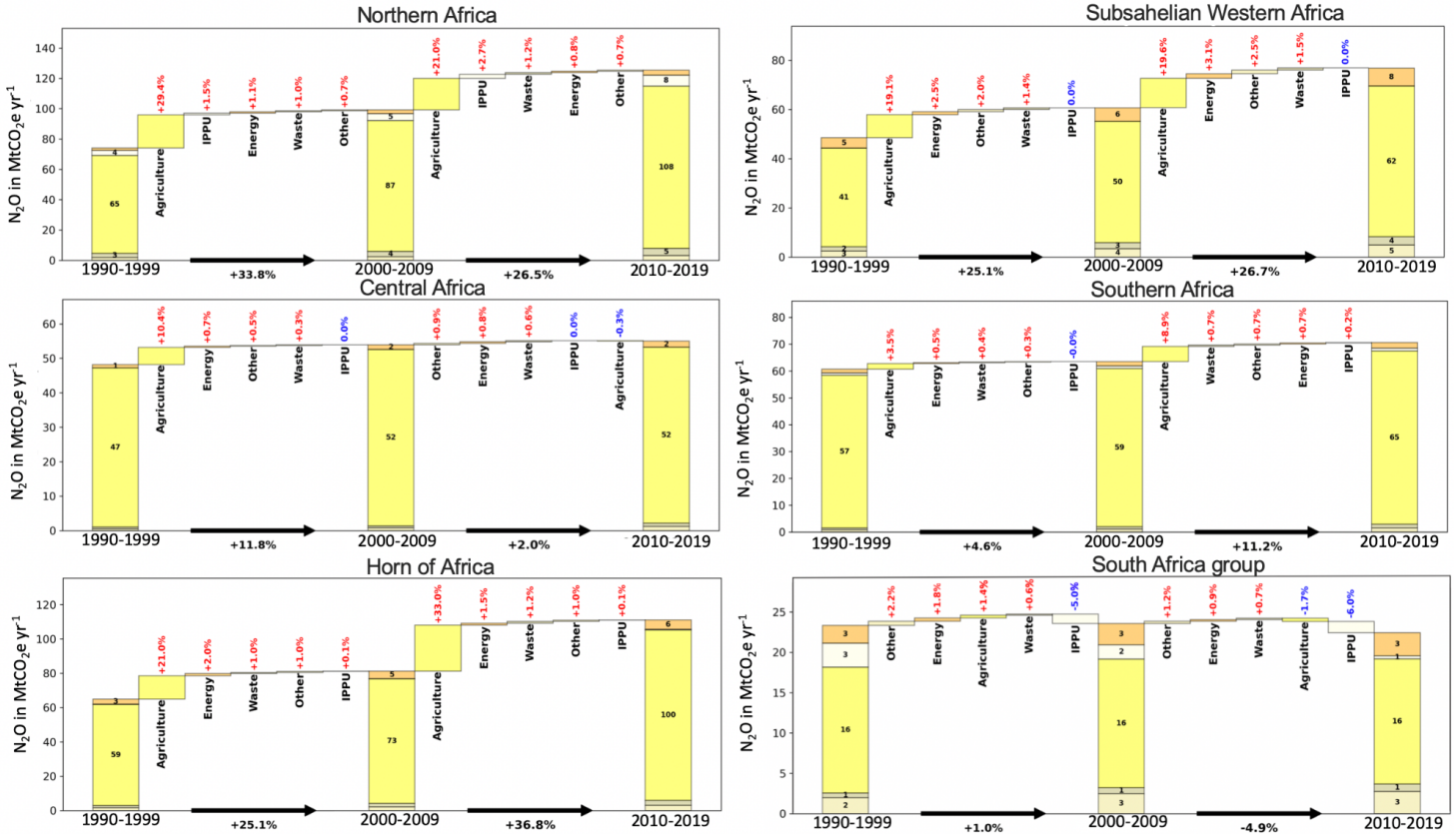

804

Figure 8. (a) African anthropogenic N_2O emissions in $MtCO_2e\ yr^{-1}$ over three decades: 1990-1998, 1999-2008 & 2009-2019. Data from PRIMAP-hist (2021). (b) Contribution of each sector to the change of African N_2O emissions between the last three decades. (c) Same for different regions regrouping several countries. Data from PRIMAP-hist (2021).

Figure 8 presents anthropogenic N_2O emissions from PRIMAP-hist, for five sectors (for country values, see Fig. 4). Over the last three decades, the mean African emissions are 378 $MtCO_2e\ yr^{-1}$, three times less than CH_4 emissions. The mean decadal N_2O emissions increased from 319 $MtCO_2e\ yr^{-1}$ in 1990-1999, to 382 $MtCO_2e\ yr^{-1}$ in 2000-2009 (+20%), and further to 431 $MtCO_2e\ yr^{-1}$ in 2010-2018. Over the last three decades, the main emitting sector remained Agriculture. The N_2O emissions increase also originates from Agriculture, with an increase from 283 $MtCO_2e\ yr^{-1}$ to 335 $MtCO_2e\ yr^{-1}$ between 1990-1999 and 2000-2009, that is, +16.3 % compared to of the total emission increase of +19.5%. The three other sectors show a smaller contribution to the emissions increase: Energy (+1.4%), Other (+1%) and Waste (+0.8%). IPPU shows no change. Similarly, between 2000-2009 and 2010-2019, the N_2O emissions increase also came from the sector of Agriculture, with an increase from 335 $MtCO_2e\ yr^{-1}$ to 399 $MtCO_2e\ yr^{-1}$ between 1990-1999 and 2000-2009.

The main contributing regions to the continental emissions are Northern Africa and the Horn of Africa (Fig. 8a). Between 2000-2009 and 2010-2019, the North African contribution increased from 99 $MtCO_2e\ yr^{-1}$ to 125 $MtCO_2e\ yr^{-1}$ (+27%). The main sectoral contribution is always Agriculture, which increased in that region from 86 $MtCO_2e\ yr^{-1}$ to 107 $MtCO_2e\ yr^{-1}$ (+21%). Emissions from the second largest emitting region, the Horn of Africa, increased from 81.19 $MtCO_2e\ yr^{-1}$ in 2000-2009 to 111 $MtCO_2e\ yr^{-1}$ in 2010-2019 (+37%), mainly from Agriculture. In the third most emitting region, Sub-Sahelian Africa, emissions increased from 61 $MtCO_2e\ yr^{-1}$ in 2000-2009 to 77 $MtCO_2e\ yr^{-1}$ in 2010-2019 (+27%), also from Agriculture. The least contributing region to the increase of the total N_2O emissions from 2000-2009 to 2010-2019 is South Africa which had a very small decrease, mainly from IPPU (-6%) followed by Agriculture (-2%). On the contrary, there is a slight increase of N_2O emissions for the group of South Africa for the Other (+1%), Energy (+1%) and Waste (+1%) sectors.

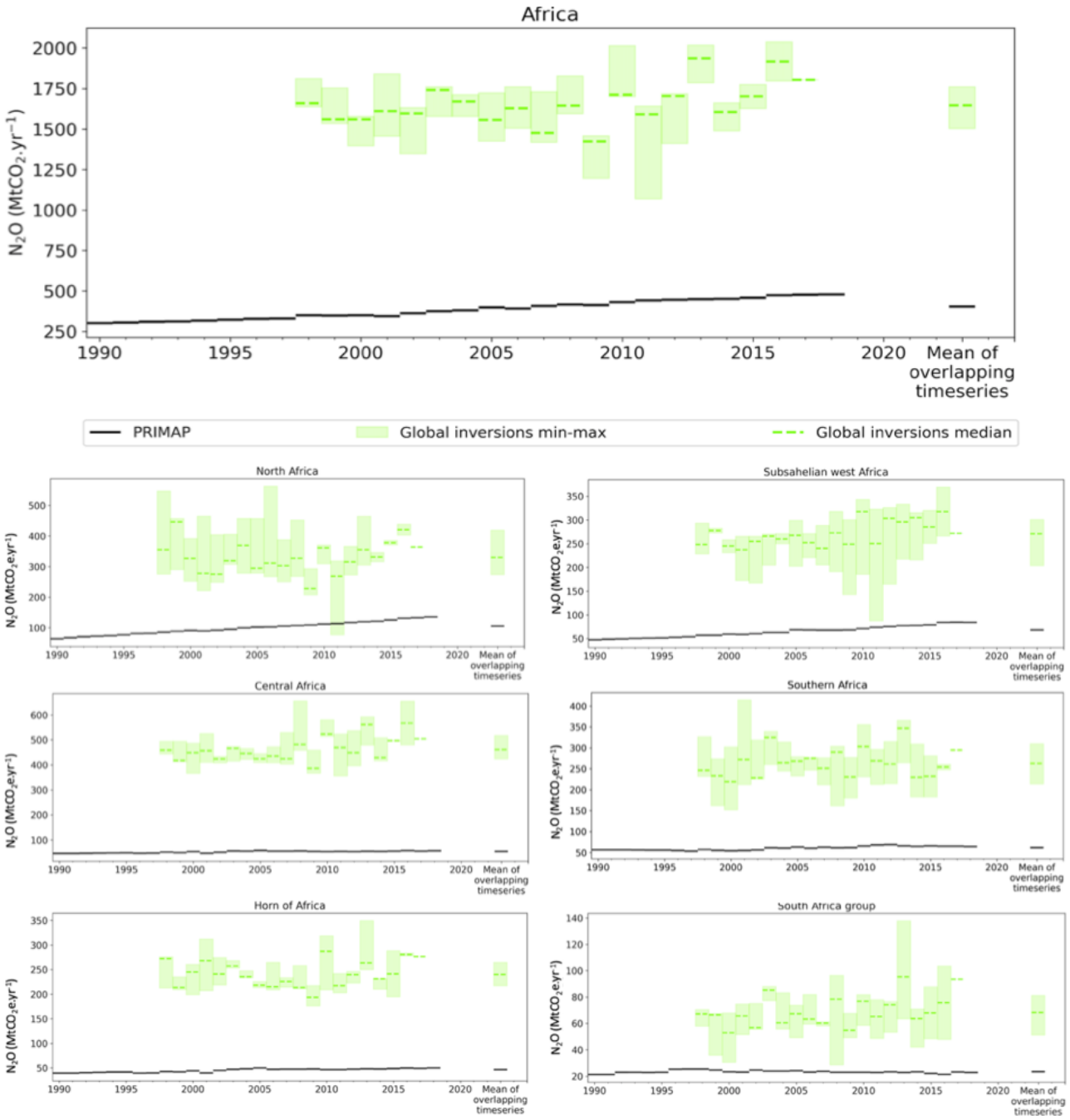

Figure 9. Total N_2O emissions from PRIMAP-hist in $MtCO_2e$ yr^{-1} (black line) from three GCP atmospheric inversions for the entire African continent and for six African sub-regions. The green line is the median of the three inversions and the light green areas the maximum-minimum range.

Figure 9 compares N_2O emissions from PRIMAP-hist and inversions. For total Africa, the mean of inversions emissions over the overlapping time period 1998-2017 is 1647^{1760}_{1502} $MtCO_2e$ yr^{-1}, much larger than the PRIMAP-hist estimate of 360 $MtCO_2e$ yr^{-1}. According to PRIMAP-hist, total African emissions increased by

28% between 1998 and 2017, while the trend of emissions from the inversions is 16 ± 8%. At regional scale, emissions from inversions ranked in decreasing order are: Central Africa (461^{517}_{424} $MtCO_2e$ yr^{-1} $MtCO_2e$ yr^{-1}) > North Africa ($330^{419}_{274}MtCO_2e$ yr^{-1}) > Sub-Sahelian West Africa ($271^{330}_{68}MtCO_2e$ yr^{-1}) > Southern Africa ($263^{310}_{214}MtCO_2e$ yr^{-1} > Horn of Africa $240^{265}_{217}MtCO_2e$ yr^{-1} > South Africa ($68^{81}_{51}MtCO_2e$ yr^{-1}). According to PRIMAP-hist, the ranking is: North Africa (106 $MtCO_2e$ yr^{-1}) > Sub-Sahelian West Africa (68 $MtCO_2e$ yr^{-1}) > Southern Africa (62 $MtCO_2e$ yr^{-1}) > Central Africa (54 $MtCO_2e$ yr^{-1}) > the Horn of Africa (46 $MtCO_2e$ yr^{-1}) > South Africa (24 $MtCO_2e$ yr^{-1}) (See also Table S132). Emissions from PRIMAP-hist are smaller than inversions by a factor of 16. This is likely due to the fact that we did not attempt to separate natural from anthropogenic emissions in inversions. Other studies (Ciais et al., 2021; Petrescu et al., 2021 in Europe) showed that even after subtracting N_2O natural estimates, inversions always point to higher estimates than BU methods.

3 Discussion: uncertainties, ~~synthesis of the three main GHG and~~ comparison between BU and TD methods, and synthesis for the three main GHG

3.1~~5~~ Uncertainties specific to DGVMs / inversions for LULUCF CO_2

In Fig. 5, we showed important disagreements among models regarding LULUCF CO_2 on whether Africa has been a small source over the last 20 years (as shown by inversions) or a net sink (as shown by DGVMs and UNFCCC except with the Grassi et al. correction). There is also more interannual variability in the DGVMs results, mainly from climate variability, which is absent from UNFCCC as inventories provide only decadal smoothed flux estimates. The larger sink in the DGVMs compared to the corrected UNFCCC estimates using the method of Grassi et al. (2022) may be due to the fact that non-Annex I UNFCCC estimates generally do not include dead biomass or harvested wood products. If forest biomass is estimated by a stock-change approach, therefore, changes in living biomass due to transfer to dead biomass and harvested wood products will be considered emitted in that year, while in the DGVMs it will decay more slowly over time. Another difference is the treatment of land use change emissions, based on historical global land use change maps for the DGVMs, which can significantly differ from national land use datasets. On the other hand, DGVMs do not represent forestry and may underestimate sinks in intensively managed young forests. DGVMs do not separate between unmanaged and managed lands, while UNFCCC inventories only account for managed land, yet including conservation areas and indigenous territories. Grassi et al. (2022) showed that the difference between the global UNFCCC sink (1100 $MtCO_2$ yr-1) and the global land carbon sink (4767 $MtCO_2e$ yr-1) must be explained by the contribution of non-managed lands. But in the case of Africa, it was not possible to extract from UNFCCC reports the national areas of unmanaged land, and we had to also look at UNFCCC Technical

Assessment Reports (TAR) as well as REDD+ reports to extract information. Methods of assessment have not been fully standardized since 1990, and they differ depending on the countries analyzed, and on the emissions categories considered. In this context, when comparing UNFCCC estimates with data from DGVM and inversion models, different layers of aggregated uncertainties affect the analysis. (Deng et al., 2021; Petrescu et al., 2021; Grassi et al., 2018). The fact that LULUCF CO_2 fluxes have the greatest uncertainties is true globally.

3.~~6~~ 2 Differences and sources of uncertainties between ~~bottom-up~~ BU and TD CH_4 emissions

The methodology used for removing natural CH_4 emissions from inversions is key for comparing with ~~bottom-up~~ BU estimates of anthropogenic emissions only. In this paper, we used a separation based on the natural emissions solved by each inversion (section 2.3 method 1). Using an alternative method from Deng et al. (2022) based on natural emissions from the median of all inversions gives smaller anthropogenic emissions than PRIMAP-hist (Fig. S10).

3.~~7~~3 Differences and sources of uncertainties between ~~bottom-up~~ BU and ~~top-down~~ TD N_2O emissions

For N_2O emissions, discrepancies between inventories and inversions are very high, especially for the group of Central African countries, where the vegetation covers an important land area with likely large natural N2O (Deng et al., 2022). We can suppose that more broadly for all African groups, the lack of accounting of natural emissions is the main reason why PRIMAP-hist estimates are much smaller than inversions. All African countries used Tier 1 emission factors and include only direct N_2O emissions. The study by Deng et al. (2022) underlined that indirect anthropogenic emissions notably coming from "atmospheric nitrogen deposition and leaching from anthropogenic nitrogen additions to aquifers and inland water are usually not reported by non-Annex I countries" and that this under-reported source of anthropogenic emissions tends to represent about 5% to 10% of anthropogenic N_2O. According to Deng et al. (2022), the global situation from inversions for main emitters is similarly affected by the potential contribution of natural sources as well, which is difficult to estimate and separate. Figure 11 from Deng et al. (2022) shows that even when removing "intact / non-managed lands" from inversions, in many countries, especially tropical countries, the inversions give a systematically much higher anthropogenic level of N_2O than inventories, suggesting that there are either missing anthropogenic sources or some "natural" sources (e.g. conservation areas) in managed lands being underestimated by inventories.

3.4~~1~~ Synthesis of the steps for assessing net GHG trends over Africa

Here, we propose a first step towards the elaboration of what could become a more systematic method for a scientific benchmark of non-Annex I national inventories: 1) correct outliers, 2) check the plausibility of estimates, 3) have an independent evaluation of inventory data by experts, 4) a comparison between UNFCCC data corrected thanks to expert judgment and other BU and TD methods, 5) computation of the mean of all BU and TD methods, 6) computation of "best fitted BU values" (meaning "best fitted BU values" excluding uncorrected UNFCCC data), and "TD values" (meaning "best fitted TD values": without considering N_2O inversions replaced with PRIMAP-hist values), 7) identification of ranking anomalies.

3.5~~3~~ Net GHG budget from inversions

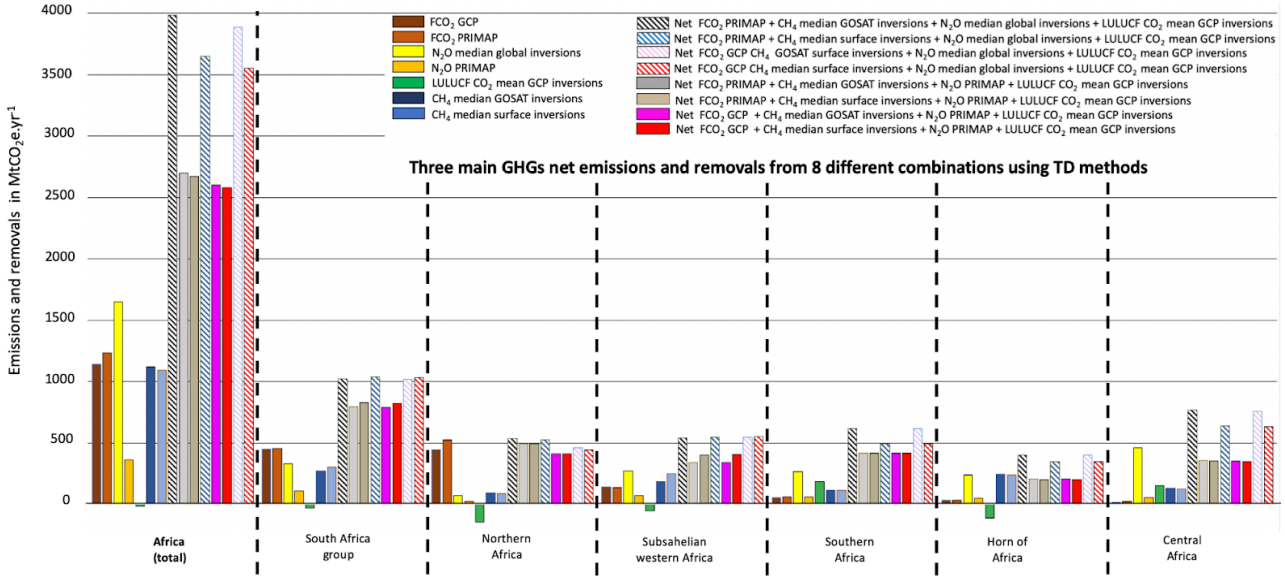

Figure 10~~2~~. Synthesis for the three main GHG with net African budget computation by all TD methods for Africa as a whole and for six sub-groups of African countries across overlapping time series (2001-2017). Following the atmospheric convention, positive numbers represent an emission to the atmosphere and the negative values represent a sink. The CO_2 emissions and sinks from LULUCF are represented in green, they are taken from GCP 2020 dataset. Unit is $MtCO_2e\ yr^{-1}$.

Figure 10 shows different combinations of inversion GHG budgets and individual gasses contributions.

For total Africa, the mean net GHG budget from inversions where N_2O inversions are replaced by PRIMAP-hist is 2638^{5873}_{1761} $MtCO_2e\ yr^{-1}$. Regional GHG budgets in decreasing order are: North Africa (810^{1170}_{279} $MtCO_2e\ yr^{-1}$) > South Africa group (452^{751}_{161} $MtCO_2e\ yr^{-1}$) > Southern Africa (416^{1465}_{-334} $MtCO_2e\ yr^{-1}$) > Sub-Sahelian West Africa (373^{1051}_{36} $MtCO_2e\ yr^{-1}$) > Central Africa (352^{1592}_{-1133} $MtCO_2e\ yr^{-1}$) > Horn of Africa

(204^{873}_{-456} $MtCO_2e\ yr^{-1}$) (Table S17~~6~~). The mean net of inversions including N_2O inversions is substantially higher, 3879^{7341}_{1320} $MtCO_2e\ yr^{-1}$. Regional GHG budgets in decreasing order are: North Africa (1034^{1475}_{600} $MtCO_2e\ yr^{-1}$) > Central Africa (759^{2054}_{-763} $MtCO_2e\ yr^{-1}$) > Southern Africa (616^{1713}_{-262} $MtCO_2e\ yr^{-1}$) > Sub-Sahelian West Africa (576^{1313}_{-61} $MtCO_2e\ yr^{-1}$) > South Africa group (496^{814}_{138} $MtCO_2e\ yr^{-1}$) (Table S17~~6~~).

3.~~4~~ 6 Comparison between ~~bottom-up~~ BU and ~~top-down~~TD methods

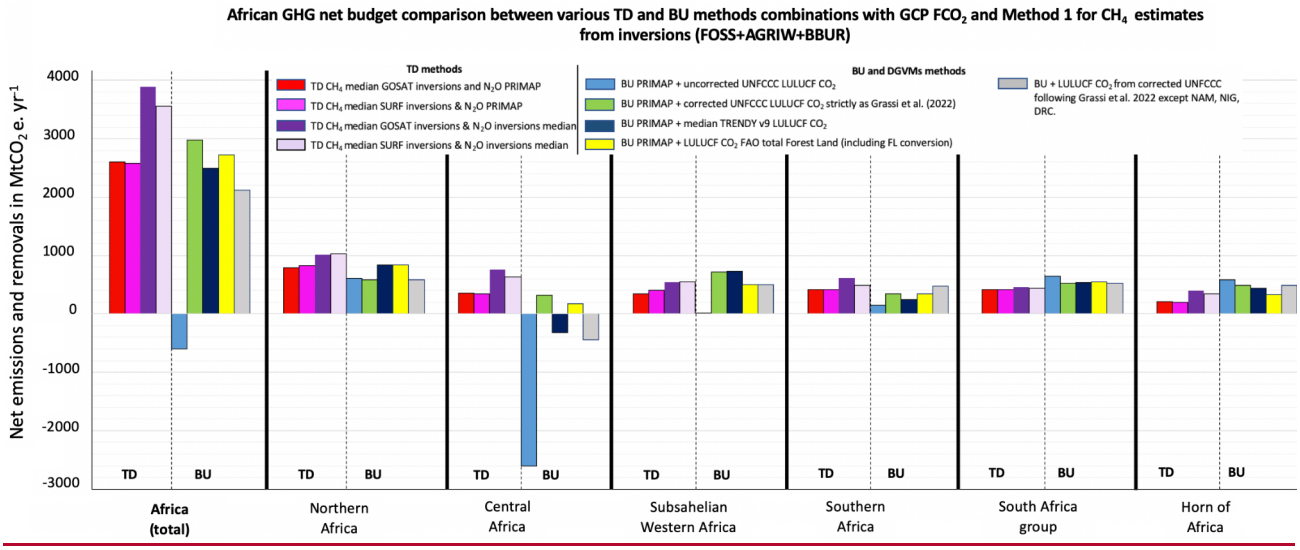

Figure 1~~3~~. Synthesis for the three main GHG net African budget from TD and BU methods, using Method 1 ~~regarding~~ for separating anthropogenic CH_4 emissions ~~estimated~~ from inversions (FOSS+AGRIW+BBUR) ~~for comparative net emissions and removals computation by BU and TD methods for Africa as a whole and for six sub-groups of African countries across the overlapping period (~~during 2001-2017~~). FCO_2 data from GCP. N_2O from global inversions and from PRIMAP-hist. For TD methods, anthropogenic CH_4 from both GOSAT and surface inversions are used, and LULUCF from GCP inversions only. For BU methods, anthropogenic CH_4 and N_2O from PRIMAP are used, and with five different methods for assessing LULUCF CO_2: from uncorrected UNFCCC data; from corrected UNFCCC data according Grassi et al. (2022); from corrected UNFCCC except Namibia, Nigeria and DRC; from TRENDY v9; from FAO FL including FL conversions. Following the atmospheric convention, positive numbers represent an emission to the atmosphere and the negative values represent a sink. All values are in $MtCO_2e$.

Figure 1~~3~~ shows the GHG budgets from all combinations of ~~bottom-up~~ BU and ~~top-down~~TD ~~–~~methods. The mean of all methods after filtering outliers (Grassi et al. (2022) UNFCCC corrections, using PRIMAP instead of inversions for N_2O) is 2630^{4557}_{1974} $MtCO_2e\ yr^{-1}$, which represents only 7.3 % of global FCO_2 emissions. The mean of all estimates points out to a source in the six African regions ranked in decreasing order as: North

Africa (761^{988}_{460} $MtCO_2e\ yr^{-1}$) > South Africa group (513^{702}_{161} $MtCO_2e\ yr^{-1}$) > Horn of Africa (318^{699}_{-80} $MtCO_2e\ yr^{-1}$) > Sub-Sahelian West Africa (492^{913}_{286} $MtCO_2e\ yr^{-1}$) > Southern Africa (354^{998}_{-78} $MtCO_2e\ yr^{-1}$) > Central Africa (143^{882}_{-670} $MtCO_2e\ yr^{-1}$).

We initially did not make any assumption regarding which approach is "better" between TD and BU method, as it actually depends on the considered gas, sector and spatial scale. Comparability between TD and BU results is not completely obvious either, as they do not represent the same processes (example of LULUCF CO_2 for DGVM as explained in paragraph 3.1). For N_2O specifically, we highlighted in paragraph 3.3 the large uncertainty of the TD estimates, underlining the importance to separate natural N_2O emissions from total estimates in order to deliver appropriate anthropogenic assessments thanks to the inversions.

We showed in the results of this paper that inversions in general tend to have larger uncertainties than inventories, and large differences in terms of min / max and at annual scale even among similar typologies of the methods. But at a decadal scale, they deliver reliable overall trends (with good match among the median values of various estimates on the overlapping time period) especially at the spatial scale of groups of countries and of a continent. Under such conditions, TD estimates help identify or confirm outliers / large uncertainties in inventories that may occur especially for Non-annex I countries like Africa.

Inversions therefore can't be a substitute but rather a complement to check trends consistency of inventories and help to identify and correct main outliers. That's why we chose BU estimates to deliver a final budget over Africa (with CO_2 LULUCF corrections) as synthesis figures (see Fig.12 and Fig.13 in the next paragraph). Possibilities to reduce the gap BU and TD estimates are the following: 1) For inversions: to have a coarser network of surface stations and coarser spatial resolution. 2) For DGVM: see paragraph 3.1. 3) For national UNFCCC inventories: to have regularly updated activity data and use country-specific emissions data and include indirect emissions, which is not the case to date for African countries, and use expert judgment for correcting outliers as done by Grassi et al. (2022) and in this study for CO_2 LULUCF emissions.

3.~~7~~2 Net GHG budget from ~~bottom-up~~ BU estimates

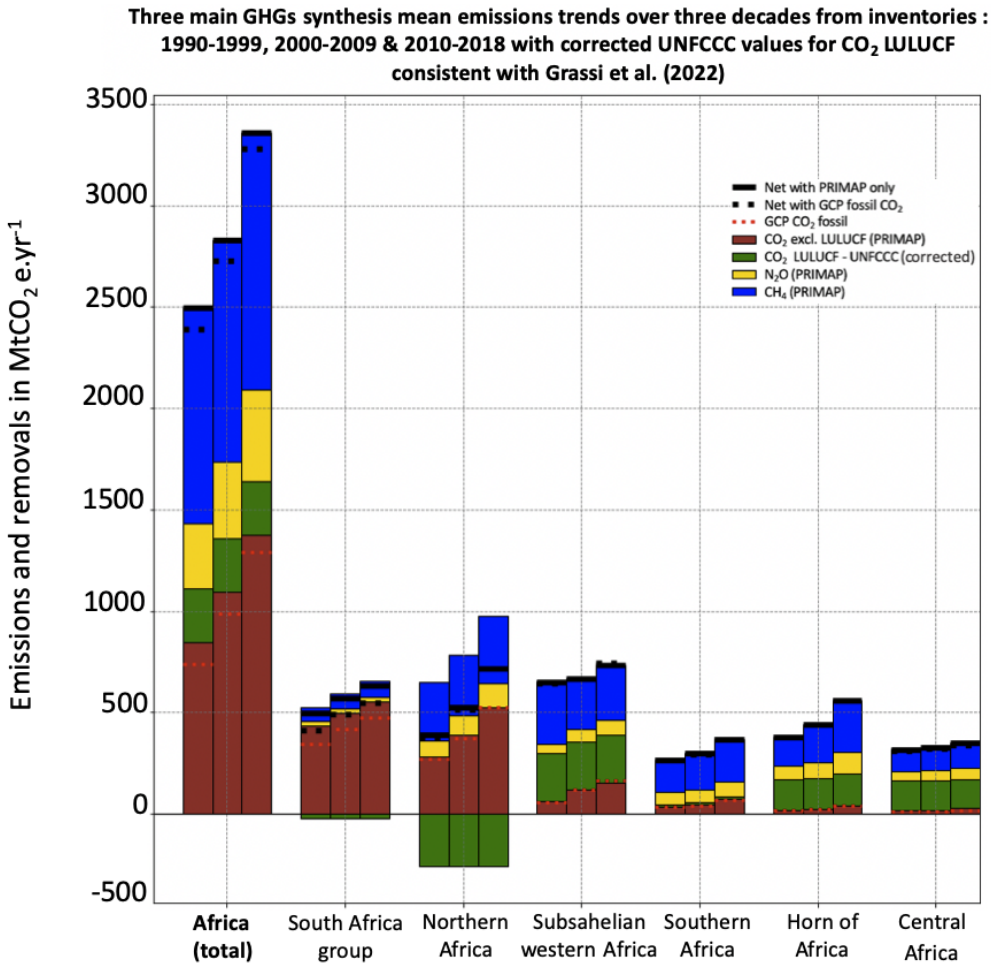

Figure 1~~2~~0. Synthesis for the three main GHG from inventories (after UNFCCC LULUCF CO_2 corrections consistent with Grassi et al. (2022)) for the three main GHG with net African budget computation by BU inventories for Africa as a whole and for six sub-groups of African countries across three different decades (1990-1999, 2000-2010, 2010-2018) using data and corrections from country inventories. Following the atmospheric convention, positive numbers represent an emission to the atmosphere and the negative values represent a sink. Black horizontal lines represent a net flux resulting from the addition of the three main GHG using PRIMAP-hist only, dashed black horizontal lines also represent the net flux resulting from the addition of the three main GHG but using the GCP dataset for FCO_2. Dashed red lines represent the fluxes from GCP FCO_2 available in the most recent GCP paper, to compare them with PRIMAP-hist results which are represented with the brown bar plots. The N_2O and CH_4 fluxes from PRIMAP-hist are respectively represented with yellow and blue bars. CO_2 emissions and sinks from LULUCF are represented in green, they are taken from NC/BUR UNFCCC datasets with corrections applied. Unit is $MtCO_2e\ yr^{-1}$.

Figure 12~~0~~ shows the budget for the three GHG from UNFCCC data with LULUCF data corrected using the second approach. There is a clear increase of African total GHG emissions during the last 3 decades. The differences between ~~bottom-up~~ BU datasets are mainly due to different sectoral allocations. However, the trends are consistent and comparable, and differences among inventories tend to be less for the most recent decade.

Table 5. Mean net total Africa and regional groups' emissions and removals from BU methods using either GCP or PRIMAP-hist for FCO_2 over 2001-2017 in $MtCO_2e.yr^{-1}$.

Region	Type of dataset									
	BU methods with GCP FCO_2					BU methods with PRIMAP FCO_2				
	GCP + uncorrected UNFCCC LULUCF CO_2	GCP + corrected UNFCCC LULUCF CO_2 as Grassi et al. (2022)	GCP + corrected UNFCCC LULUCF CO_2 as Grassi et al. (2022) but for DRC, NAM, NIG	GCP + median TRENDY v9 LULUCF CO_2 (min/max)	GCP + LULUCF CO_2 FAO total FL	PRIMAP + uncorrected UNFCCC LULUCF CO_2	PRIMAP + corrected UNFCCC LULUCF CO_2 as Grassi et al. (2022)	PRIMAP + corrected UNFCCC LULUC CO_2 as Grassi et al. (2022) but for DRC, NAM, NIG	PRIMAP + median TRENDY v9 LULUCF CO_2 (min/max)	PRIMAP + LULUCF CO_2 FAO total FL
Africa total	-599	2975	2122	2478^{4806}_{732}	2728	-502	3069	2216	2572^{4899}_{827}	2822
North Africa	613	589	589	835^{1216}_{549}	839	620	597	597	842^{1224}_{557}	846
Central Africa	-2605	316	-448	-318^{633}_{-879}	171	-2598	324	-440	-310^{641}_{-871}	179
Subsahelian West Africa	19	718	501	726^{1382}_{433}	503	15	714	497	723^{1378}_{430}	500
Southern Africa	149	346	473	251^{953}_{-453}	345	151	347	475	252^{955}_{-452}	346
South Africa group	640	524	524	542^{860}_{179}	546	719	603	603	621^{939}_{258}	625
Horn of Africa	586	484	484	438^{805}_{-109}	325	587	484	484	439^{806}_{-108}	326

At the country level, a small number of countries showed an increasing difference between PRIMAP-hist and GCP estimates of fossil CO_2 emissions over time, but they are small FCO_2 emitters. The differences may also be partly explained by changes in accounting methods as mentioned in Gütschow et al. (2016). The biggest discrepancies are noticeable for Mali (64%), Cameroon (-62%), and the DRC (-38%), but those three countries are not major FCO_2 emitters (Fig. 4.a-b).

Table 5 shows the differences of net African budget from various BU methods using GCP or PRIMAP-hist for FCO_2 over 2001-2017 that are also illustrated on Fig. 11.

~~Bottom-up~~ BU LULUCF budget from UNFCCC corrected by Grassi (2022)

Over 2001-2017 the net ~~bottom-up~~ BU GHG budget is 2975 $MtCO_2e\ yr^{-1}$. Regionally the ranking in decreasing order is: Sub-Sahelian West Africa (718 $MtCO_2e\ yr^{-1}$) > North Africa (588 $MtCO_2e\ yr^{-1}$) > South Africa group (524 $MtCO_2e\ yr^{-1}$) > Horn of Africa (484 $MtCO_2e\ yr^{-1}$) > Southern Africa (346 $MtCO_2e\ yr^{-1}$) > Central Africa (316 $MtCO_2e\ yr^{-1}$).

~~Bottom-up~~ BU LULUCF budget CO_2 from FAO

The ~~bottom-up~~ BU budget from FAO data is 2728 $MtCO_2e\ yr^{-1}$, 8% less than above. The ranking of regions in decreasing order is: North Africa (838 $MtCO_2e\ yr^{-1}$) > South Africa group (546 $MtCO_2e\ yr^{-1}$) > Sub-Sahelian West Africa (503 $MtCO_2e\ yr^{-1}$) > Southern Africa (345 $MtCO_2e\ yr^{-1}$) > Horn of Africa (325 $MtCO_2e\ yr^{-1}$) > Central Africa (171 $MtCO_2e\ yr^{-1}$).

~~Bottom-up~~ BU LULUCF budget from DGVMs

The net GHG budget for Africa is $2478^{4806}_{733}\ MtCO_2e\ yr^{-1}$, 9% less than with FAO. The ranking of regions in decreasing order is: North Africa ($835\ ^{1216}_{549}\ MtCO_2e\ yr^{-1}$) > Sub-Sahelian West Africa ($726\ ^{1382}_{433} MtCO_2e\ yr^{-1}$) > South Africa ($542\ ^{859}_{179}\ MtCO_2e\ yr^{-1}$) > Horn of Africa ($438^{805}_{-109}\ MtCO_2e\ yr^{-1}$) > Southern Africa ($251\ ^{953}_{-453} MtCO_2e\ yr^{-1}$ > Central Africa ($-318\ ^{633}_{-879}\ MtCO_2e\ yr^{-1}$).

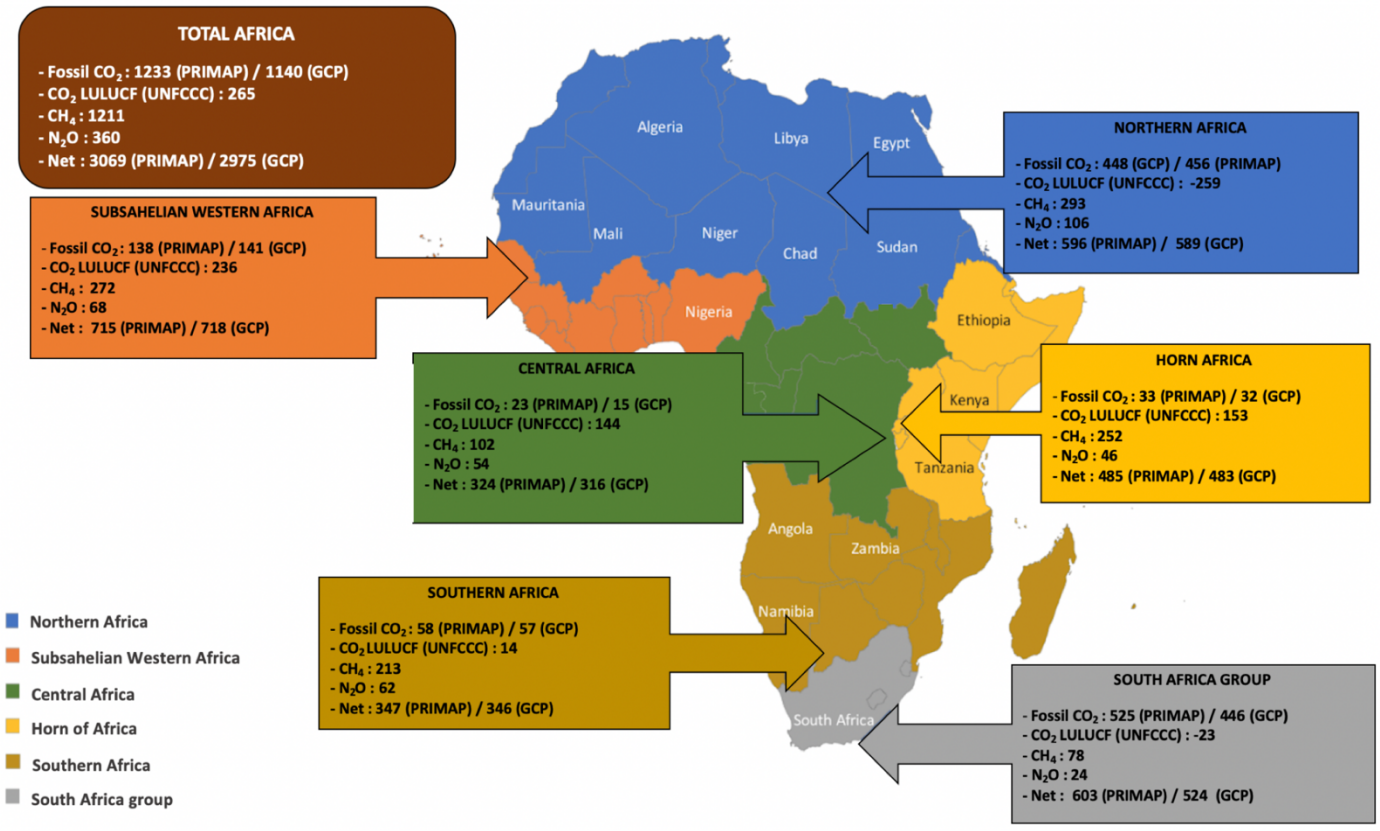

Figure 13~~1~~. 2001-2018 emissions in $MtCO_2e\ yr^{-1}$ for fossil CO_2 (GCP and PRIMAP-hist), LULUCF CO_2 (corrected UNFCCC data consistent with Grassi et al. (2022), CH_4 (PRIMAP-hist), N_2O (PRIMAP-hist) for Africa, and for six regions.

For information, in the supplement section Fig. S13 and Fig. S14 illustrate the differences in $MtCO_2e$ and in % for CH_4, N_2O and for the total net GHG budget that would result from the use of AR6 GWP100 compared to AR4 GWP100 currently in used by UNFCCC non-Annex I countries, for the six African regions considered on Fig.13 as well as for Africa total. The net difference on the total African budget for the use of GWP100 AR6 instead of AR4 is: +4.6%, which means a relatively small increasing impact on the net budget, with a prevailing effect of the slight increase of CH_4 GWP100 in the AR6 as compared to AR4, over the strong decrease of N_2O GWP-100. The two African regions that are the most impacted in terms of net budget are: Southern Countries (+7.2%) and the Horn of Africa (+6.3%). The least impacted region in terms of overall net budget with an updated AR6 GWP-100 for CH_4 and $N_2O$is South Africa (+1.7%).

4 Summary, concluding remarks and perspectives

Africa is a large continent gathering 56 countries, and some countries are major GHG emitters. Because of its rapidly growing population and high industrial potential, Africa is a critical geography regarding climate change mitigation and adaptation policy. Depending on the emissions pathways, Africa, which is already a big emitting region, is expected to represent between at least a bit more than 10% of the global share by 2050, and could become as high as 18% of global emissions by 2050 (van der Zwaan, 2018).

This paper delivers both a continental view and a detailed analysis of the three main GHG trends during the last thirty years across this continent as a whole, across relevant groups of countries given the inversions' resolutions, and also considering country details. Thanks to the comparison of different methods and datasets, the uncertainty about the net emissions and removals of GHG lowers. The interest of studying Africa is high not only from a scientific point of view, but also from a climate-policy perspective, as under the UNFCCC principle of "common but differentiated responsibility" about global warming, the credibility of the PA lies in the effective participation and inclusiveness of all parties, including non-Annex I countries. Our effort of comparing BU datasets and inversions and analyzing differences for African GHG emissions and removals assessment by looking at trends since 1990 will also be useful for future updates on a regular basis within the 2023 GST perspective.

At the scale of Africa, there is a rapid increase of FCO_2 emissions that roughly doubled since 1990. This increase is dominated by coal emissions for the decade 1990-1998 compared to 1999-2008 (+9%), and by oil for the decade 1999-2008 compared to the decade 2008-2017 (+16%). As for CO_2 LULUCF, we found that BU estimates are featured with important annual fluctuations, as opposed to periodic national inventories assessments, the reconciliation between the sectoral classification for anthropogenic estimates between TD and BU has to be done "manually" and is not uniform to date, which doesn't facilitate the comparability of those different approaches. There are also differences among GCP inversions for CO_2, due to the fact that choices of model transport may differ among models, because prior fluxes can also differ between modeling teams, and because the African GHG observation network is featured with few stations and relatively scarce data. The lack of integration of CO_2 lateral anthropogenic and river fluxes is also an issue to be taken into account when trying to compare BU and TD methods (Ciais et al., 2022), and in the present study we did integrate those lateral fluxes. Anthropogenic CH_4 from PRIMAP-hist estimates indicate that out of the total African emissions increase from 1064 $MtCO_2e\ yr^{-1}$ to 1116 $MtCO_2e\ yr^{-1}$ between 1990-2000 and 2001-2009 (+5%), only two sectors contributed: Agriculture, in a dominant way (+8%) and Waste (+5%). Energy contributes to emissions decrease (-8%) that is however too small to offset other sectors' CH_4 emissions that represent a net increase. The main regional contributions come from North Africa and from the Agriculture sector (+12%). Over the same period, the least contributing emitter is the group of South Africa (+12%), with only one decreasing emissions sector: Agriculture (-1%). The mean 2001-2009 emissions increased by +15% over 2010-2018 with

contribution from all sectors except IPPU. This increase is dominated by Agriculture (+8%) and Waste (+ 6%). For 2010-2018, the two main contributing regions for CH_4 emissions are Northern Africa and Sub-Sahelian Western Africa, Agriculture being the dominant emitting sector. From inversions, after withdrawing natural emissions and wildfires using the GFED dataset from total CH_4 emissions, median values are almost always below PRIMAP-hist estimates. CH_4 natural emissions have an important impact in Africa especially in the Central African region as well as in the Southern countries. N_2O TD estimates are always higher than the ones from PRIMAP-hist, underlining the importance to separate natural N_2O emissions from total estimates in order to deliver appropriate anthropogenic assessments thanks to the inversions.

To compute a net budget for the three main GHG emissions and removals and for comparability we used the $MtCO_2e\ yr^{-1}$ metric and the latest IPCC report recommended GWP. The choice of a constructed GWP metric, however, creates additional associated uncertainties notably due to the selected time horizon. By computing the mean of methods excluding uncorrected UNFCCC and N_2O inversions data from twenty different ways for assessing GHG emissions and removals in Africa, we found that the most recent net from the three main GHG in Africa is a source of 2630^{4557}_{1974} $MtCO_2e\ yr^{-1}$.

Our assessment of African GHG emissions trends over 30 years through different methods can enable comparisons of *ex post* with *ex ante* pledges of the PA, whose baseline year is often 1990. However, given the global geopolitics to date featured with the prevailing principle of national sovereignty, a scientific assessment of GHG can only work as a supporting tool (Janssens-Maenhout et al., 2020) and cannot be directly policy-prescriptive. We note a relatively good match among the various types of estimates in terms of overall trends, especially at a regional level and on a decadal basis, but large differences in terms of min / max and at annual scale even among similar typologies of the methods (TD or BU). The large discrepancies are a scientific limit to the possibility of precise verification of the African country-reported emissions, but they are good enough to indicate trends. To compute a net from the three main GHG, no purely "TD" method is available due to the necessity to replace N_2O inversions data with BU data. An original result of this study is that we proposed at a small scale what may become a systematic formalized methodological protocol for independent verification of a net estimate using country-reported data, to be possibly implemented at the UNFCCC secretariat scale in a centralized way. The African GHG increasing trend is not in line with the mitigation aims of the PA towards net-zero globally. Research teams focusing on inversion methods (Nickless et al., 2020), underline that uncertainties should not be above 15% in order to deliver a reasonable verification support capacity. A major source of complexity for the evaluation of the respect of the Paris Agreement comes from the fact that national pledges generally fall below the discrepancies between different scientific independent estimates. This calls for investments not only in improvements of atmospheric measurement devices but also in the research efforts for standardizing verification methods. At the policy level, the extrapolation of this study to the climate policy

field could also serve as a compelling argument for the creation of a global dedicated "Climate Inspection task force" of the UNFCCC.

5 Data availability

The datasets from the three main greenhouse gasses used in this paper (CO_2, CH_4, N_2O) from the various BU inventories, TD inversions and DGVM over Africa will be made publicly available. This database is available from Zenodo at: https://doi.org/10.5281/zenodo.7347077 (Mostefaoui et al., 2022).

This dataset contains 32 data files:

- CO_2 inversions (annual flux for LULUCF CO_2)

- African CO_2 TD inversions GCB2020 1990-2019: annual CO_2 flux from GCB inversion models
- African CO_2 lateral flux 2001-2019: annual CO_2 lateral flux including river transport, crop and wood product trade.
- African CO_2 TRENDYv9 1990-2019: annual CO_2 flux from 14 DGVM
- FAO 1990-2019: annual emissions and removals from FAO dataset
- Inventory IPCC 1990-2019: annual flux from inventory data collected from UNFCCC national inventories in the IPCC categories

- CH_4 inversions 2000-2017 (annual flux)

- African CH_4 global inversion 2000-2017: CH_4 flux over 2000-2017 from 11 surface inversion and 11 satellite inversion models from four sectors; fossil refers to emissions from the fossil sector; agriculture and waste refers to emissions from both the agriculture and waste sector; biomass burning refers to emissions from biomass burning
- GFEDv4 1997-2016: wildfire emissions from the Global Fires Emission Dataset (GFED) version 4

- N_2O inversions 1998-2017 (annual flux)

- N_2O PYVAR 1998-2017: total N_2O emissions from PyVAR inversions;
- N_2O TOMCAT-INVICAT 1998-2015: total N_2O emissions from TOMCAT-INVICAT model;
- N_2O MIROC4 - ACTM 1998-2016: total N_2O emissions from MIROC4-ACTM model;

Data used in this study are also included in the Supplementary Information (for example, from FAO data) and on public websites (CDIAC, PRIMAP-hist, World Bank data). Any other data that support the findings of this study are available from the corresponding author upon request.

Author contributions. MM, PC, PP and MJM designed research and led the discussions; MM wrote the initial draft of the paper and edited all the following versions; MM made all figures ; MJM and PP processed the original data from inversions and DGVM; MM processed the UNFCCC data and corrections; PC, PP and YE

gave valuable suggestions to the manuscript structure; PC, MJM and PPP read, gave comments and advice on previous versions of the manuscript; all co-authors commented on specific parts related to their datasets; PC, MJM, PP, FC, SS, CR, IL, MS, PP are data providers.

Competing interests. The authors declare that they have no conflict of interest.

Disclaimer. The views expressed in this publication are those of the authors.

Acknowledgements

MM acknowledges funding from Sorbonne University, Institute of the Environmental Transition. PC, PP, and MJM were supported by the European Commission, Horizon 2020 Framework Program (VERIFY, grant no. 776810). PC and YE are also supported by the RECCAP2 project (grant no. ESRIN/4000123002/18/I-NB). We acknowledge Stephen Sitch and Trendy modelers for the use of their dataset. We also acknowledge Christian Rödenbeck for the use of CarboScope, Frédéric Chevallier for CAMS, Ingrid Luijkx for CTE, Marielle Saunois for CH_4 inversions. The PyVAR-N_2O modeling results were provided by Rona Thompson (NILU) and were funded through the Copernicus Atmosphere Monitoring Service (https://atmosphere.copernicus.eu/), implemented by ECMWF on behalf of the European Commission, and were generated using computing resources from LSCE.

References

Andrew, R. M.: A comparison of estimates of global carbon dioxide emissions from fossil carbon sources, Earth Syst. Sci. Data, 12, 1437–1465, https://doi.org/10.5194/essd-12-1437-2020, 2020.

Ayompe, L. M., Davis, S. J., and Egoh, B. N.: Trends and drivers of African fossil fuel CO 2 emissions 1990–2017, Environ. Res. Lett., 15, 124039, https://doi.org/10.1088/1748-9326/abc64f, 2020.

BP. BP Statistical Review of World Energy, 2020.

Beck, H. E., Zimmermann, N. E., McVicar, T. R., Vergopolan, N., Berg, A., and Wood, E. F.: Present and future Köppen-Geiger climate classification maps at 1-km resolution, Sci. Data, 5, 180214, https://doi.org/10.1038/sdata.2018.214, 2018.

Bombelli, A., Henry, M., Castaldi, S., Adu-Bredu, S., Arneth, A., de Grandcourt, A., Grieco, E., Kutsch, W. L., Lehsten, V., Rasile, A., Reichstein, M., Tansey, K., Weber, U., and Valentini, R.: An outlook on the Sub-Saharan Africa carbon balance, Biogeosciences, 6, 2193–2205, https://doi.org/10.5194/bg-6-2193-2009, 2009.

Canadell, J. G., Raupach, M. R., and Houghton, R. A.: Anthropogenic CO2 emissions inAfrica, Biogeosciences, 6, 463–468, https://doi.org/10.5194/bg-6-463-2009, 2009.

Chevallier, F., Fisher, M., Peylin, P., Serrar, S., Bousquet, P., Bréon, F.-M., Chédin, A., and Ciais, P.: Inferring CO2 sources and sinks from satellite observations: Method and application to TOVS data, J. Geophys. Res. Atmospheres, 110, https://doi.org/10.1029/2005JD006390, 2005.

Ciais, P., Bastos, A., Chevallier, F., Lauerwald, R., Poulter, B., Canadell, J. G., Hugelius, G., Jackson, R. B., Jain, A., Jones, M., Kondo, M., Luijkx, I. T., Patra, P. K., Peters, W., Pongratz, J., Petrescu, A. M. R., Piao, S., Qiu, C., Von Randow, C., Regnier, P., Saunois, M., Scholes, R., Shvidenko, A., Tian, H., Yang, H., Wang, X., and Zheng, B.: Definitions and methods to estimate regional land carbon fluxes for the second phase of the REgional Carbon Cycle Assessment and Processes Project (RECCAP-2), Geosci. Model Dev., 15, 1289–1316, https://doi.org/10.5194/gmd-15-1289-2022, 2022.

Deng, Z., Ciais, P., Tzompa-Sosa, Z. A., Saunois, M., Qiu, C., Tan, C., Sun, T., Ke, P., Cui, Y., Tanaka, K., Lin, X., Thompson, R. L., Tian, H., Yao, Y., Huang, Y., Lauerwald, R., Jain, A. K., Xu, X., Bastos, A., Sitch, S., Palmer, P. I., Lauvaux, T., d'Aspremont, A., Giron, C., Benoit, A., Poulter, B., Chang, J., Petrescu, A. M. R., Davis, S. J., Liu, Z., Grassi, G., Albergel, C., and Chevallier, F.: Comparing national greenhouse gas budgets reported in UNFCCC inventories against atmospheric inversions, Earth Syst. Sci. Data Discuss., 1–59, https://doi.org/10.5194/essd-2021-235, 2021.

Dorfman, R.: A formula for the Gini Coefficient. The Review of Economics and Statistics Vol. 61, No. 1 , https://doi.org/10.2307/1924845,1979.

FAOSTAT: available at: https://www.fao.org/faostat/en/#data/GF, last access: 3 May 2022.

FAO FRA: FAO Global Forests Resource Assessment, available at fra-data.fao.org, last access: June 2022, 2022.

Friedlingstein, P., Jones, M. W., O'Sullivan, M., Andrew, R. M., Hauck, J., Peters, G. P., Peters, W., Pongratz, J., Sitch, S., Le Quéré, C., Bakker, D. C. E., Canadell, J. G., Ciais, P., Jackson, R. B., Anthoni, P., Barbero, L., Bastos, A., Bastrikov, V., Becker, M., Bopp, L., Buitenhuis, E., Chandra, N., Chevallier, F., Chini, L. P., Currie, K. I., Feely, R. A., Gehlen, M., Gilfillan, D., Gkritzalis, T., Goll, D. S., Gruber, N., Gutekunst, S., Harris, I., Haverd, V., Houghton, R. A., Hurtt, G., Ilyina, T., Jain, A. K., Joetzjer, E., Kaplan, J. O., Kato, E., Klein Goldewijk, K., Korsbakken, J. I., Landschützer, P., Lauvset, S. K., Lefèvre, N., Lenton, A., Lienert, S., Lombardozzi, D., Marland, G., McGuire, P. C., Melton, J. R., Metzl, N., Munro, D. R., Nabel, J. E. M. S., Nakaoka, S.-I., Neill, C., Omar, A. M., Ono, T., Peregon, A., Pierrot, D., Poulter, B., Rehder, G., Resplandy, L., Robertson, E., Rödenbeck, C., Séférian, R., Schwinger, J., Smith, N., Tans, P. P., Tian, H., Tilbrook, B., Tubiello, F. N., van der Werf, G. R., Wiltshire, A. J., and Zaehle, S.: Global Carbon Budget 2019, Earth Syst. Sci. Data, 11, 1783–1838, https://doi.org/10.5194/essd-11-1783-2019, 2019.

Friedlingstein, P., O'Sullivan, M., Jones, M. W., Andrew, R. M., Hauck, J., Olsen, A., Peters, G. P., Peters, W., Pongratz, J., Sitch, S., Le Quéré, C., Canadell, J. G., Ciais, P., Jackson, R. B., Alin, S., Aragão, L. E. O. C., Arneth, A., Arora, V., Bates, N. R., Becker, M., Benoit-Cattin, A., Bittig, H. C., Bopp, L., Bultan, S., Chandra, N., Chevallier, F., Chini, L. P., Evans, W., Florentie, L., Forster, P. M., Gasser, T., Gehlen, M., Gilfillan, D., Gkritzalis, T., Gregor, L., Gruber, N., Harris, I., Hartung, K., Haverd, V., Houghton, R. A., Ilyina, T., Jain, A. K., Joetzjer, E., Kadono, K., Kato, E., Kitidis, V., Korsbakken, J. I., Landschützer, P., Lefèvre, N., Lenton, A., Lienert, S., Liu, Z., Lombardozzi, D., Marland, G., Metzl, N., Munro, D. R., Nabel, J. E. M. S., Nakaoka, S.-I., Niwa, Y., O'Brien, K., Ono, T., Palmer, P. I., Pierrot, D., Poulter, B., Resplandy, L., Robertson, E., Rödenbeck, C., Schwinger, J., Séférian, R., Skjelvan, I., Smith, A. J. P., Sutton, A. J., Tanhua, T., Tans, P. P., Tian, H., Tilbrook, B., van der Werf, G., Vuichard, N., Walker, A. P., Wanninkhof, R., Watson, A. J., Willis,

D., Wiltshire, A. J., Yuan, W., Yue, X., and Zaehle, S.: Global Carbon Budget 2020, Earth Syst. Sci. Data, 12, 3269–3340, https://doi.org/10.5194/essd-12-3269-2020, 2020.

Gilfillan, D., and Marland G.: CDIAC-FF: global and national CO2 emissions from fossil fuel combustion and cement manufacture: 1751–2017, https://doi.org/10.5194/essd-13-1667-2021 , 2021.

Grassi, G., House, J., Kurz, W. A., Cescatti, A., Houghton, R. A., Peters, G. P., Sanz, M. J., Viñas, R. A., Alkama, R., Arneth, A., Bondeau, A., Dentener, F., Fader, M., Federici, S., Friedlingstein, P., Jain, A. K., Kato, E., Koven, C. D., Lee, D., Nabel, J. E. M. S., Nassikas, A. A., Perugini, L., Rossi, S., Sitch, S., Viovy, N., Wiltshire, A., and Zaehle, S.: Reconciling global-model estimates and country reporting of anthropogenic forest CO2 sinks, Nat. Clim. Change, 8, 914–920, https://doi.org/10.1038/s41558-018-0283-x, 2018.

Grassi, G., Stehfest, E., Rogelj, J., van Vuuren, D., Cescatti, A., House, J., Nabuurs, G.-J., Rossi, S., Alkama, R., Viñas, R. A., Calvin, K., Ceccherini, G., Federici, S., Fujimori, S., Gusti, M., Hasegawa, T., Havlik, P., Humpenöder, F., Korosuo, A., Perugini, L., Tubiello, F. N., and Popp, A.: Critical adjustment of land mitigation pathways for assessing countries' climate progress, Nat. Clim. Change, 11, 425–434, https://doi.org/10.1038/s41558-021-01033-6, 2021.

Grassi, G., Conchedda, G., Federici, S., Abad Viñas, R., Korosuo, A., Melo, J., Rossi, S., Sandker, M., Somogyi, Z., and Tubiello, F. N.: Carbon fluxes from land 2000–2020: bringing clarity on countries' reporting, Biogeosciences and biodiversity, https://doi.org/10.5194/essd-2022-104, 2022.

Gütschow, J., Jeffery, M. L., Gieseke, R., Gebel, R., Stevens, D., Krapp, M., and Rocha, M.: The PRIMAP-hist national historical emissions time series, Earth Syst. Sci. Data, 8, 571–603, https://doi.org/10.5194/essd-8-571-2016, 2016.

Gütschow, J., Günther, A., Jeffery, M. L., and Gieseke, R.: The PRIMAP-hist national historical emissions time series (1850-2018) v2.2, https://doi.org/10.5281/zenodo.4479172, 2021.

Houghton, R. A., House, J. I., Pongratz, J., van der Werf, G. R., DeFries, R. S., Hansen, M. C., Le Quéré, C., and Ramankutty, N.: Carbon emissions from land use and land-cover change, Biogeosciences, 9, 5125–5142, https://doi.org/10.5194/bg-9-5125-2012, 2012.

IMF: International Monetary Fund: International Monetary Fund website, available at: https://www.imf.org/en/Publications/fandd/issues/Series/Back-to-Basics/gross-domestic-product-GDP, last access : February 2022.

IPCC: Good practice guidance for land use, land-use change and forestry /The Intergovernmental Panel on Climate Change. Edited by: Penman, J., Hayama, Kanagawa, 2006.

IPCC: Climate Change and Land: an IPCC special report on climate change, desertification, land degradation, sustainable land management, food security, and greenhouse gas fluxes in terrestrial ecosystems, [Shukla, P.R., Skea, J., CalvoBuendia,E., Masson-Delmotte, V., Pörtner, H.-O., Roberts, D. C., Zhai, P., Slade, R., Connors, S., van Diemen, R., Ferrat, M., Haughey, E., Luz, S., Neogi, S., Pathak, M., Petzold, J., Portugal Pereira, J., Vyas, P., Huntley, E., Kissick, K., Belkacemi, M., Malley,J. (eds.)]. In press, 2019.

IPCC: Revised 1996 IPCC Guidelines for National Greenhouse Inventories, IPCC/OECD/IEA, Paris, France, ISBN 92-64-15578- 3, 1997.

IPCC: 2006 IPCC guidelines for National Greenhouse Gas Inventories, IGES, ISBN 4-88788-032-4, 2006.

IPCC: 2019 Refinement to the 2006 IPCC Guidelines for National Greenhouse Gas Inventories, edited by: Buendia, E., Tanabe, K., Kranjc, A., Baasansuren, J., Fukuda, M., Ngarize, S., Osako, A., Pyrozhenko, Y., Shermanau, P., and Federici, S., Intergovernmental Panel on Climate Change (IPCC), Switzerland, ISBN 978-4-88788-232-4, 2019.

IPCC: Climate Change 2021: The Physical Science Basis. Contribution of Working Group I to the Sixth Assessment Report of the Intergovernmental Panel on Climate Change[Masson-Delmotte, V., P. Zhai, A. Pirani, S.L. Connors, C. Péan, S. Berger, N. Caud, Y. Chen, L. Goldfarb, M.I. Gomis, M. Huang, K. Leitzell, E. Lonnoy, J.B.R. Matthews, T.K. Maycock, T. Waterfield, O. Yelekçi, R. Yu, and B. Zhou (eds.)]. Cambridge University Press, Cambridge, United Kingdom and New York, NY, USA, In press, doi:10.1017/9781009157896, 2021.

Janssens-Maenhout, G., Pinty, B., Dowell, M., Zunker, H., Andersson, E., Balsamo, G., Bézy, J.-L., Brunhes, T., Bösch, H., Bojkov, B., Brunner, D., Buchwitz, M., Crisp, D., Ciais, P., Counet, P., Dee, D., Gon, H. D. van der, Dolman, H., Drinkwater, M. R., Dubovik, O., Engelen, R., Fehr, T., Fernandez, V., Heimann, M., Holmlund, K., Houweling, S., Husband, R., Juvyns, O., Kentarchos, A., Landgraf, J., Lang, R., Löscher, A., Marshall, J., Meijer, Y., Nakajima, M., Palmer, P. I., Peylin, P., Rayner, P., Scholze, M., Sierk, B., Tamminen, J., and Veefkind, P.: Toward an Operational Anthropogenic CO2 Emissions Monitoring and Verification Support Capacity, Bull. Am. Meteorol. Soc., 101, E1439–E1451, https://doi.org/10.1175/BAMS-D-19-0017.1, 2020.

van der Laan-Luijkx, I. T., van der Velde, I. R., van der Veen, E., Tsuruta, A., Stanislawska, K., Babenhauserheide, A., Zhang, H. F., Liu, Y., He, W., Chen, H., Masarie, K. A., Krol, M. C., and Peters, W.: The CarbonTracker Data Assimilation Shell (CTDAS) v1.0: implementation and global carbon balance 2001–2015, Geosci. Model Dev., 10, 2785–2800, https://doi.org/10.5194/gmd-10-2785-2017, 2017.

Liousse, C., Assamoi, E., Criqui, P., Granier, C., and Rosset, R.: Explosive growth in African combustion emissions from 2005 to 2030, Environ. Res. Lett., 9, 035003, https://doi.org/10.1088/1748-9326/9/3/035003, 2014.

Mostefaoui, M., Ciais, P., McGrath, M. J., Peylin, P., Prabir, P. K., Saunois, M., Chevallier, F., Sitch, S., Rodenbeck, C., Luijkx, I., and Thompson, R.: Datasets for greenhouse gasses emissions and removals from inventories and global models over Africa v0.1, Zenodo [data set], https://doi.org/10.5281/zenodo.7347077, 2022.

Monks, S. A., Arnold, S. R., Hollaway, M. J., Pope, R. J., Wilson, C., Feng, W., Emmerson, K. M., Kerridge, B. J., Latter, B. L., Miles, G. M., Siddans, R., and Chipperfield, M. P.: The TOMCAT global chemical transport model v1.6: description of chemical mechanism and model evaluation, Geosci. Model Dev., 10, 3025–3057, https://doi.org/10.5194/gmd-10-3025-2017, 2017.

Nickless, A., Scholes, R. J., Vermeulen, A., Beck, J., López-Ballesteros, A., Ardö, J., Karstens, U., Rigby, M., Kasurinen, V., Pantazatou, K., Jorch, V., and Kutsch, W.: Greenhouse gas observation network design for Africa, Tellus B Chem. Phys. Meteorol., 72, 1–30, https://doi.org/10.1080/16000889.2020.1824486, 2020.

Patra, P. K., Takigawa, M., Watanabe, S., Chandra, N., Ishijima, K., and Yamashita, Y.: Improved Chemical Tracer Simulation by MIROC4.0-based Atmospheric Chemistry-Transport Model (MIROC4-ACTM), Sola, 14, 91–96, https://doi.org/10.2151/sola.2018-016, 2018.

Perugini, L., Pellis, G., Grassi, G., Ciais, P., Dolman, H., House, J. I., Peters, G. P., Smith, P., Günther, D., and Peylin, P.: Emerging reporting and verification needs under the Paris Agreement: How can the research community effectively contribute?, Environ. Sci. Policy, 122, 116–126, https://doi.org/10.1016/j.envsci.2021.04.012, 2021.

Petrescu, A. M. R., Qiu, C., Ciais, P., Thompson, R. L., Peylin, P., McGrath, M. J., Solazzo, E., Janssens-Maenhout, G., Tubiello, F. N., Bergamaschi, P., Brunner, D., Peters, G. P., Höglund-Isaksson, L., Regnier, P., Lauerwald, R., Bastviken, D., Tsuruta, A., Winiwarter, W., Patra, P. K., Kuhnert, M., Oreggioni, G. D., Crippa, M., Saunois, M., Perugini, L., Markkanen, T., Aalto, T., Groot Zwaaftink, C. D., Tian, H., Yao, Y., Wilson, C., Conchedda, G., Günther, D., Leip, A., Smith, P., Haussaire, J.-M., Leppänen, A., Manning, A. J., McNorton, J., Brockmann, P., and Dolman, A. J.: The consolidated European synthesis of CH4 and N2O emissions for the European Union and United Kingdom: 1990–2017, Earth Syst. Sci. Data, 13, 2307–2362, https://doi.org/10.5194/essd-13-2307-2021, 2021.

Pongratz, J., Reick, C. H., Houghton, R. A., & House, J. I.: Terminology as a key uncertainty in net land use and land cover change carbon flux estimates. Earth System Dynamics, 5(1), 177-195. https://doi.org/10.5194/esd-5-177-2014, 2014.

PRIMAP-hist: PRIMAP-hist dataset, available at: https://www.pik-potsdam.de/paris-reality-check/primap-hist (last access: April 2022), 2021.

Rödenbeck, C.: Estimating CO2 sources and sinks from atmospheric mixing ratio measurements using a global inversion of atmospheric transport, undefined, 2005.

Rodgers, C. D.: Inverse Methods For Atmospheric Sounding: Theory And Practice, World Scientific, 256 pp., 2000.

Saunois, M., Stavert, A. R., Poulter, B., Bousquet, P., Canadell, J. G., Jackson, R. B., Raymond, P. A., Dlugokencky, E. J., Houweling, S., Patra, P. K., Ciais, P., Arora, V. K., Bastviken, D., Bergamaschi, P., Blake, D. R., Brailsford, G., Bruhwiler, L., Carlson, K. M., Carrol, M., Castaldi, S., Chandra, N., Crevoisier, C., Crill, P. M., Covey, K., Curry, C. L., Etiope, G., Frankenberg, C., Gedney, N., Hegglin, M. I., Höglund-Isaksson, L., Hugelius, G., Ishizawa, M., Ito, A., Janssens-Maenhout, G., Jensen, K. M., Joos, F., Kleinen, T., Krummel, P. B., Langenfelds, R. L., Laruelle, G. G., Liu, L., Machida, T., Maksyutov, S., McDonald, K. C., McNorton, J., Miller, P. A., Melton, J. R., Morino, I., Müller, J., Murguia-Flores, F., Naik, V., Niwa, Y., Noce, S., O'Doherty, S., Parker, R. J., Peng, C., Peng, S., Peters, G. P., Prigent, C., Prinn, R., Ramonet, M., Regnier, P., Riley, W. J., Rosentreter, J. A., Segers, A., Simpson, I. J., Shi, H., Smith, S. J., Steele, L. P., Thornton, B. F., Tian, H., Tohjima, Y., Tubiello, F. N., Tsuruta, A., Viovy, N., Voulgarakis, A., Weber, T. S., van Weele, M., van der Werf, G. R., Weiss, R. F., Worthy, D., Wunch, D., Yin, Y., Yoshida, Y., Zhang, W., Zhang, Z., Zhao, Y., Zheng, B., Zhu, Q., Zhu, Q., and Zhuang, Q.: The Global Methane Budget 2000–2017, Earth Syst. Sci. Data, 12, 1561–1623, https://doi.org/10.5194/essd-12-1561-2020, 2020.

Schulz, E., Speekenbrink, M., Krause, A.: A tutorial on Gaussian process regression: Modelling, exploring, and exploiting functions, Journal of Mathematical Psychology, https://doi.org/10.1016/j.jmp.2018.03.001, 2018.

Sitch, S., Huntingford, C., Gedney, N., Levy, P. E., Lomas, M., Piao, S. L., Betts, R., Ciais, P., Cox, P., Friedlingstein, P., Jones, C. D., Prentice, I. C., and Woodward, F. I.: Evaluation of the terrestrial carbon cycle,

future plant geography and climate-carbon cycle feedbacks using five Dynamic Global Vegetation Models (DGVMs), Glob. Change Biol., 14, 2015–2039, https://doi.org/10.1111/j.1365-2486.2008.01626.x, 2008.

Thompson, R. L., Chevallier, F., Crotwell, A. M., Dutton, G., Langenfelds, R. L., Prinn, R. G., Weiss, R. F., Tohjima, Y., Nakazawa, T., Krummel, P. B., Steele, L. P., Fraser, P., O'Doherty, S., Ishijima, K., and Aoki, S.: Nitrous oxide emissions 1999 to 2009 from a global atmospheric inversion, Atmospheric Chem. Phys., 14, 1801–1817, https://doi.org/10.5194/acp-14-1801-2014, 2014.

Tian, H., Xu, R., Canadell, J. G., Thompson, R. L., Winiwarter, W., Suntharalingam, P., Davidson, E. A., Ciais, P., Jackson, R. B., Janssens-Maenhout, G., Prather, M. J., Regnier, P., Pan, N., Pan, S., Peters, G. P., Shi, H., Tubiello, F. N., Zaehle, S., Zhou, F., Arneth, A., Battaglia, G., Berthet, S., Bopp, L., Bouwman, A. F., Buitenhuis, E. T., Chang, J., Chipperfield, M. P., Dangal, S. R. S., Dlugokencky, E., Elkins, J. W., Eyre, B. D., Fu, B., Hall, B., Ito, A., Joos, F., Krummel, P. B., Landolfi, A., Laruelle, G. G., Lauerwald, R., Li, W., Lienert, S., Maavara, T., MacLeod, M., Millet, D. B., Olin, S., Patra, P. K., Prinn, R. G., Raymond, P. A., Ruiz, D. J., van der Werf, G. R., Vuichard, N., Wang, J., Weiss, R. F., Wells, K. C., Wilson, C., Yang, J., and Yao, Y.: A comprehensive quantification of global nitrous oxide sources and sinks, Nature, 586, 248–256, https://doi.org/10.1038/s41586-020-2780-0, 2020.

Tongwane, M. I. and Moeletsi, M. E.: A review of greenhouse gas emissions from the agriculture sector in Africa, Agric. Syst., 166, 124–134, https://doi.org/10.1016/j.agsy.2018.08.011, 2018.

UNFCCC: UNFCCC: National Inventory Submissions, available at: https://unfccc.int/ (last access : March 2021), 2021.

UNFCCC REDD+: REDD+ National Reports, available at: https://redd.unfccc.int/submissions.html?topic=6 (last access: July 2022), 2022.

United Nations Department of Economic and Social Affairs, Population Division: World Population Prospects 2019: Summary of Results, 2019.

Valentini, R., Arneth, A., Bombelli, A., Castaldi, S., Cazzolla Gatti, R., Chevallier, F., Ciais, P., Grieco, E., Hartmann, J., Henry, M., Houghton, R. A., Jung, M., Kutsch, W. L., Malhi, Y., Mayorga, E., Merbold, L., Murray-Tortarolo, G., Papale, D., Peylin, P., Poulter, B., Raymond, P. A., Santini, M., Sitch, S., Vaglio Laurin, G., van der Werf, G. R., Williams, C. A., and Scholes, R. J.: A full greenhouse gases budget of Africa: synthesis, uncertainties, and vulnerabilities, Biogeosciences, 11, 381–407, https://doi.org/10.5194/bg-11-381-2014, 2014.

van der Werf, G. R., Randerson, J. T., Giglio, L., van Leeuwen, T. T., Chen, Y., Rogers, B. M., Mu, M., van Marle, M. J. E., Morton, D. C., Collatz, G. J., Yokelson, R. J., and Kasibhatla, P. S.: Global fire emissions estimates during 1997–2016, Earth Syst. Sci. Data, 9, 697–720, https://doi.org/10.5194/essd-9-697-2017, 2017.

Wilson, C., Chipperfield, M. P., Gloor, M., and Chevallier, F.: Development of a variational flux inversion system (INVICAT v1.0) using the TOMCAT chemical transport model, Geosci. Model Dev., 7, 2485–2500, https://doi.org/10.5194/gmd-7-2485-2014, 2014.

World Bank: GDP exchange rate estimates, available at https://data.worldbank.org/indicator/NY.GDP.MKTP.CD last accessed, 2019.

World Bank: World Bank economic data, available at: https://www.worldbank.org/ (last access: May 2022), 2022.

Zhu, Y., Merbold, L., Pelster, D., Diaz-Pines, E., Wanyama, G. N., and Butterbach-Bahl, K.: Effect of Dung Quantity and Quality on Greenhouse Gas Fluxes From Tropical Pastures in Kenya, Glob. Biogeochem. Cycles, 32, 1589–1604, https://doi.org/10.1029/2018GB005949, 2018.

van der Zwaan, B., Kober, T., Longa, F. D., van der Laan, A., and Jan Kramer, G.: An integrated assessment of pathways for low-carbon development in Africa, Energy Policy, 117, 387–395, https://doi.org/10.1016/j.enpol.2018.03.017, 2018.

Supplementary figures and methods

Table S1. Surface flasks characteristics over the African continent. Data synthetized from NOAA website: https://www.noaa.gov.

Station name, Country	Parameter	First sample date	Status for the three GHG	Frequency	Elevation (in meters above mean sea level)	Cooperating Agencies
Assekrem, Algeria	CO_2 CH_4 N_2O	12/09/1995 12/09/1995 12/09/1995	Terminated since 26/08/2020	Discrete Monthly	2710	Algerian National Office of Meteorology
Gobabeb, Namibia	CO_2 CH_4 N_2O	13/01/1997 13/01/1997 13/01/1997	Ongoing	Discrete Monthly	456	Gobabeb Training and Research Center
Mahe Island, Seychelles	CO_2 CH_4 N_2O	15/01/1980 12/05/1983 13/06/1997	Ongoing	Discrete Monthly	2	Seychelles Bureau of Standards
Cape Point, South Africa	CO_2 CH_4 N_2O	5/01/1980 12/05/1983 13/06/1997	Ongoing	Discrete Monthly	230	South African Weather Service
Mt. Kenya, Kenya	CO_2 CH_4 N_2O	11/02/2010 11/02/2010 11/02/2010	Inactive since 21/06/2011	Discrete Monthly	3644	Kenya Meteorological Department

Table S2. List of African countries per group.

Country name	Group
Algeria Chad Egypt Eritrea Libya Mali Mauritania Morocco Niger Sudan Tunisia	Northern Africa
Benin Burkina Faso Cape verde Ivory Cote Gambia Ghana Guinea Guinea-Bissau Liberia Nigeria Sao Tome and Principe Senegal Sierra Leone Togo	Subsahelian Western Africa
Cameroon Central African Republic Democratic Republic of the Congo Gabon Republic of the Congo South Sudan	Central African countries
Burundi Comoros Djibouti Ethiopia Kenya Rwanda Seychelles Somalia Uganda United Republic of Tanzania	Horn of Africa
Angola Botswana Madagascar Malawi Mauritius Mozambique Namibia Zambia Zimbabwe	Southern countries
Lesotho South Africa Swaziland	Group of South Africa

Methodological Supplementary M1 - discussion about the rescaling for CO_2 inversions

Supprimé: 2

We operated a rescaling by subtracting back the prescribed fossil fuel fluxes to make sure that the inversions do not differ regarding prior fluxes for better comparability.

Figure S1. Comparison of PRIMAP-hist, GCP versus prescribed fossil fluxes for three CO_2 inversion models at the regional scale.

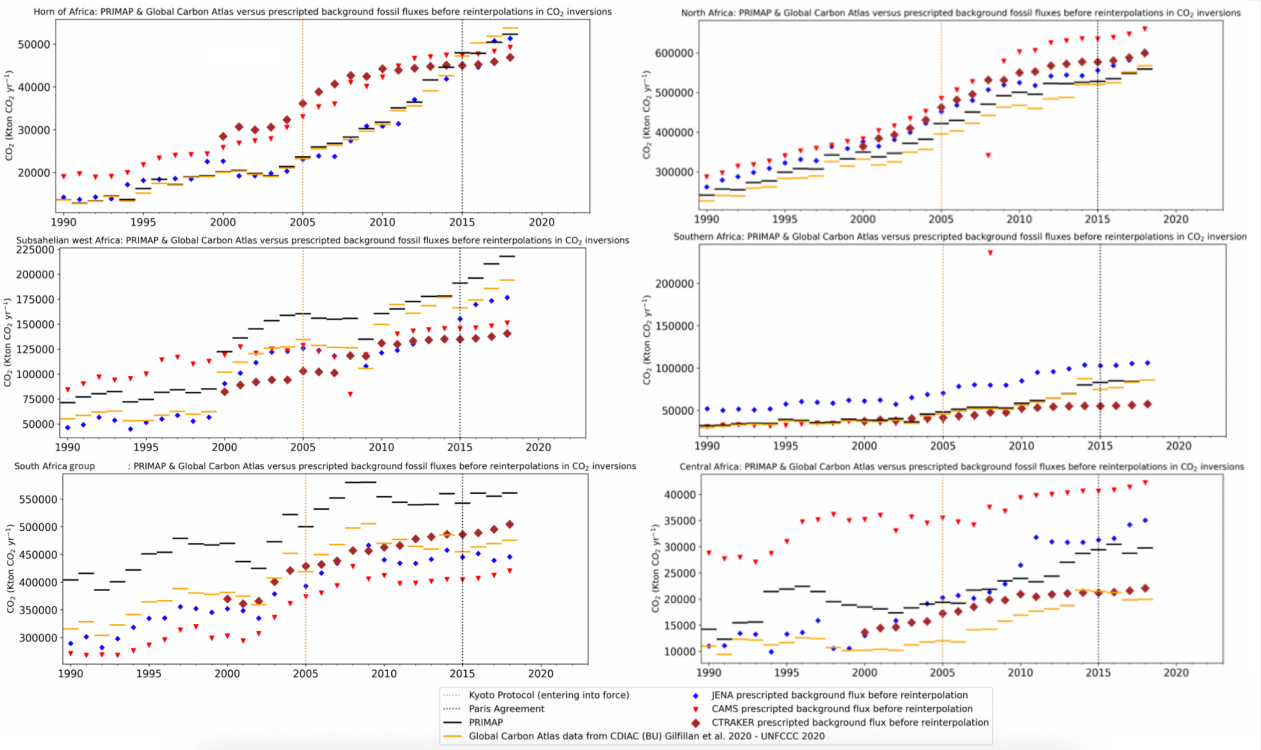

Figure S2. Map of six African groups.

Supprimé: 1

Table S3. Data sources for the anthropogenic fossil CO_2 emissions included in this study.

Method	Product type / file name	Species	Overall period covered	References
BU	GCP/CDIAC	CO_2 fossil country totals with detailed emissions separating different subsectors	1990-2019	-GCP (Le Quéré et al., 2018; Friedlingstein et al., 2019) -CDIAC https://cdiac.ess-dive.lbl.gov/
BU	PRIMAP-hist	CO_2, CH_4 and N_2O fossil country totals (excluding LULUCF) with detailed emissions separating different subsectors	1990-2019	-PRIMAP https://www.pik-potsdam.de/paris-reality-check/primap-hist/

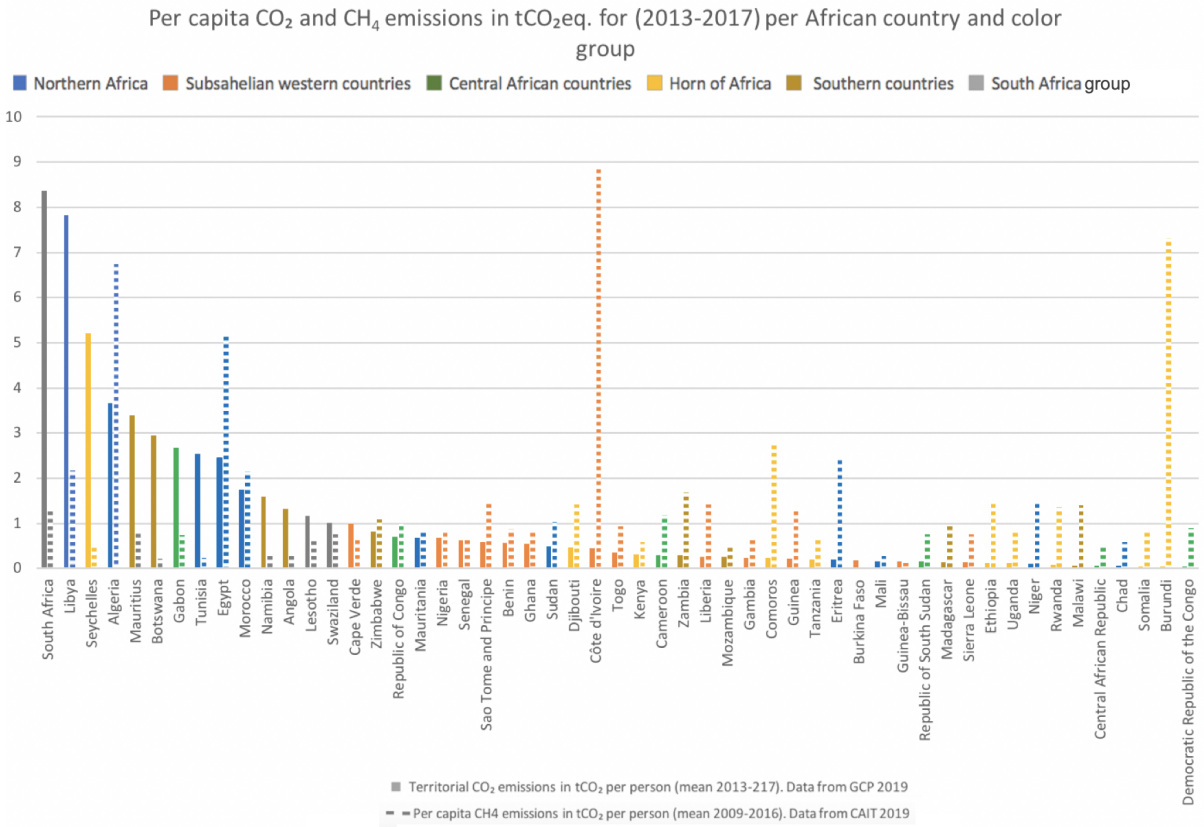

Figure S3. Bar plots of detailed African emissions for the mean values of the recent five years for fossil CO_2 and anthropogenic CH_4 in tCO_2e per capita, and by group color for 2009-2016.

Supprimé: 2

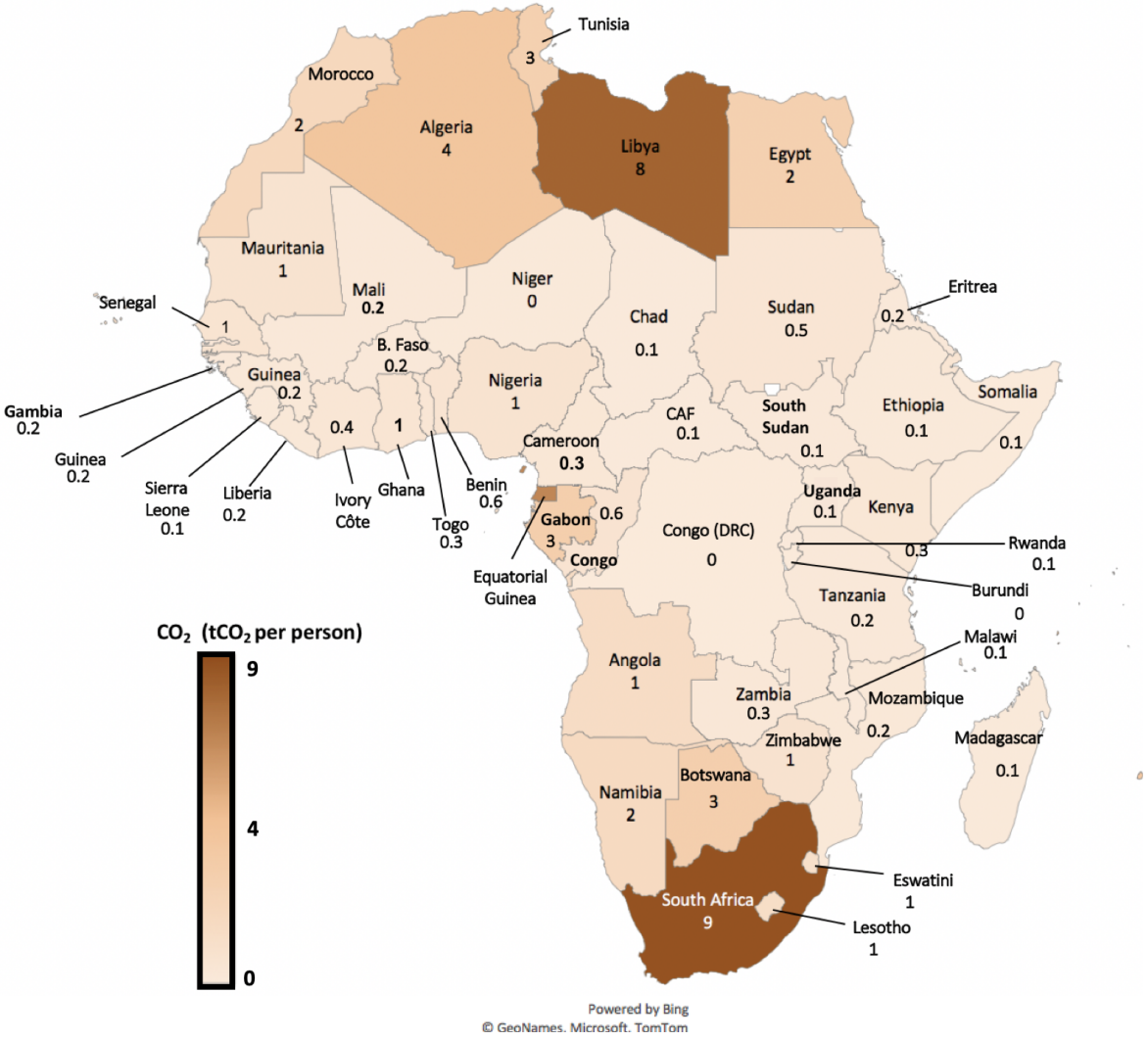

Figure S4. Map of African decennial 2009-2018 GCP CO_2 fossil fuel emissions per capita in tCO_2 per person - CDIAC.

Supprimé: 3

Methodological supplementary M2. Steps for computing the GINI index of African country emissions.

Supprimé: 1

The GINI index is a metric assessing the level of dispersion and therefore the level of inequalities among the values of a given dataset. To show the inequalities of per capita emissions among the African countries, we computed the continent GINI index for each of the last three decades using the Pareto principle for the following fluxes: fossil CO_2 per capita emissions, CH_4 fossil + agriculture per capita emissions, CH_4 from agriculture per capita emissions.

We computed the GINI using the Paretto method also named 20/80 or ABC method, using an excel file for the several countries' data manipulation. We obtained the GINI index (γ) thanks to the formula:

$$\gamma = \frac{[(\sum_{1}^{n} y_i \times x) - 5000\ ]}{5000}$$

When γ is bigger than 0.6, it means that the area delimited by the curve of the cumulated criterion and the graph diagonal represents more than 60% of the surface of half of the graph, and that the dispersion of the dataset is high. This method was built in the 19th century based on Vilfredo Paretto's observations regarding the inequalities of repartition of the volume of housing taxes among the taxpayers (he realized that 80% of this tax was paid by 20% of the taxpayer.) The different steps that we followed to compute the GINI are detailed below:

1) computation of the territorial emissions per capita in every African country,
2) ranking in a decreasing order (from the highest to the smallest one),
3) computation of the cumulative emissions,
4) creation of a column with the cumulative emissions expressed as a percentage,
5) creation of a column with a rank (integer) for those ordered emissions from the biggest to the smallest,
6) conversion of this rank as a percentage in another column,
7) distinction of the emissions representing less than 25% of emissions, less than 50%, and less than 75% of emissions.
8) computation of the GINI index (γ) thanks to the Paretto's formula given above.

Methodological supplementary M3. Computation of correlation coefficient.

In mathematics, the linear correlation between two variables that we can call X and Y implies that two variables have a linear relationship between each other. If there is a linear relation between two variables, it can be represented by a straight line. To compute this linear correlation coefficient, we use the Pearson formula that is the computation of the covariance among variables (cov(X,Y)) , divided by the product of their standard deviation (σ_X and σ_Y). Thus, we can compute the linear correlation $\rho_{X,Y}$ among two variables by using the following formula: $\rho_{X,Y} = \frac{\mathrm{cov}(X,Y)}{\sigma_X \sigma_Y}$

The higher the absolute value of a linear correlation coefficient between two variables, the more the variables are linearly correlated.

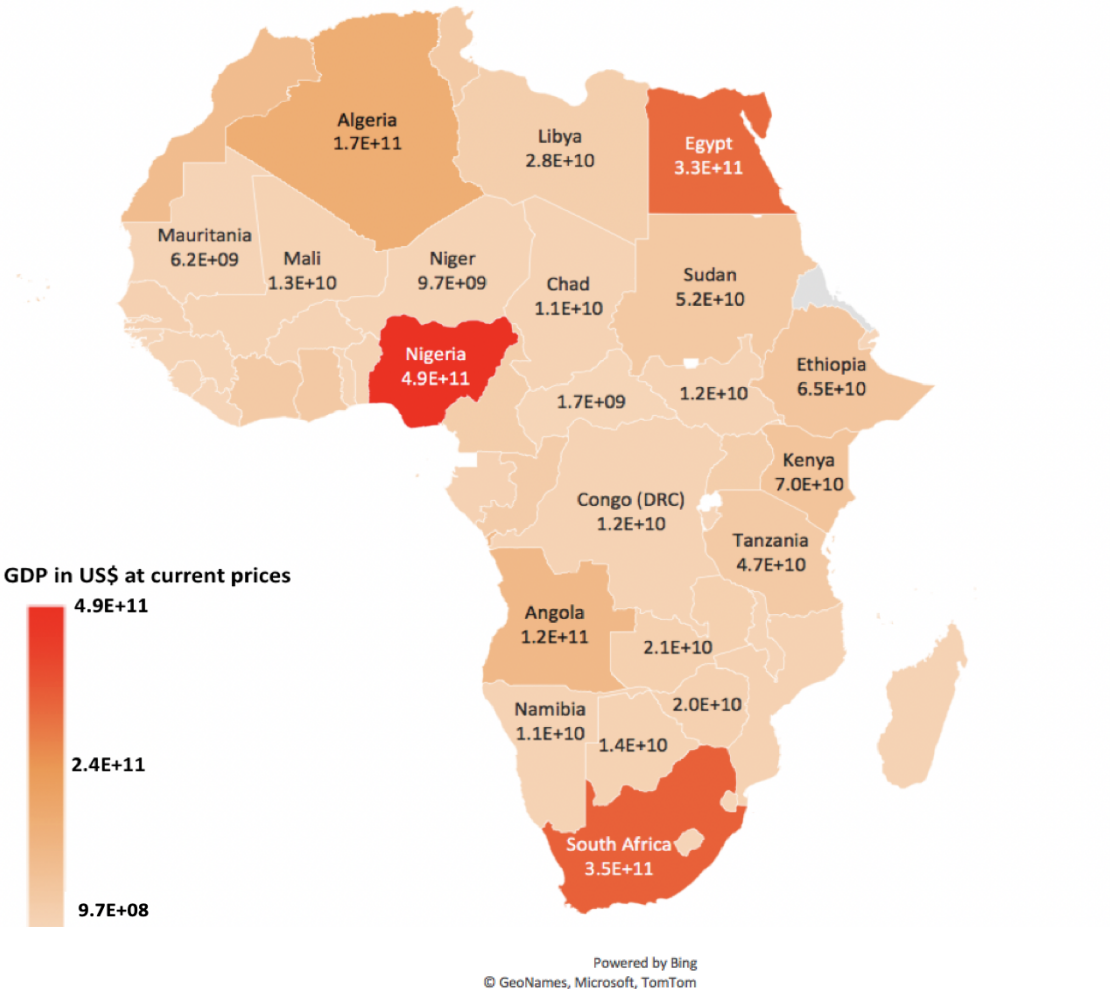

Figure S5. Bar plots and associated map of African GDP in US$ for the year 2015, dataset taken from World Bank national accounts data/OECD (2020).

Supprimé: 4

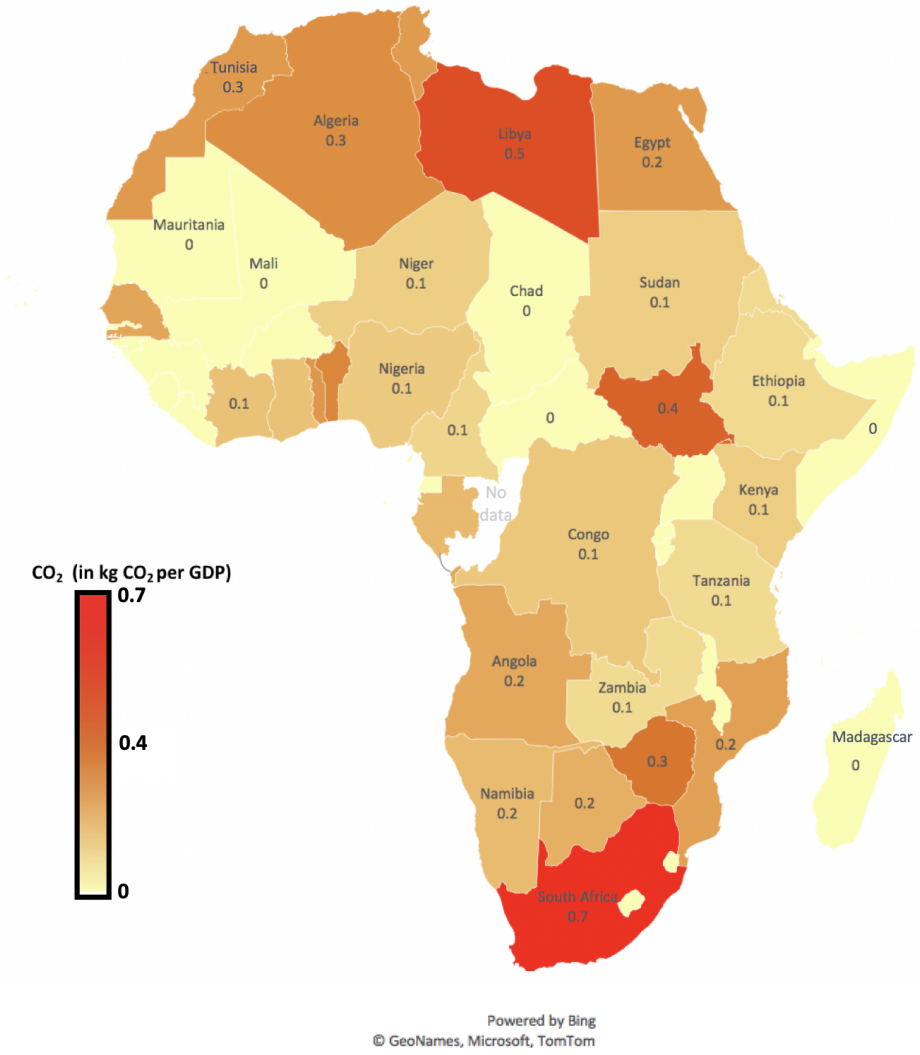

Figure S6. Map of territorial mean 2013-2017 emissions and its associated bar plots in kg CO_2 of GDP, dataset taken from GCP 2019 (CDIAC).

Supprimé: 5

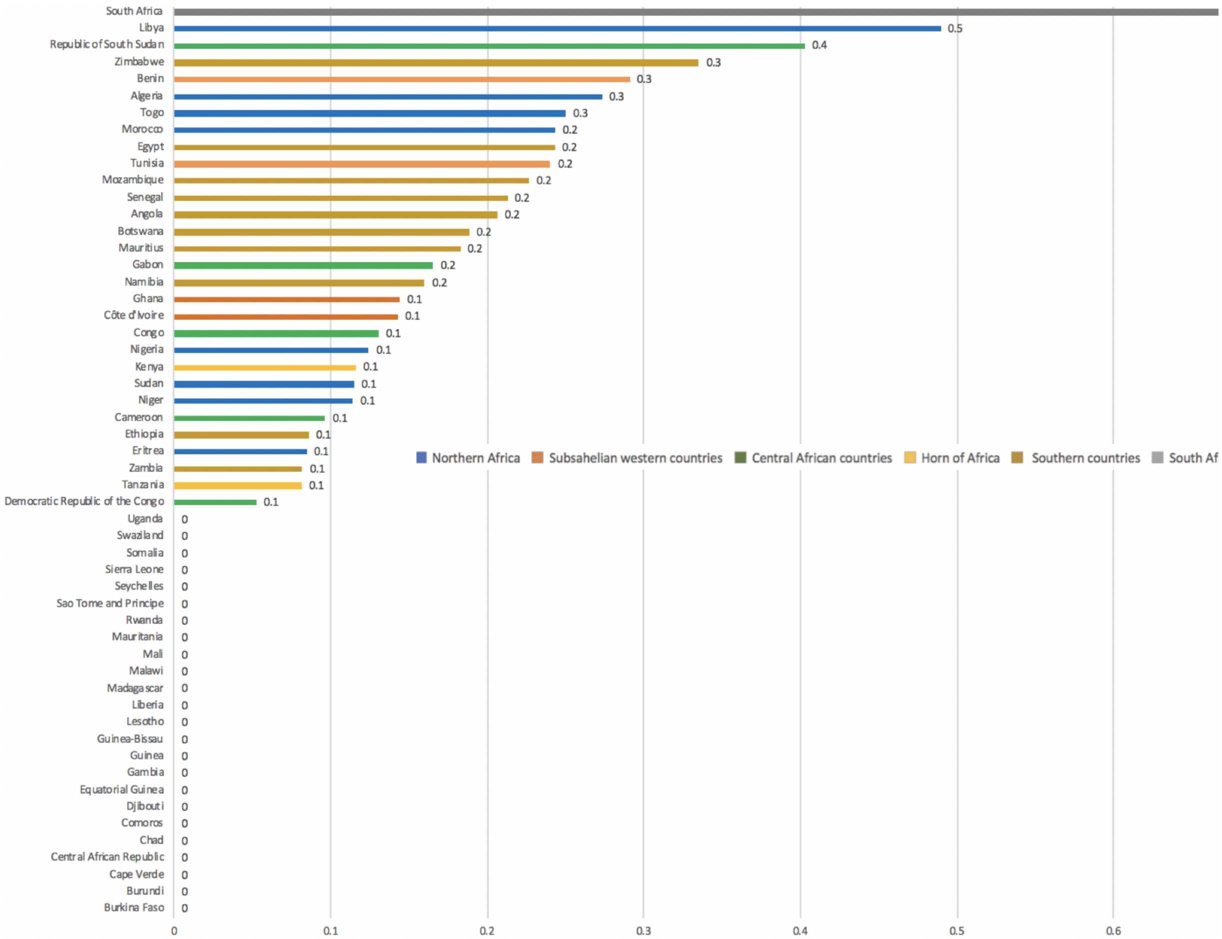

Figure S6 bis. Map of territorial mean 2013-2017 emissions and its associated bar plots in kgCO_2 per GDP, dataset taken from GCP 2019 (CDIAC).

Supprimé: 5

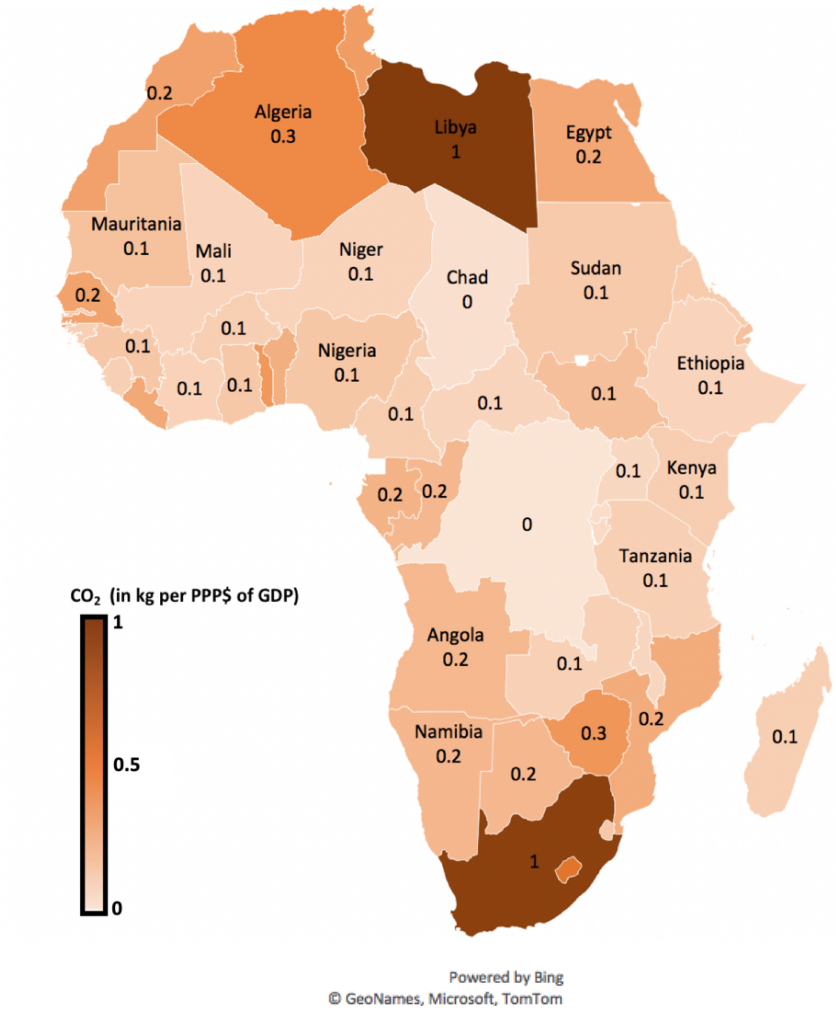

Figure S7. Map of African CO_2 emissions expressed in kg per PPP$ of GDP in 2016 - CDIAC.

Supprimé: 6

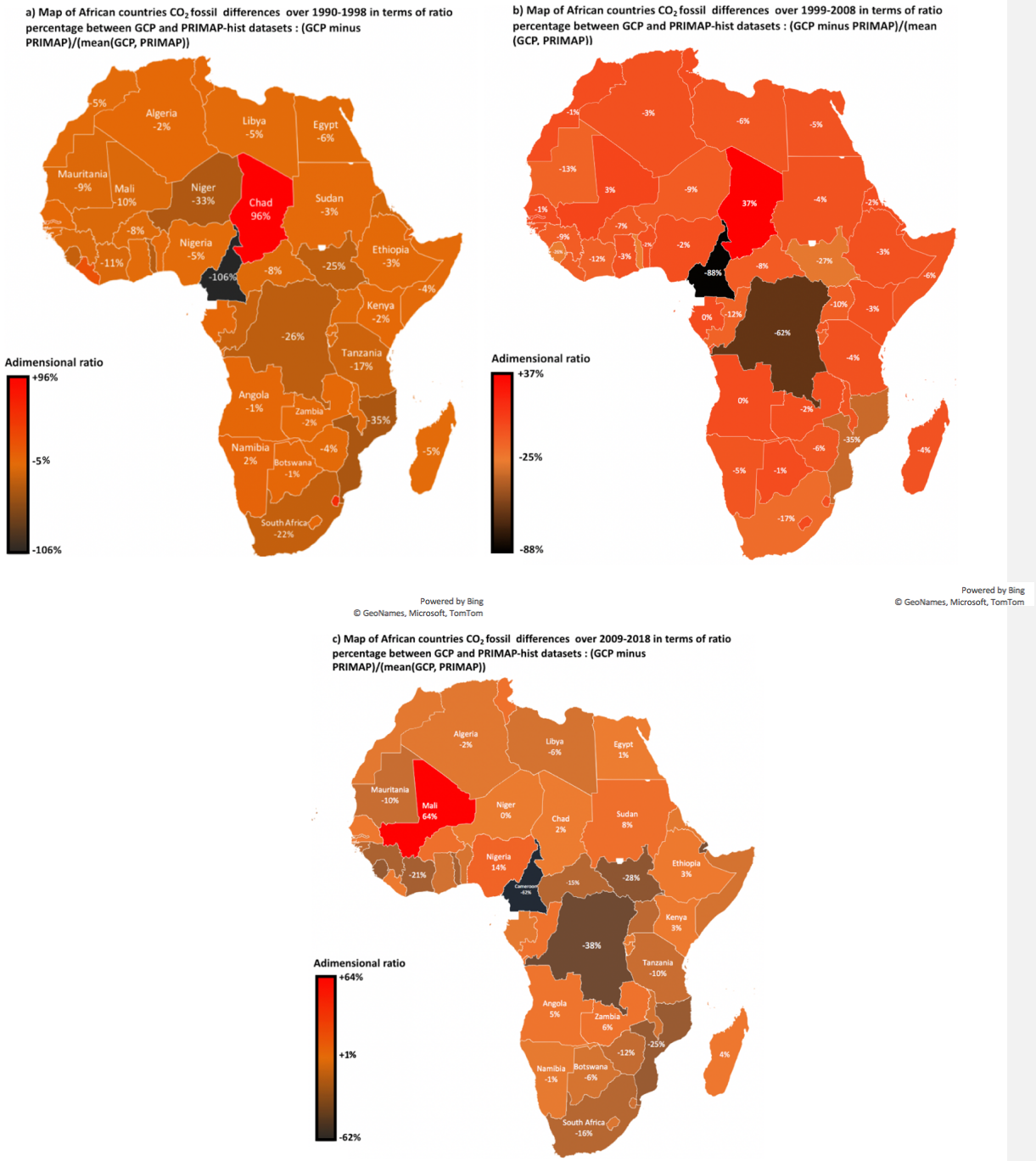

Figure S8. Three maps of African countries fossil CO_2 emissions per decade: ratio percentage showing the discrepancies between GCP and PRIMAP-hist datasets over three decades (1990-2018).

Supprimé: 7

Table S4. List of Least Developed Countries and Small Islands Developing States in Africa.

Supprimé: 3

33 Least Developed Countries (LDCs)	6 Small Islands Developing States (SIDS)
Angola, Benin, Burkina Faso, Burundi, Central African Republic, Chad, Comoros, D.R. Congo, Djibouti, Eritrea, Ethiopia, Gambia, Guinea, Guinea-Bissau, Lesotho, Liberia, Madagascar, Malawi, Mali, Mauritania, Mozambique, Niger, Rwanda, São Tomé and Príncipe, Senegal, Sierra Leone, Somalia, South Sudan, Sudan, Tanzania, Togo, Uganda, Zambia.	Cape Verde, Comores, Guinea-Bissau, Mauritius, Sao Tomé and Principe, Seychelles.

Table S5. List of corrected countries for CO_2 LULUCF (in $MtCO_2$) - corrections in line with Grassi (2022)

Supprimé: 4

Country	Year of most recent outlier report	Outlier value and source	Year corrected data	Corrected data and source	Mean corrected value over 2000-2020	Mean difference over 2000-2020	Comments on the chosen correcting method.
CAF	2010	-1766 (NC2)	2016	-229 (NDC)	-229	1537	NDC 2016 because more recent than NC2 (2015), and sink in most recent NDC 2021 biophysically impossible.
Guinea-Bissau	2001	-11288 (NC1)	2010	-1 (NC2)	-1	-11287	NC1 value reports an unrealistically high sink.
Tanzania	1994	810 (NC2)	2022	77 (NDC 2022[1])	77	566	NDC is more recent and underlines a more realistic order of magnitude.
Guinea	2000	-444 (NC2)	2021	34 (NDC 2021)	34	478	NDC 2021 chosen because more recent than NC2 (2018), and the sink in NC2 is biophysically impossible (-444 $MtCO_2.yr^{-1}$over only 5 Mha of forest). However, a remaining problem with the corrected value from nc2 is that no forest sink at all is reported.
Namibia	2000	11 (NC3)	2019	-117 (NIR 2019[2])	-106	-117	NIR 2019 chosen because more recent than NC3 (2015) and more complete than NDC 2021 which is more recent.
Mali	2010	-245 (NC3)	Mean 2000 and 2010	-221 (mean of NC2 and NC3)	-155	66	Mean of NC2 and NC3 as more complete than REDD+. The sink in NC3 is high and here considered implausible, but it is however consistently reported in various official UNFCCC documents.
Democratic Republic of the Congo	2015	-235 (NC3)	2021	529 (NDC 2021)	529	761	NDC 2021 chosen because more recent than the NC3 (2015) and broadly consistent with REDD+ (2018). But a weakness of this correction source is that it does not report any carbon sink from forest.
Madagascar	2010	-97 (NC3)	2017	34 (REDD+ 2018)	34	131	REDD+ (2018) chosen because more recent than NC3 (2017), but it covers only deforestation. NC3 reports a biophysically impossible sink over only 9 Mha of forest.
Nigeria	2014	98 (NC2)	2017	315 (BUR2)	287	189	BUR2 (2021) chosen because more recent than NC2 (2014) and more detailed than NDC 2021 which report different numbers.
Zimbabwe	2006	-83 NC3 (2017)	2021	16 (BUR1)	11	95	BUR1 (2021) as more recent than the NC3 (2017) and more complete than NDC 2021.
Congo	Since 2000	-83 (NC2)	2009	-18 (NC2)	-18	65	NDC2021 chosen because more recent than the NC2 (2009).
Angola	2012	0.7 (NC1)	2021	55 (NC2)	55	54	NC2 (2021) chosen because more recent that NC1 (2012).
Mauritius	2013	-490 (NC3)	2016	0 (NIR 2021)	0	490	NIR 2021 more recent than NC3 (with unrealistically high value).

[1]Using Tanzania GHGs Inventory Report and MRV System (2018).
[2]NIR = National Inventory Report (NIR).

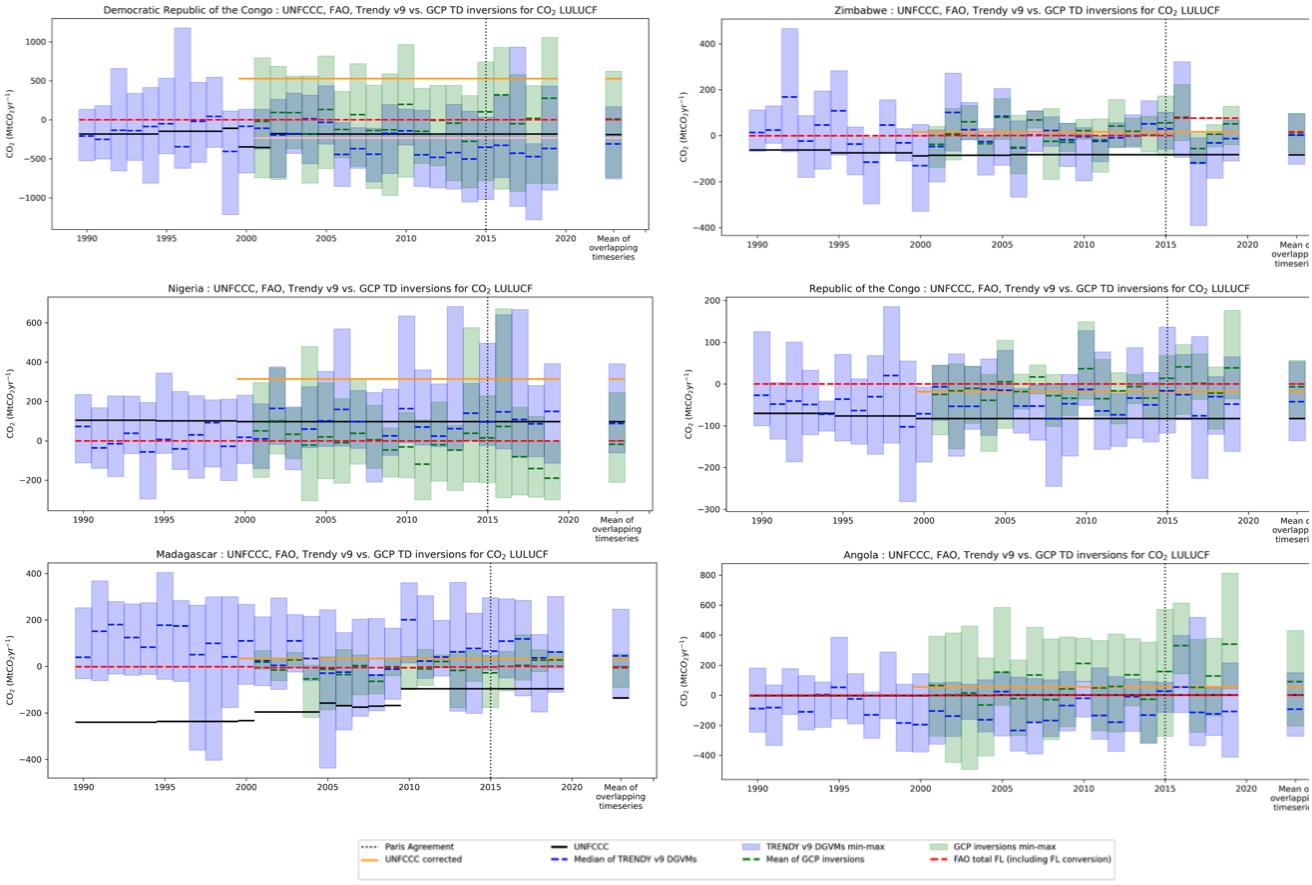
Democratic Republic of the Congo : UNFCCC, FAO, Trendy v9 vs. GCP TD inversions for CO_2 LULUCF
Zimbabwe : UNFCCC, FAO, Trendy v9 vs. GCP TD inversions for CO_2 LULUCF
Nigeria : UNFCCC, FAO, Trendy v9 vs. GCP TD inversions for CO_2 LULUCF
Republic of the Congo : UNFCCC, FAO, Trendy v9 vs. GCP TD inversions for CO_2 LULUCF
Madagascar : UNFCCC, FAO, Trendy v9 vs. GCP TD inversions for CO_2 LULUCF
Angola : UNFCCC, FAO, Trendy v9 vs. GCP TD inversions for CO_2 LULUCF
CO_2 ($MtCO_2yr^{-1}$)
1990
1995
2000
2005
2010
2015
2020
Mean of overlapping timeseries
Paris Agreement
UNFCCC corrected
UNFCCC
Median of TRENDY v9 DGVMs
TRENDY v9 DGVMs min-max
Mean of GCP inversions
GCP inversions min-max
FAO total FL (including FL conversion)

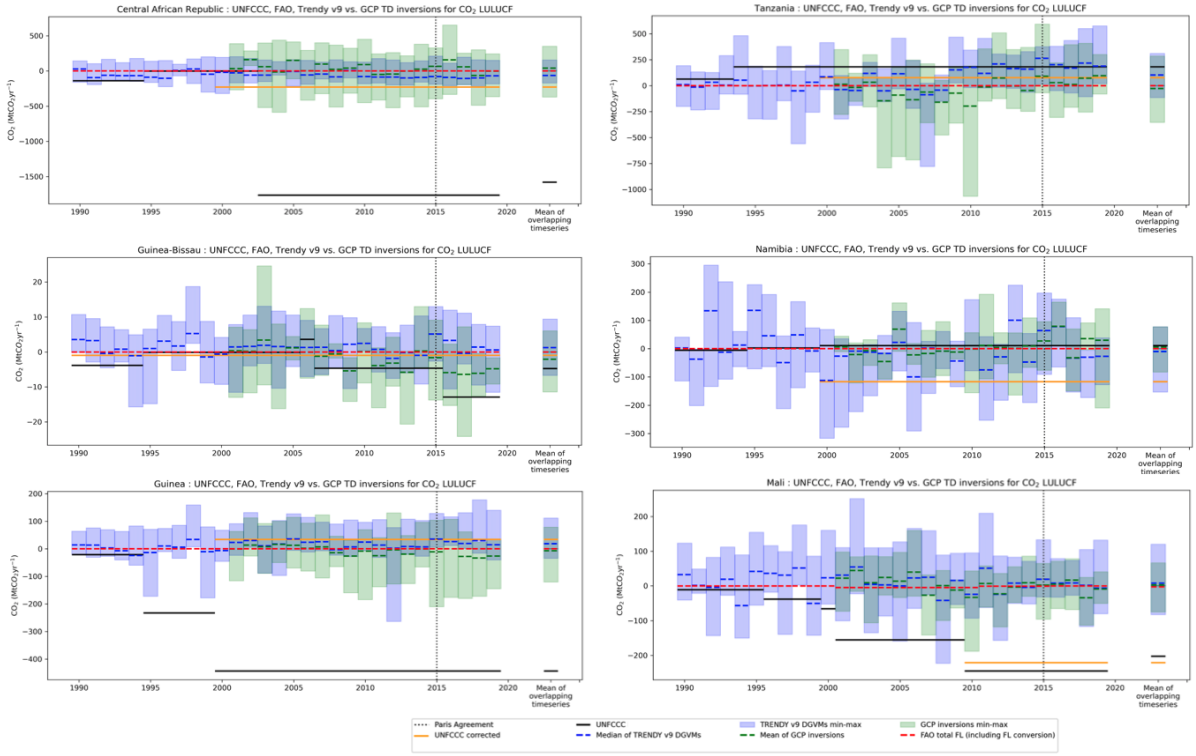

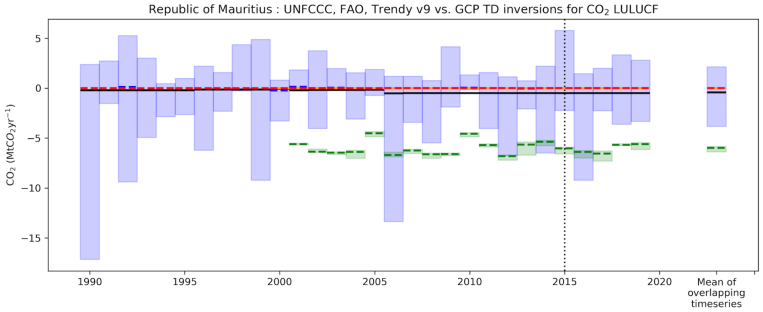

Figure S9. Country details for LULUCF CO_2 emissions and sinks from UNFCCC corrected (strictly consistent with Grassi et al. 2022) for 13 African countries that we identified as outliers vs. UNFCCC uncorrected data, TRENDY v9, DGVMs and GCP (2020) inversions. Unit is in $MtCO_2$. Black lines denote the PRIMAP-hist estimates for total anthropogenic emissions including all IPCC sectors. Shaded green areas represent the minimum and maximum ranges from GCP inversions. Shaded blue areas represent the minimum and maximum ranges for TRENDY v9 DGVMs. Green dashes denote the median of GCP inversions, blue dashes denote the median of TRENDY v9 DGVMs, green dashes the median of GCP inversions. The positive values represent a source while the negative values refer to a sink.

Table S6. Data sources for the land CO_2 emissions in this analysis.

Supprimé: 5

Method	Product type / file name	Species	Overall period covered	References
BU	TRENDY v9 (2019) 14 DGVMs : CABLE, CLASS, CLM5, DLEM, ISAM, JSBACH, JULES, LPJ, LPX, OCN, ORCHIDEE-CNP, ORCHIDEE, SDGVM, SURFEX	Land-related Carbon emissions (Net Biome Productivity)	1900-2019	Met Office UK/ Le Quéré et al. (2018) www.icos-cp.eu/GCP
BU	UNFCCC	LULUCF Net CO_2 emissions / removals	1990-2015	UNFCCC https://unfccc.int/non-annex-I-NCs
TD	GCB 2019	Total CO_2 inverse flux (Net Biome Productivity)	2000-2018	Friedlingstein et al. (2020)
	Carbon Tracker Europe (CTE)		2000-2018	van der Laan-Luijke et al. (2017)
	CAMS (in-situ)		2000-2018	Chevallier et al. (2005) Rödenbeck (2005)
	Jena CarboScopeReg (in situ)		2006-2010	Kountouris et al. (2018)

Table S7. Data sources for total CH_4 emissions in this analysis.

Method/observations	Product type / number of inversions	Overall period covered	References
TD (surface stations)	Carbon Tracker-Europe CH_4 CTE_SURF (FMI)/ 1	2000-2017	Tsuruta et al. (2017)
TD (GOSAT NIES L2 v2.72)	Carbon Tracker-Europe CH_4 CTE_GOSAT (FMI)/ 1	2000-2017	Tsuruta et al. (2017)
TD (surface stations)	GELCA_SURF (NIES)/ 1	2000-2015	Ishizawa et al. (2016)
TD (surface stations)	LMDZ_PYVAR (LSCE)/ 2	2010-2016	Yin et al. (2020)
TD (GOSAT 7.2 Leicester v2)	LMDZ_PYVAR (LSCE)/ 4	2010-2016	Yin et al. (2020)
TD (GOSAT 7.2 Leicester v2)	LMDZ_PYVAR (LSCE)/ 2	2010-2017	Zheng et al. (2018)
TD (surface stations)	MIROC4- ACTM (JAMSTEC)/ 1	2010-2016	Patra et al. (2016)
TD (surface stations)	NICAM-TM (NIES)/ 1	2000-2017	Niwal et al. (2017)
TD (surface stations)	NIES-TM-FLEXPART-VAR (NETFVAR), (NIES)/ 1	2010-2017	Maksyutov et al. (2020); Wang et al. (2019)
TD (GOSAT NIES L2 v2.72)	NIES-TM-FLEXPART-VAR (NETFVAR), (NIES)/ 1	2010-2017	Maksyutov et al. (2020); Wang et al. (2019)
TD (surface stations)	TM5-CAMS (TNO)/1	2000-2017	Segers and Houweling (2018). Bergamaschi et al. (2013, 2018)
TD (GOSAT/CCI v2.3.8 and surface observations)	TM5-CAMS (TNO)/1	2010-2017	Segers and Houweling (2018). Bergamaschi et al. (2013, 2018)
TD (surface stations)	TM5-4DVAR (EC_JRC)/2	2000-2017	Bergamaschi et al. (2013, 2018)
TD (GOSAT/CCI v2.3.8 and surface observations)	TM5-4DVAR(EC_JRC)/2	2010-2017	Bergamaschi et al. (2013, 2018)
TD (surface stations)	TOMCAT (University of Leeds)/	2003-2015	McNorton (2018)

Supprimé: 6

Table S8. Data sources for total N_2O inverse flux over Africa (in situ).

Method	Product type / file name	Period covered	References
TD	PyVAR	1998-2017	Thompson et al. (2014), Tian et al. (2020)
TD	TOMCAT- INVICAT	1998-2015	Wilson et al. (2014), Tian et al. (2020)
TD	MIROC4- ACTM (JAMSTEC)	1998-2016	Patra et al. (2018), Tian et al. (2020)

Supprimé: 7

Table S9. Area of managed land reported in NC/BUR/REDD+ versus FAO forest land (2015) and FAO forest land + other woodlands (2015) for Africa.

Supprimé: 8

Country	Forest area in Mha. Data: FAO (2015)	Inventories forest area in Mha. Data: UNFCCC/REDD+	Forest land area + other woodland area in Mha. Data : FAO (2015)
Mauritius	0.04	0.00	0.05
Rwanda	0.27	0.00	0.53
Cape Verde	0.04	0.04	0.08
Burundi	0.28	0.71	0.28
Togo	1.22	1.00	3.33
Eritrea	1.07	1.59	7.03
Algeria	1.96	2.14	4.53
Guinea-Bissau	2.02	2.46	2.19
Eq. Guinea	2.49	2.50	2.49
Mauritania	0.34	3.00	2.74
Côte d'Ivoire	3.40	3.40	5.96
Benin	3.39	3.59	5.34
Liberia	7.77	4.52	8.07
Guinea	6.39	4.60	12.24
Kenya	3.52	4.75	35.14
Botswana	15.85	5.83	42.34
Morocco	5.68	6.00	6.97
Namibia	6.99	7.00	61.07
Niger	1.14	8.00	4.28
Ghana	7.88	8.97	7.88
Madagascar	12.50	9.00	26.96
Malawi	2.45	9.00	2.45
Nigeria	22.44	14.00	22.44
Senegal	8.27	14.00	13.42
Zimbabwe	17.67	16.00	25.13
Ethiopia	17.43	17.43	39.83
Gabon	23.59	18.27	23.59
Cameroon	20.62	20.00	33.34
South Africa	17.23	23.00	66.91
Congo	22.02	23.52	26.39
Burkina Faso	6.47	27.30	16.45
Mozambique	37.94	34.00	52.36
Tanzania	48.09	48.00	63.38
Zambia	45.76	48.00	58.97
Angola	69.38	53.00	95.31
Sudan	19.21	70.00	39.96
Dem. Rep. Congo	131.66	152.00	143.17

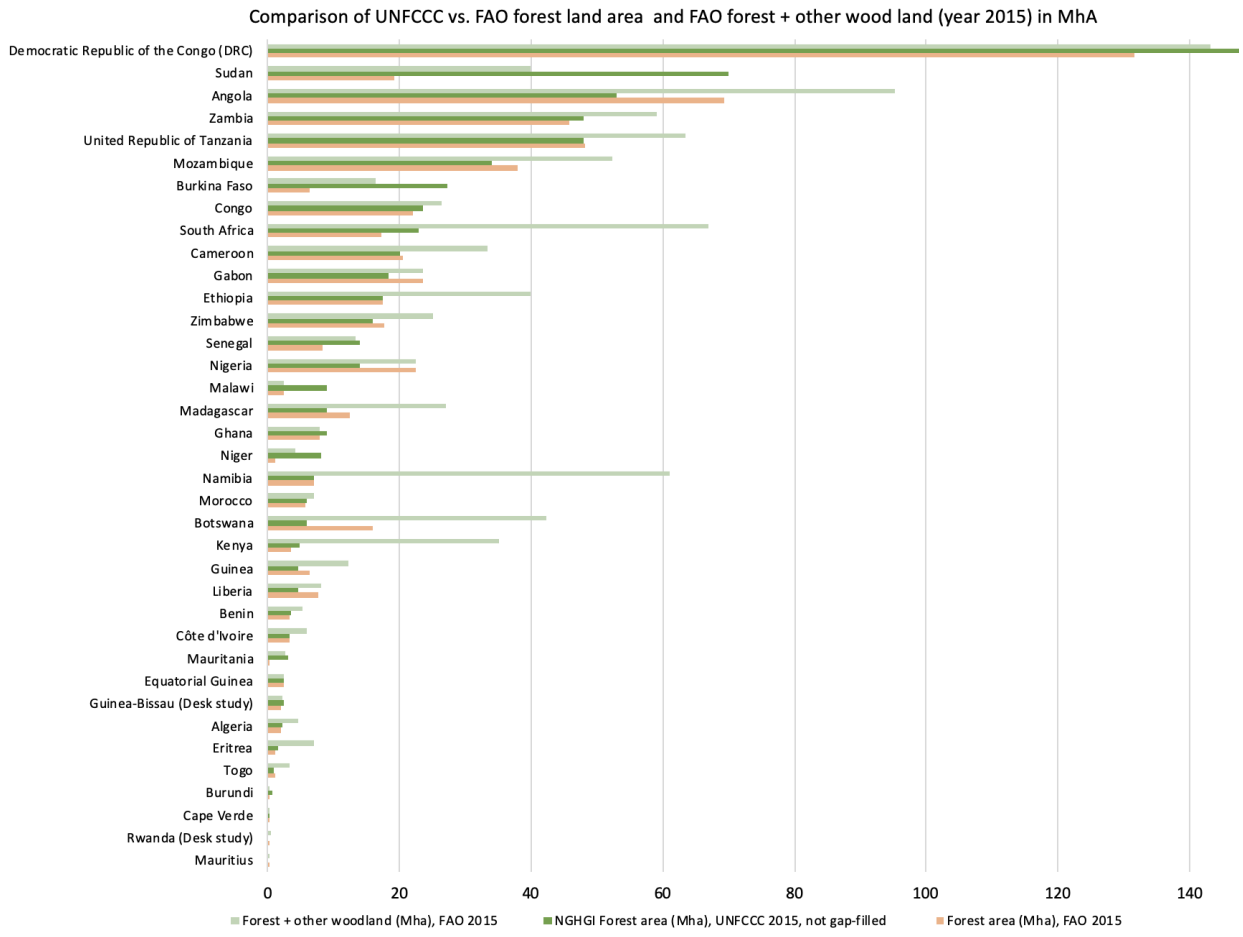

Figure S10. Bar plots comparing areas of managed land reported in Mha for NC/BUR/REDD+ versus FAO forest land (2015) in Mha and FAO forest land + other woodlands areas (2015) for African countries. (Source: Forest Resource Assessment, FAO). See also Table S7 for detailed values.

Table S10. Synthesis of TD and BU mean CH_4 emissions and removals in $MtCO_2e.yr^{-1}$ for the overlapping time series (2010-2017) for whole Africa and for the six groups using Method 1 (Foss+ AGRIW + BBUR - wildfires).

Region	Rank median PRIMAP	Rank median GOSAT	Rank median surface inversions	Rank wetlands median GMB	Rank wildfires	Rank wetlands median GMB
North Africa	**1**	**1**	**1**	**5**	3	**5**
Subsahelian West Africa	**2**	3	**2**	**4**	5	**4**
Horn of Africa	**3**	2	**3**	**3**	4	**3**
Southern Africa	4	**5**	**5**	**2**	1	**2**
Central Africa	5	**4**	**4**	**1**	2	**1**
South Africa Group	**6**	**6**	**6**	**6**	**6**	**6**

Supprimé: 9

Table S11. Anomalies in ranking for TD and BU mean values on the overlapping time periods (2010-2017) for whole Africa, and for six African groups using Method 1 for anthropogenic CH_4 (FOSS + AGRIW + BBUR - wildfires) in $MtCO_2e.yr^{-1}$.

Region	PRIMAP	Median GOSAT inv.	Max GOSAT inv.	Min GOSAT inv.	Median surface inv.	Max surface inv.	Min surface inv.	Max wetlands GCB	Median wetlands GCB	Min wetlands GCB	Wildfires
Africa Total	1231	1117	1390	903	1094	1330	853	946	827	481	110
North Africa	293	270	330	174	302	396	245	146	69	34	11
Subsahelian West Africa	272	186	329	174	249	396	245	161	77	48	8
Horn of Africa	252	242	551	206	237	302	183	171	86	47	9
Southern Africa	212	114	173	99	114	146	91	214	102	65	41
Central Africa	123	130	170	106	123	142	88	615	428	195	40
South Africa Group	78	91	168	75	88	124	65	21	13	2	1

Table S12. Synthesis of wetlands (GCB) mean CH_4 emissions and removals in $MtCO_2e.yr^{-1}$ for the overlapping time series (2010-2017) for the whole Africa and six African groups.

Region	Max wetlands GCB	Median wetlands GCB	Min wetlands GCB
Africa	946	827	481
North Africa	146	69	34
Subsahelian West Africa	161	77	48
Horn of Africa	171	86	47
Southern Africa	214	102	65
Central Africa	615	428	195
South Africa group	21	13	2

Supprimé: 0

Supprimé: 1

Table S13. Comparison between N_2O PRIMAP-hist mean values and the median of inversions on the overlapping period (2010-2017) for Africa and the six African groups in $MtCO_2e.yr^{-1}$.

Region	PRIMAP-hist	Median global inversions
Africa total	360	1647 (1502 to 1760)
North Africa	106	330 (274 to 419)
Subsahelian West Africa	68	271 (68 to 330)
Horn of Africa	46	240 (217 to 265)
Southern Africa	62	263 (214 to 310)
Central Africa	182	461 (424 to 517)
South Africa group	24	68 (51 to 81)

Table S14. Synthesis for the three main GHGs net African budget: comparative net emissions and removals computation by TD methods for Africa as a whole and for six sub-groups of African countries over the overlapping period (2001-2017), in $MtCO_2e$. Use of Method 1 for CH_4 (FOS+AGRIW+BBUR-wildfires) excluding UNFCCC outliers, and including the range for GCP CO_2 LULUCF.

Region	TD Method 1 and GCP for FCO_2				TD Method 1 and PRIMAP for FCO_2			
	CH_4 median GOSAT inversions + median N_2O inversions	CH_4 median SURF inversions + median N_2O inversions	CH_4 median SURF inversions + PRIMAP N_2O	CH_4 median GOSAT inversions + PRIMAP N_2O	CH_4 median GOSAT inversions + median N_2O inversions	CH_4 median SURF inversions + median N_2O inversions	CH_4 median SURF inversions + PRIMAP N_2O	CH_4 median GOSAT inversions + PRIMAP N_2O
Africa total	3889^{7257}_{1296}	3866^{7197}_{1246}	2579^{5797}_{104}	2602^{5857}_{154}	3983^{7621}_{1390}	3960^{7291}_{1340}	2673^{5890}_{198}	2696^{5950}_{248}
North Africa	1014^{1438}_{553}	1046^{1504}_{624}	822^{1190}_{456}	790^{1124}_{385}	1022^{1446}_{591}	1054^{1511}_{632}	830^{1232}_{464}	798^{1132}_{393}
Central Africa	758^{2064}_{-758}	751^{2036}_{-776}	344^{1573}_{-1145}	351^{1602}_{-1128}	766^{2072}_{-750}	759^{2043}_{-768}	352^{1582}_{-1138}	359^{1610}_{-1120}
Subsahelian West Africa	546^{1282}_{-95}	609^{1349}_{-24}	406^{1086}_{-24}	343^{1019}_{95}	542^{1278}_{-98}	605^{1345}_{-27}	403^{1083}_{-27}	340^{1016}_{98}
Southern Africa	616^{1726}_{-175}	616^{1699}_{-186}	415^{1451}_{-338}	415^{1478}_{-331}	618^{1728}_{-340}	618^{1701}_{-348}	416^{1452}_{-337}	416^{1479}_{-329}
South Africa group	458^{710}_{103}	455^{747}_{93}	411^{689}_{116}	414^{734}_{126}	537^{871}_{184}	534^{927}_{172}	490^{769}_{196}	493^{813}_{206}
Horn of Africa	399^{1215}_{-274}	394^{966}_{-297}	201^{748}_{-467}	206^{997}_{-444}	401^{1216}_{-273}	395^{967}_{-296}	202^{749}_{-467}	207^{998}_{-444}

Table S15. Synthesis for the three main GHGs net African budget: comparative net emissions and removals computation by TD methods for Africa as a whole and for six sub-groups of African countries over the overlapping period (2001-2017), in $MtCO_2e$. Use of Method 1 for CH_4 (FOS+AGRIW+BBUR-wildfires) excluding UNFCCC outliers, and excluding the range for GCP CO_2 LULUCF (possible outliers).

Region	TD Method 1 and GCP FCO_2				TD Method 1 and PRIMAP FCO_2			
	CH_4 median GOSAT inversions + median N_2O inversions	CH_4 median SURF inversions + median N_2O inversions	CH_4 median SURF inversions + PRIMAP N_2O	CH_4 median GOSAT inversions + PRIMAP N_2O	CH_4 median GOSAT inversions + median N_2O inversions	CH_4 median SURF inversions + median N_2O inversions	CH_4 median SURF inversions + PRIMAP N_2O	CH_4 median GOSAT inversions + PRIMAP N_2O
Africa total	3889^{4276}_{3530}	3866^{4216}_{3480}	2579^{2815}_{2338}	2602^{2875}_{2388}	3983^{4639}_{3624}	3960^{4309}_{3574}	2673^{2909}_{2432}	2696^{2969}_{2482}
North Africa	1014^{1164}_{862}	$1046^{1230}_{933.1}$	822^{916}_{765}	790^{850}_{694}	1022^{1171}_{870}	1054^{1237}_{941}	830^{958}_{773}	798^{858}_{702}
Central Africa	758^{853}_{697}	751^{826}_{679}	344^{363}_{309}	351^{391}_{327}	766^{862}_{705}	759^{833}_{687}	352^{371}_{317}	359^{399}_{335}
Subsahelian West Africa	546^{748}_{331}	609^{815}_{402}	406^{553}_{402}	343^{486}_{331}	542^{745}_{328}	605^{812}_{399}	403^{550}_{399}	340^{483}_{328}
Southern Africa	616^{722}_{552}	616^{695}_{544}	415^{447}_{392}	415^{474}_{400}	618^{724}_{390}	618^{697}_{382}	416^{448}_{393}	416^{475}_{401}
South Africa group	458^{467}_{374}	455^{504}_{364}	411^{446}_{388}	414^{491}_{398}	537^{628}_{453}	534^{584}_{443}	490^{526}_{467}	493^{570}_{477}
Horn of Africa	399^{733}_{340}	394^{484}_{317}	201^{266}_{147}	206^{515}_{179}	400^{734}_{341}	395^{485}_{318}	202^{267}_{148}	207^{516}_{171}

Supprimé: 4

Table S16. Mean net total Africa and regional groups from mean TD (excluding the range for CO_2 LULUCF due to outliers) and mean best fitted BU Methods excluding outliers. (For TD approaches, N_2O inversions were excluded and replaced by PRIMAP estimates. For DGVMs the range for GCP CO_2 LULUCF was not considered due to probable outliers. UNFCCC outliers are also excluded.) Net emissions and removals are expressed in $MtCO_2e.yr^{-1}$ over the overlapping period (2001-2017).

Region	Mean of TD methods excluding N_2O inversions replaced with N_2O PRIMAP and excluding the range for GCP CO_2 LULUCF (with probable outliers)	Ranking with TD methods	Mean net of best fitted BU methods (excluding uncorrected UNFCCC data)	Ranking with BU methods
North Africa	806^{883}_{730} (GCP FCO_2) 814^{908}_{737} (PRIMAP FCO_2) Mean GCP & PRIMAP (FCO_2): 810^{895}_{733}	1	713^{807}_{641} (GCP FCO_2) 720^{816}_{649} (PRIMAP FCO_2) Mean GCP & PRIMAP (FCO_2): 717^{812}_{645}	1
South Africa group	412^{468}_{393} (GCP FCO_2) 491^{547}_{472} (PRIMAP FCO_2) Mean GCP & PRIMAP (FCO_2): 452^{508}_{432}	2	534^{613}_{443} (GCP FCO_2) 613^{692}_{522} PRIMAP FCO_2) Mean GCP & PRIMAP (FCO_2): 574^{653}_{483}	3
Horn of Africa	203^{390}_{158} (GCP FCO_2) 204^{391}_{159}(PRIMAP FCO_2) Mean GCP &PRIMAP (FCO_2): 204^{391}_{159}	6	432^{524}_{296}(GCP FCO_2) 433^{525}_{297}(PRIMAP FCO_2) Mean GCP & PRIMAP (FCO_2): 433^{525}_{297}	4
Subsahelian West Africa	375^{520}_{367}(GCP FCO_2) 371^{516}_{363} (PRIMAP FCO_2) Mean GCP & PRIMAP (FCO_2): 373^{518}_{365}	4	612^{776}_{539} (GCP FCO_2) 609^{772}_{535} (PRIMAP FCO_2) Mean GCP & PRIMAP (FCO_2): 610^{774}_{537}	2
Southern Africa	415^{460}_{396}(GCP FCO_2) 416^{462}_{397} (PRIMAP FCO_2) Mean GCP & PRIMAP (FCO_2): 416^{461}_{397}	3	228^{529}_{178}(GCP FCO_2) 355^{531}_{179}(PRIMAP FCO_2) Mean GCP & PRIMAP (FCO_2): 292^{530}_{178}	5
Central Africa	348^{377}_{318}(GCP FCO_2) 356^{385}_{326} (PRIMAP FCO_2) Mean GCP & PRIMAP (FCO_2): 352^{381}_{322}	5	-70^{168}_{-210}(GCP FCO_2) -62^{176}_{-202}(PRIMAP FCO_2) Mean GCP & PRIMAP (FCO_2): -66^{172}_{-206}	6
Africa total	2591^{2845}_{2363}(GCP FCO_2) 2684^{2939}_{2457} (PRIMAP FCO_2) Mean GCP &PRIMAP (FCO_2): 2638^{2892}_{2410}		2576^{3228}_{2140} (GCP FCO_2) 2669^{3251}_{2233} (PRIMAP FCO_2) Mean GCP & PRIMAP (FCO_2): 2623^{3240}_{2186}	

Supprimé: 5

Tableau mis en forme

Table S17. Mean net total Africa and regional groups from best fitted mean TD and mean BU Methods excluding outliers. For TD approaches, N_2O inversions were excluded and replaced by PRIMAP estimates. For DGVMs, the range for GCP CO_2 LULUCF was considered. UNFCCC outliers are also excluded. Net emissions and removals are expressed in $MtCO_2.yr^{-1}$ over the overlapping period (2001-2017).

Region	Mean net of TD methods (including range for CO_2 LULUCF from GCP inversions with outliers but excluding N_2O inversions (N_2O PRIMAP)	Ranking with TD methods	Mean net of best fitted BU methods (excluding uncorrected UNFCCC data)	Ranking with BU methods
North Africa	$806\,^{1157}_{129}$(GCP FCO_2) 814^{1182}_{428} (PRIMAP FCO_2) Mean GCP & PRIMAP: 810^{1170}_{279}	1	713^{807}_{641} (GCP FCO_2) 720^{816}_{649} (PRIMAP FCO_2) Mean GCP & PRIMAP (FCO_2): 717^{812}_{645}	1
South Africa group	412^{712}_{121} (GCP FCO_2) 491^{791}_{201} (PRIMAP FCO_2) Mean GCP & PRIMAP: 452^{751}_{161}	2	534^{613}_{443} (GCP FCO_2) 613^{692}_{522} PRIMAP FCO_2) Mean GCP & PRIMAP (FCO_2): 574^{653}_{483}	3
Horn of Africa	$203\,^{872}_{-456}$ (GCP FCO_2) 204^{873}_{-455} (PRIMAP FCO_2) Mean GCP & PRIMAP: 204^{873}_{-456}	6	432^{524}_{296}(GCP FCO_2) 433^{525}_{297}(PRIMAP FCO_2) Mean GCP & PRIMAP (FCO_2): 433^{525}_{296}	4
Subsahelian West Africa	$375\,^{1053}_{36}$ (GCP FCO_2) 371^{1050}_{36} (PRIMAP FCO_2) Mean GCP & PRIMAP: 373^{1051}_{356}	4	612^{776}_{539} (GCP FCO_2) 609^{772}_{535} (PRIMAP FCO_2) Mean GCP & PRIMAP (FCO_2): 610^{774}_{537}	2
Southern Africa	$415\,^{1464}_{-335}$(GCP FCO_2) 416^{1466}_{-333} (PRIMAP FCO_2) Mean GCP &PRIMAP: 416^{1465}_{-334}	3	228^{529}_{178}(GCP FCO_2) 355^{531}_{179}(PRIMAP FCO_2) Mean GCP & PRIMAP (FCO_2): 292^{530}_{178}	5
Central Africa	$348\,^{1588}_{-1137}$(GCP FCO_2) 356^{1596}_{-1129}(PRIMAP FCO_2) Mean GCP & PRIMAP (FCO_2): 352^{1592}_{-1133}	5	-70^{168}_{-210}(GCP FCO_2) -62^{176}_{-202}(PRIMAP FCO_2) Mean GCP & PRIMAP (FCO_2): -66^{172}_{-206}	6
Africa total	2583^{3037}_{2251} (GCP FCO_2) 2654^{3089}_{2322} (PRIMAP FCO_2) Mean GCP & PRIMAP (FCO_2): 2638^{5873}_{1761}		2576^{3228}_{2140} (GCP FCO_2) 2669^{3251}_{2233} (PRIMAP FCO_2) Mean GCP & PRIMAP (FCO_2): 2623^{3240}_{2186}	

Table S18. Mean net total of best fitted mean TD and mean BU methods excluding N_2O inversions (replaced by PRIMAP estimates), using Method 1 for CH_4 (FOS+AGRIW+BBUR-wildfires) excluding UNFCCC outliers, and including the range for GCP CO_2 LULUCF, for Africa total and for regional groups, with associated ranking.

Region	Mean of best fitted TD and BU methods using both GCP and PRIMAP FCO_2 (excluding UNFCCC outliers and N_2O inversions, but including range for CO_2 LULUCF from GCP inversions)	Ranking with TD methods
North Africa	761^{988}_{460}	1
South Africa group	513^{702}_{161}	2
Horn of Africa	318^{699}_{-80}	5
Subsahelian West Africa	492^{913}_{286}	3
Southern Africa	354^{998}_{-78}	4
Central Africa	143^{882}_{-670}	6
Africa total	2630^{4557}_{1974}	

Supprimé: 7

Table S19. Mean net total Africa and regional groups from TD inversions only including N_2O inversions (and the range for CO_2 LULUCF from GCP inversions). For BU methods, UNFCCC outliers are excluded.

Supprimé: 8

Region	Mean TD from inversions only (including range for CO_2 LULUCF from GCP inversions and N_2O inversions)	Ranking with BU methods
North Africa	1030^{1471}_{589} (GCP FCO_2) 1038^{1479}_{512} (PRIMAP FCO_2) Mean GCP & PRIMAP (FCO_2): 1034^{1475}_{600}	1
South Africa group	457^{729}_{98} (GCP FCO_2) 536^{899}_{178} (PRIMAP FCO_2) Mean GCP & PRIMAP (FCO_2): 496^{814}_{138}	5
Horn of Africa	397^{1090}_{-286} (GCP FCO_2) 398^{1091}_{-285} (PRIMAP FCO_2) Mean GCP & PRIMAP (FCO_2): 397^{1091}_{-285}	6
Subsahelian West Africa	577^{1315}_{-60} (GCP FCO_2) 574^{1312}_{-63} (PRIMAP FCO_2) Mean GCP & PRIMAP (FCO_2): 576^{1313}_{-61}	4
Southern Africa	616^{1713}_{-181} (GCP FCO_2) 618^{1714}_{-344} (PRIMAP FCO_2) Mean GCP & PRIMAP (FCO_2): 617^{1713}_{-262}	3
Central Africa	755^{2050}_{-767} (GCP FCO_2) 763^{2058}_{-759} (PRIMAP FCO_2) Mean GCP & PRIMAP (FCO_2): 759^{2054}_{-763}	2
Africa total	3787^{7226}_{1274} (GCP FCO_2) 3971^{7456}_{1365} (PRIMAP FCO_2) Mean GCP & PRIMAP (FCO_2): 3879^{7341}_{1320}	

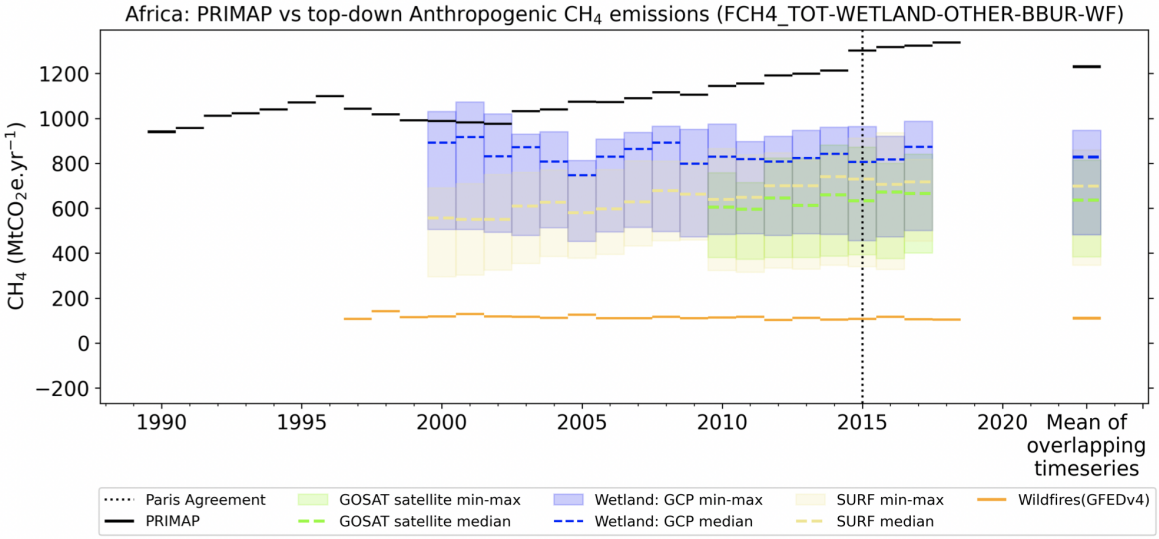

414

415 **Figure S11. Comparison of the total anthropogenic CH_4 emissions from PRIMAP-hist and 22 top-down global**
416 **ensembles using Method 2 for total Africa, including wildfire emissions. Anthropogenic CH_4 emissions from TD**
417 **methods were computed by withdrawing the sum of available data regarding natural emissions from the total flux**
418 **(wetlands, "other natural" emissions, biomass burning, and wildfires (GFEDv4)). Black lines denote the PRIMAP-**
419 **hist estimates for total anthropogenic emissions including all IPCC sectors. Shaded green areas represent the**
420 **minimum and maximum ranges from satellite concentration observations (GOSAT) inversions. Shaded blue areas**
421 **represent the minimum and maximum ranges for wetlands. Shaded yellow areas represent the minimum and**
422 **maximum ranges for surface stations (SURF). Green dashes denote the median of 11 global GOSAT satellites, blue**
423 **dashes denote the median of wetlands, yellow dashes the median of inversions using surface stations (SURF). The**
424 **orange lines represent wildfire emissions. Following the atmospheric convention, positive numbers represent an**
425 **emission to the atmosphere.**

426

427

428

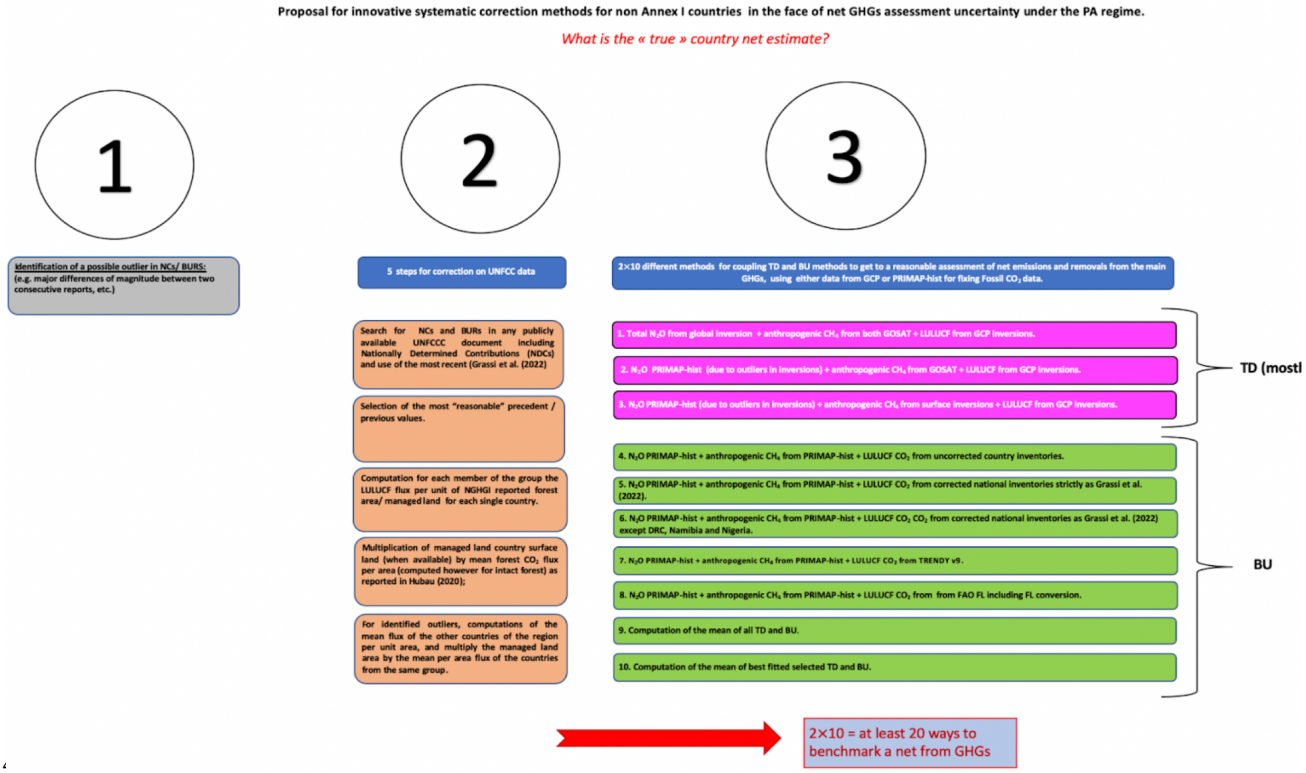

Figure S12. Synthesis of the different methodological steps used in this paper for assessing net African GHG trends.

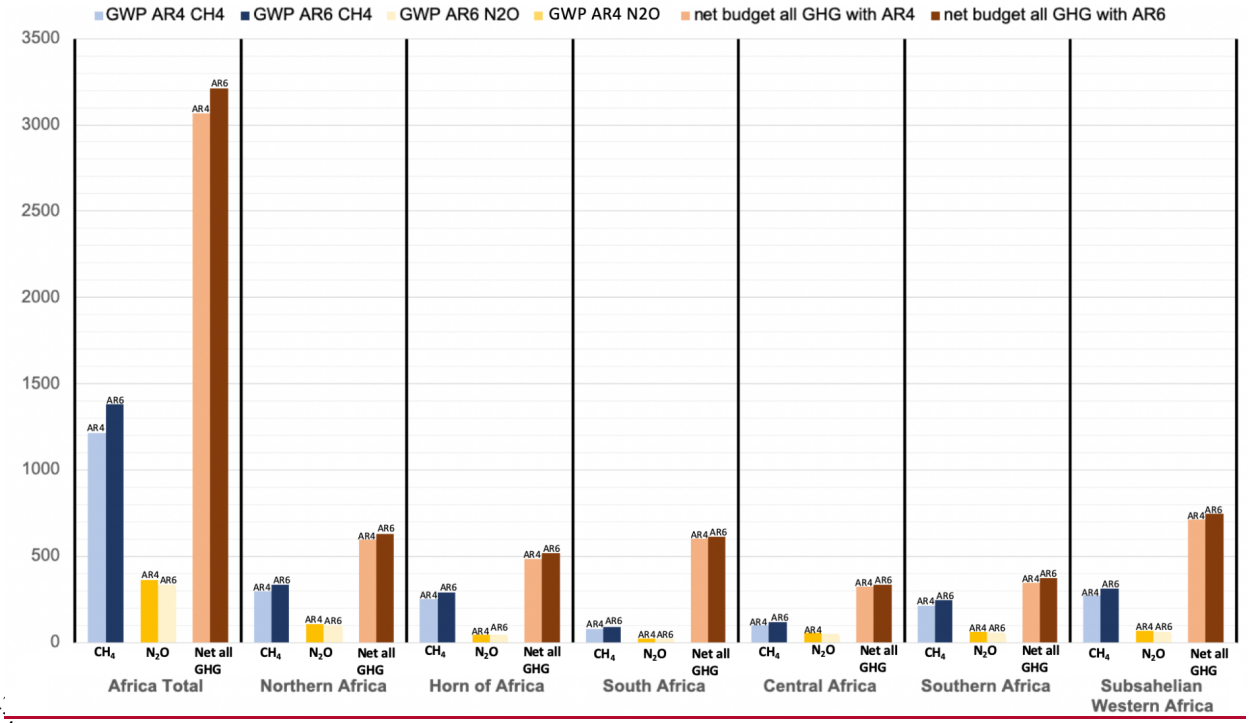

Figure S13. Differences in $MtCO_2e$ in the CH_4 emissions, N_2O emissions and total GHG net budget coming from the use of AR4 and AR6 GWP-100 for CH_4 and N_2O with PRIMAP fossil CO_2 emissions and LULUCF CO_2 for the 6 African regions and Africa total, using PRIMAP-hist for fossil CO_2 and UNFCCC data consistent with Grassi et al. (2022).

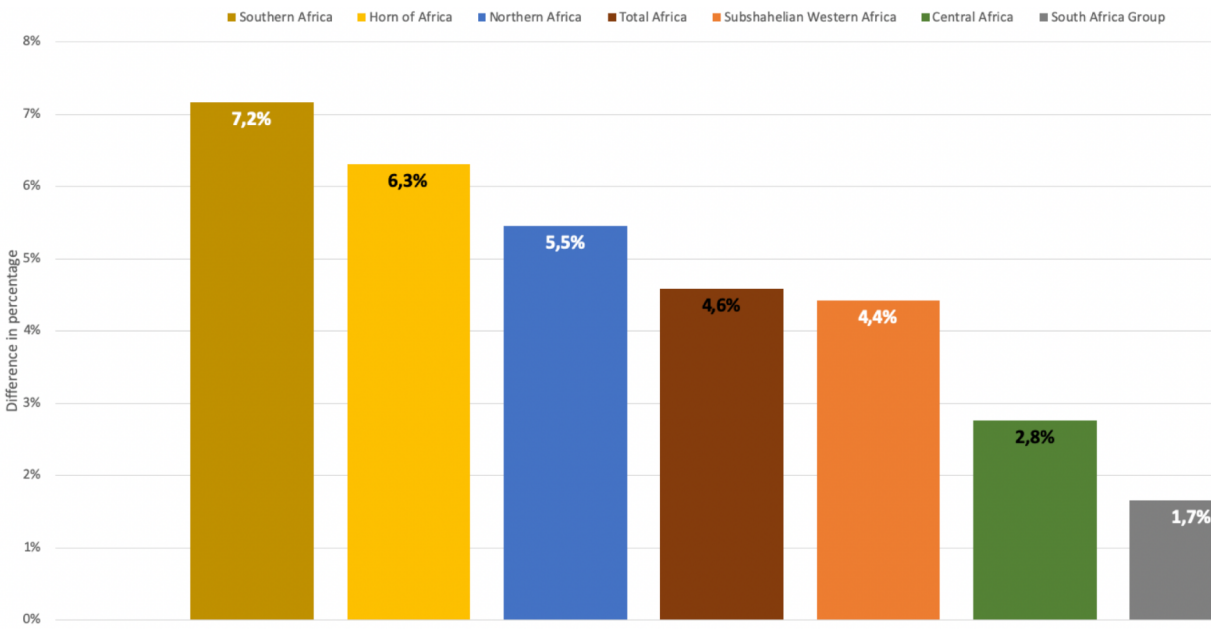

Figure S14. Percentage of difference in the 2001-2018 net budget coming from the difference between the use of AR6 GWP-100 and AR4 GWP-100 for CH_4 and N_2O, with PRIMAP fossil CO_2 emissions and UNFCCC LULUCF CO_2 (Grassi, 2022) for the 6 African regions and Africa total.

References

Andrew, R. M.: A comparison of estimates of global carbon dioxide emissions from fossil carbon sources, Earth Syst. Sci. Data, 12, 1437–1465, https://doi.org/10.5194/essd-12-1437-2020, 2020.

Chevallier, F., Fisher, M., Peylin, P., Serrar, S., Bousquet, P., Bréon, F.-M., Chédin, A., and Ciais, P.: Inferring CO2 sources and sinks from satellite observations: Method and application to TOVS data, J. Geophys. Res. Atmospheres, 110, https://doi.org/10.1029/2005JD006390, 2005.

FAO FRA: FAO Global Forests Resource Assessment, available at fra-data.fao.org, last access: June 2022, 2022.

Friedlingstein, P., O'Sullivan, M., Jones, M. W., Andrew, R. M., Hauck, J., Olsen, A., Peters, G. P., Peters, W., Pongratz, J., Sitch, S., Le Quéré, C., Canadell, J. G., Ciais, P., Jackson, R. B., Alin, S., Aragão, L. E. O. C., Arneth, A., Arora, V., Bates, N. R., Becker, M., Benoit-Cattin, A., Bittig, H. C., Bopp, L., Bultan, S., Chandra, N., Chevallier, F., Chini, L. P., Evans, W., Florentie, L., Forster, P. M., Gasser, T., Gehlen, M., Gilfillan, D., Gkritzalis, T., Gregor, L., Gruber, N., Harris, I., Hartung, K., Haverd, V., Houghton, R. A., Ilyina, T., Jain, A. K., Joetzjer, E., Kadono, K., Kato, E., Kitidis, V., Korsbakken, J. I., Landschützer, P., Lefèvre, N., Lenton, A., Lienert, S., Liu, Z., Lombardozzi, D., Marland, G., Metzl, N., Munro, D. R., Nabel, J. E. M. S., Nakaoka, S.-I., Niwa, Y., O'Brien, K., Ono, T., Palmer, P. I., Pierrot, D., Poulter, B.,

Resplandy, L., Robertson, E., Rödenbeck, C., Schwinger, J., Séférian, R., Skjelvan, I., Smith, A. J. P., Sutton, A. J., Tanhua, T., Tans, P. P., Tian, H., Tilbrook, B., van der Werf, G., Vuichard, N., Walker, A. P., Wanninkhof, R., Watson, A. J., Willis, D., Wiltshire, A. J., Yuan, W., Yue, X., and Zaehle, S.: Global Carbon Budget 2020, Earth Syst. Sci. Data, 12, 3269–3340, https://doi.org/10.5194/essd-12-3269-2020, 2020.

Gilfillan, D., and Marland G.: CDIAC-FF: global and national CO2 emissions from fossil fuel combustion and cement manufacture: 1751–2017, https://doi.org/10.5194/essd-13-1667-2021 , 2021.

Grassi, G., Stehfest, E., Rogelj, J., van Vuuren, D., Cescatti, A., House, J., Nabuurs, G.-J., Rossi, S., Alkama, R., Viñas, R. A., Calvin, K., Ceccherini, G., Federici, S., Fujimori, S., Gusti, M., Hasegawa, T., Havlik, P., Humpenöder, F., Korosuo, A., Perugini, L., Tubiello, F. N., and Popp, A.: Critical adjustment of land mitigation pathways for assessing countries' climate progress, Nat. Clim. Change, 11, 425–434, https://doi.org/10.1038/s41558-021-01033-6, 2021.
Gütschow, J., Jeffery, M. L., Gieseke, R., Gebel, R., Stevens, D., Krapp, M., and Rocha, M.: The PRIMAP-hist national historical emissions time series, Earth Syst. Sci. Data, 8, 571–603, https://doi.org/10.5194/essd-8-571-2016, 2016.

Gütschow, J., Günther, A., Jeffery, M. L., and Gieseke, R.: The PRIMAP-hist national historical emissions time series (1850-2018) v2.2, https://doi.org/10.5281/zenodo.4479172, 2021.

IMF: International Monetary Fund: International Monetary Fund website, available at: https://www.imf.org/en/Publications/fandd/issues/Series/Back-to-Basics/gross-domestic-product-GDP, last access : February 2022.

IPCC: *Climate Change 2021: The Physical Science Basis. Contribution of Working Group I to the Sixth Assessment Report of the Intergovernmental Panel on Climate Change*[Masson-Delmotte, V., P. Zhai, A. Pirani, S.L. Connors, C. Péan, S. Berger, N. Caud, Y. Chen, L. Goldfarb, M.I. Gomis, M. Huang, K. Leitzell, E. Lonnoy, J.B.R. Matthews, T.K. Maycock, T. Waterfield, O. Yelekçi, R. Yu, and B. Zhou (eds.)]. Cambridge University Press, Cambridge, United Kingdom and New York, NY, USA, In press, doi:10.1017/9781009157896, 2021.

Mostefaoui, M., Ciais, P., McGrath, M. J., Peylin, P., Prabir, P. K., Saunois, M., Chevallier, F., Sitch, S., Rodenbeck, C., Luijkx, I., and Thompson, R.: Datasets for greenhouse gasses emissions and removals from inventories and global models over Africa v0.1, Zenodo [data set], https://doi.org/10.5281/zenodo.7347077, 2022.

NOAA Website, available at: **https://www.noaa.gov.** (last access: August 2023), 2023.

Patra, P. K., Takigawa, M., Watanabe, S., Chandra, N., Ishijima, K., and Yamashita, Y.: Improved Chemical Tracer Simulation by MIROC4.0-based Atmospheric Chemistry-Transport Model (MIROC4-ACTM), Sola, 14, 91–96, https://doi.org/10.2151/sola.2018-016, 2018.

World Bank: GDP exchange rate estimates, available at https://data.worldbank.org/indicator/NY.GDP.MKTP.CD last accessed, 2019.

World Bank: World Bank economic data, available at: https://www.worldbank.org/ (last access: May 2022), 2022.